THESIS APPROVAL

GRADUATE SCHOOL, KASETSART UNIVERSITY

Master of Science (Genetic Engineering)

DEGREE

Genetic Engineering | Interdisciplinary Graduate Program

FIELD | **PROGRAM**

TITLE: Pyruvate Kinase from *Streptomyces antibioticus* and *S. coelicolor*: Characterization of the Nucleotide Sequence and Kinetic Property

NAME: Miss Nalumon Thadtapong

THIS THESIS HAS BEEN ACCEPTED BY

THESIS ADVISOR

(Assistant Professor Somchai Pornbanlualap, Ph.D.)

THESIS CO-ADVISOR

(Assistant Professor Nonlawat Boonyalai, Ph.D.)

GRADUATE COMMITTEE CHAIRMAN

(Assistant Professor Siriwan Prapong, Ph.D.)

APPROVED BY THE GRADUATE SCHOOL ON _____

DEAN

(Associate Professor Gunjana Theeragool, D.Agr.)

THESIS

PYRUVATE KINASE FROM *Streptomyces antibioticus* AND *S. coelicolor*: CHARACTERIZATION OF THE NUCLEOTIDE SEQUENCE AND KINETIC PROPERTY

NALUMON THADTAPONG

A Thesis Submitted in Partial Fulfilment of
the Requirements for the Degree of
Master of Science (Genetic Engineering)
Graduate School, Kasetsart University
2013

Nalumon Thadtapong 2013: Pyruvate Kinase from *Streptomyces antibioticus* and *S. coelicolor*: Characterization of the Nucleotide Sequence and Kinetic Property. Master of Science (Genetic Engineering), Major Field: Genetic Engineering, Interdisciplinary Graduate Program. Thesis Advisor: Assistant Professor Somchai Pornbanlualap, Ph.D. 130 pages.

2'-Deoxynucleoside triphosphates (dNTP) are becoming indispensible reagents used for amplification of DNA in PCR techniques. This thesis describes an enzymatic method for the synthesis of dNTPs at 100 mM-scale and cloning of pyruvate kinase from *Streptomyces coelicolor* and *S. antibioticus*. The first step in synthesis of dNTP involves phosphorylation to 2'-deoxynucleoside monophosphates (dNMP) to their diphosphoric forms, using 2'-deoxynucleoside monophosphate (dNMP kinases). However, because no one single dNMP kinase was found to able to convert all four dNMPs to dNDPs, phosphorylation of 2'-dAMP and 2'-dCMP to their respective diphosphoric forms was accomplished using *Escherichia coli* adenylate kinase (ADK) and cytidine monophosphate kinase (CMK), respectively. The phosphorylation of 2'-dGMP and 2'-dTMP were accomplished using one enzyme, T_4 phage deoxynucleotides kinase (DNK). All of the enzymes described had been previously cloned and over-expressed in laboratory. The second step involves phosphorylation of 2'-dNDP to 2'-dNTP with pyruvate kinase (PYK). Although the type II *E. coli* PYK had been cloned and over-expressed in *E. coli*, this recombinant was unstable and aggregated upon prolonged incubation at 37°C. This enzyme was replaced by type I PYK from *E. coli* and from other organisms such as *Streptomyces antibioticus* and *S. coelicolor.* The *pyk* gene from *S. coelicolor* was cloned, sequenced and expressed in *E. coli* host. When induced with lactose, *S. coelicolor* PYK (ScPYK) was expressed as inclusion bodies. The purified protein contains two bands with a molecular weight of 51 and 60 kDa, respectively. The 51 kDa protein corresponds to the predicted molecular weight of ScPYK whereas the 60 kDa protein is proposed to be the phosphorylated form of PYK or protein resulted from an error during protein translation. In addition to ScPYK, the 1,437 bp *pyk* gene from *S. antibioticus* was isolated by PCR, completely sequenced and will be over-expressed and purified in the future. The putative *pyk* gene from *S. antibioticus* is predicted to encode for the type I PYK with the deduced amino acid sequence of 478 residues. To synthesized dNTP, the type I PYK from *E. coli* was chosen. Using ADK or CMK in combination with type I *E. coli* PYK, dATP or dCTP was successfully synthesized at 100 mM-scale with a yield of approximately 92%. Using DNK in combination with PYK, the synthesis of dGTP and dTTP were accomplished at 10 mM and 50 mM-scale, respectively. Synthesis of dGTP requires ATP as phosphoryl donor whereas synthesis of dTTP requires dTTP as phosphoryl donor.

Student's signature Thesis Advisor's signature

ACKNOWLEDGEMENTS

First, I would like to thank my advisor, Asst. Prof. Dr. Somchai Pornbanlualap for his advice, guidance and the opportunity that he provided me to perform the research work in his laboratory. This thesis could not be completed without his support. I would also like to thank my co-advisor, Asst. Prof. Dr. Nonlawat Boonyalai and Dr. Sasimanas Unajak for their advice and helpful suggestion regarding to thesis writing. I am grateful to Dr. Chonticha Tantitadapitark for allowing me to use her equipment in my experiment. I also would like to thank the chairman of Genetic Engineering Program, Asst. Prof. Dr. Siriwan Prapong, for her advice, encouragement and caring.

I would like to thank my friends and staffs in the Department of Biochemistry and Genetic Engineering Program, especially Budsakorn Auiyawong, Kanok-on Suwandumrong, Prapaipit Pumthong, Siripnan Artornturasuk, Pornchanok Chalopagorn, Dr. Chanthakan Nuchsuk, Rawint Narawongsanont and Jaruwan Jumnianpol for their friendship, encouragement, assistances and advice. This thesis could not be completed without them.

Special thanks for Assoc. Prof. Dr. Parin Chaivisuthangkura and my friends from Department of Biology, Faculty of Science, Srinakharinwirot University for their encouragement and care.

Finally, I would like to thank my parent for their understanding, emotional and financial supports.

Nalumon Thadtapong

May, 2013

TABLE OF CONTENTS

LIST OF TABLES

LIST OF FIGURES

LIST OF FIGURES (Continued)

LIST OF FIGURES (Continued)

LIST OF FIGURES (Continued)

LIST OF FIGURES (Continued)

LIST OF ABBREVIATIONS

ADK	=	Adenylate kinase
ADP	=	Adenosine diphosphate
AMP	=	Adenosine monophosphate
Arg	=	Arginine
ATP	=	Adenosine triphosphate
B. licheniformis	=	*Bacillus licheniformis*
B. phychrophila	=	*Bacillus phychrophila*
B. stearothermophilus	=	*Bacillus stearothermophilus*
BME	=	β-mercaptoethanol
bp	=	Base pair
CDP	=	Cytidine diphosphate
CMK	=	Cytidine monophosphate kinase
CMP	=	Cytidine monophospphate
dADP	=	Deoxyadenosine diphosphate
dAMP	=	Deoxyadenosine monophosphate
dATP	=	Deoxyadenosine triphosphate
dCDP	=	Deoxycythydine diphosphate
dCMP	=	Deoxycytidine monophosphate
dCTP	=	Deoxycytidine triphosphate
DCC	=	Dicyclohexylcarbodiimide
DEAE	=	Diethylaminoethyl
DEAE-Cellulose	=	Diethylaminoethyl-Cellulose
dGDP	=	Deoxyguanosine diphosphate
dGMP	=	Deoxyguanosine monophosphate
dGTP	=	Deoxyguanosine triphosphate
dHDP	=	5-Hydroxymethyl-dCDP
dHMP	=	5-Hydroxymethyl-dCMP
DMF	=	Dimethylformamide
DMSO	=	Dimethyl sulfoxide

LIST OF ABBREVIATIONS (Continued)

DNA	=	Deoxyribonucleic acid
DNK	=	Deoxynucleotide kinase
dNDP	=	Deoxynucleoside diphosphate
dNMP	=	Deoxynucleoside monophosphate
dNTP	=	Deoxynucleotides triphosphates
dTDP	=	Deoxythymidine diphosphate
dTMP	=	Deoxythymidine monophosphate
dTTP	=	Deoxythymidine triphosphate
dUMP	=	Deoxyuridine monophosphate
E. coli	=	*Escherichia coli*
EDTA	=	Ethylenediaminetetraacetic acid
G+C content	=	Guanine + Cytosine content
HCl	=	Hydrochloric acid
His	=	Histidine
IPTG	=	Isopropyl β-D-1-thiogalactopyranoside
ISP	=	International *Streptomyces* Project
kb	=	Kilo-base pair
KCl	=	Potassium chloride
kDa	=	Kilo-daltons
LB	=	Luria-Bertani
LDH	=	Lactate dehydrogenase
M	=	Molar
Mb	=	Mega base
mg	=	Milligram
$MgCl_2$	=	Magnesium chloride
ml	=	Milliliter
mM	=	Millimolar
µM	=	Micromolar
µl	=	Microliter

LIST OF ABBREVIATIONS (Continued)

NaCl	=	Sodium chloride
NAD^+	=	Nicotinamide adenine dinucleotide
NADH	=	Nicotinamide adenine dinucleotide, reduced form
ng	=	Nano gram
nmole	=	Nanomole
NMP	=	Nucleoside monophosphate
NTP	=	Nucleoside triphosphate
PCR	=	Polymerase chain reaction
PDB	=	Protein data bank
PEG	=	Polyethylene glycol
PEI-Cellulose	=	Polyethylenimine-Cellulose
PEP	=	Phosphoenolpyruvate
PFK	=	Phosphofructokinase
PMSF	=	Phenylmethylsulfonyl fluoride
PYK	=	Pyruvate kinase
RNA	=	Ribonucleic acid
rpm	=	Round per minute
R state	=	Relaxed or active state
S. albus	=	*Streptomyces albus*
S. antibioticus	=	*Streptomyces antibioticus*
S. avermitilis	=	*Streptomyces avermitilis*
S. coelicolor	=	*Streptomyces coelicolor*
S. griseus	=	*Streptomyces griseus*
S. hygroscopicus	=	*Streptomyces hygroscopicus*
S. lividans	=	*Streptomyces lividans*
S. scabiei	=	*Streptomyces scabiei*
S. somaliensis	=	*Streptomyces somaliensis*
S. rimosus	=	*Streptomyces rimosus*
SaPYK	=	Pyruvate kinase of *Streptomyces antibioticus*

LIST OF ABBREVIATIONS (Continued)

ScPYK	=	Pyruvate kinase of *Streptomyces coelicolor*
SDS-PAGE	=	Sodium dodecyl sulfate- polyacrylamide gel electrophoresis
T. brucei	=	*Trypanosoma brucei*
TEAB	=	Triethylammonium bicarbonate
TLC	=	Thin layer chromatography
Trp	=	Tryptophane
T state	=	Tensed or inactive state

PYRUVATE KINASE FROM *Streptomyces antibioticus* AND *S. coelicolor*: CHARACTERIZATION OF THE NUCLEOTIDE SEQUENCE AND KINETIC PROPERTY

INTRODUCTION

Polymerase chain reaction (PCR) is one of the most commonly used techniques in molecular biology and requires dNTP as the essential precursor for synthesis of DNA during amplification. The demand for dNTP is steadily increasing due to the increasing of PCR application in the both biotechnological industry and universities. Therefore, we are interested in developing an enzymatic synthesis for synthesis of dNTP at the medium and large scale. Although dNTP had been successfully synthesized by members from Pornbanlualap's laboratory, however, the scale of synthesis can only be accomplished at 1-2 mM-scale (Howhan, 2004; Poopanitpan, 2005; Narawongsanont, 2010). Limitation to large scale synthesis of dNTP is likely to be originated from the use of *E. coli* type II PYK in the synthesis. Although this enzyme can be expressed at satisfactory level in *E. coli*, however, the recombinant enzyme was found to be highly unstable and easily aggregated upon prolong in incubation at 37°C. Consequently, we are interested to employ PYK from other microorganisms for enzymatic synthesis of dNTP. In addition to being an essential enzyme in synthesis of dNTP, PYK has also been used as the model enzyme for studying of the mechanism of allosteric activation as well as a drug target.

Pyruvate kinase (PYK) (ATP-pyruvate 2-*o*-phosphotranferase, EC 2.7.1.40) is an essential enzyme in the glycolysis that is necessary to the survival of cell. This enzyme catalyzes the essentially irreversible transphosphorylation from phosphoenolpyruvate (PEP) and adenosine diphosphate (ADP) to pyruvate and adenosine triphosphate (ATP) (Valentini *et al.*, 2000). Because the pyruvate formed feeds into several other metabolic pathways, this makes PYK an essential enzyme at a primary metabolic intersection. Both eukaryotes and prokaryotes have been shown to contain a similar glycolytic pathway (Munoz and Ponce, 2003).

PYK, hexokinase and phosphofructokinase-1 (PFK) are the three main regulatory enzymes in controlling the metabolic flux in glycolysis (Munoz and Ponce, 2003; Moran *et al.*, 2012). In addition to glycolysis, PYK has been proposed to play other roles in several organisms studied (Haug *et al.*, 2006; Benjaphokee *et al.*, 2011; Chanaton and Gottlieb, 2012; Christofk *et al.*, 2008; Murphy *et al.*, 2006; D'Auria *et al.*, 2000; Sauer and Eikmanns, 2005). Because of its regulatory property, PYK from both prokaryotic and eukaryotic origin has become one of a few enzymes used in studying the molecular basis for allosteric transition (Alam *et al.*, 2010). For instance, allosteric enzymes are known to exist in two conformations, an "active" and an "inactive" state. When bind to an allosteric activator, what is the structural basic of transition from the "inactive" to the "active" state?

Streptomyces spp. are microorganisms that are found in soils of tropical area such as Thailand. *Streptomyces* sp., Gram-positive and soil-dwelling bacteria, is one of genera of Actinomycetes that known to produced antibiotic. For this reason, many researchers become interested to improve the growth condition of *Streptomyces* sp. to obtain a higher yield of antibiotics and extracellular enzyme production.

Streptomyces coelicolor is the model actinomyces generally used in research and used for improving antibiotic production (Hopwood, 1999). The genome-scale stoichiometric model of *S. coelicolor* metabolism was studied and predicted by *in silico* (Alam *et al.*, 2010; Ahmed *et al.*, 2013; Nieselt *et al.*, 2010; Cochrane, 1955). The complete genome of *S. coelicolor* had been sequenced. Analysis of the genome of *S. coelicolor* showed that two putative PYKs, type I and type II, existed (Bentley *et al.*, 2002). These enzymes had been predicted to locate at different position in the metabolic pathway. Type II PYK has encoded genes of metabolic enzymes as gene neighborhoods, but type I PYK has encoded gene of ATP-binding cassetts transporter, ABC transporters as gene neighborhoods. Since these two putative PYKs have never been biochemically characterized, their real functions can only be predicted using molecular modeling (Galperin and Koonin, 2000; Olson *et al.*, 1996; Tamames *et al.*, 1997; Yi *et al.*, 2007).

Type I PYK has been proposed to play an essential role in ABC transporter rather than in glycolysis. ABC transporters are members of protein superfamily that is one of the largest and most ancient families which existed in both prokaryote and eukaryote (Procko *et al.*, 2009). ABC transporters transport various substrates, nutrients, antibiotics and other molecules across cellular membranes. Moreover, research reported in several literatures had suggested that ABC transporter is one of factors for increasing antibiotic production (Qiu and Zhuo, 2011; Rodriguez *et al.*, 1993). Consequently, type I PYK may be part of factors for increasing antibiotic production. Thus, we are interested to study type I PYK of *S. coelicolor*.

Another PYK that captivated our interest is the PYK from *S. antibioticus*, a facultative thermophilic bacterium. However, since the complete genome of *S. antibioticus* is not currently available, therefore one approach in determination of the nucleotide sequence of *S. antibioticus* PYK is to first determine the central region of the *pyk* gene by degenerate PCR, using two primers complementary to the highly conserved regions of *pyk* gene obtained by multiple alignments. Once the central region is known, chromosomal walking PCR technique can be used to determine complete sequence of the *pyk* gene. Then, amino acid sequences of PYKs from *S. antibioticus* and *S. coelicolor* will be analyzed in terms of phylogenetic tree and structure prediction by 3D-modeling.

Therefore, the aims of this thesis are (i) to clone, over-express and purify type I PYK from *S. coelicolor* and (ii) to determine the nucleotide sequence PYK from *S. antibioticus* and predict its structure by modeling.

OBJECTIVES

1. To clone type I *pyk* gene from *S. coelicolor*
2. To overexpress and purify type I PYK from *S. coelicolor*
3. To predict structure and characterize type I PYK from *S. coelicolor*
4. To determine putative *pyk* gene from *S. antibioticus*
5. To predict structure and characterize putative PYK from *S. antibioticus*
6. To synthesize dNTP

LITERATURE REVIEW

1. Pyruvate kinase

Pyruvate kinase (PYK) (ATP-pyruvate 2-*O*-phosphotransferase, EC 2.7.1.40) is the key enzyme in the glycolytic pathway and carbon metabolism in general. The enzyme catalyzes a basically irreversible the transfer of a phosphoryl group from phosphoenolpyruvate (PEP) to adenosine diphosphate (ADP) to form pyruvate and ATP (Valentini *et al.*, 2000), which subsequently channel into the Krebs cycle. The metabolic flux through the glycolysis has been demonstrated to be controlled by only a limited number of enzymes such as PYK, hexokinase and phosphofructokinase-1 (PFK) (Allert *et al.*, 1991; Moran *et al.*, 2012).

The kinetic property, catalytic mechanism and three-dimensional structure of PYK from both prokaryotes and eukaryotes have been studied intensively over the past ten years or so. Most bacteria and lower eukaryotes contain only one isoform of PYK, although a few bacteria also have been reported to contain two (Garrido-Pertierra and Cooper, 1983; Hohn and Paznokas, 1987; Portela *et al.*, 2002). Higher eukaryotes such as plants and vertebrates are known to contain more than one isoform of PYK. Vertebrates, on the other hand, are known to contain as much as four different isoform of PYK (Baysdorfer and Bassham, 1984; Munoz and Ponce, 2003; Ponce *et al.*, 1995). Recently, PYK is known to play other functional roles in addition to glycolysis. For instance, the type M2 PYK from human has been shown to play important role in tumor growth (Aloysius *et al.*, 2009; Anastasiou *et al.*, 2012; Christofk *et al.*, 2008; Ferguson and Rathmell, 2008; Ignacak and Stachurska, 2003; Tanaka *et al.*, 1995) and PYK from *Saccharomyces cerevisiae* has been recently shown to play essential role in high-temperature tolerance (Benjaphokee *et al.*, 2011).

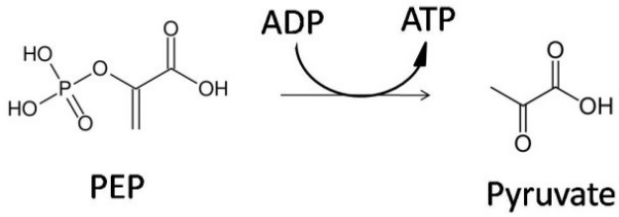

Figure 1 Diagram illustrating the reaction catalyzes by pyruvate kinase. ADP, adenosine diphosphate ; ATP, adenosine triphosphate ; PEP, phosphoenolpyruvate.

The crystal structure of PYK from *E. coli*, *Saccharomyces cerevisiae* and rabbit muscle had been determined. These studied shown that the enzymes from different source are homotetrameric protein. Each enzyme subunit is in turn consisted of three domains (Fothergill-Gilmore *et al.*, 2000; Munoz and Ponce, 2003). PYK from some organisms, however, have been shown to be a dimeric protein (Andre *et al.*, 2007; Plaxton, 1989; Rigden *et al.*, 1999; Sakai, 2004).

Figure 2 The three-dimensional structure of *E. coli* type I PYK in native form, homotetrameric protein

Source: Mettevi *et al.* (1996)

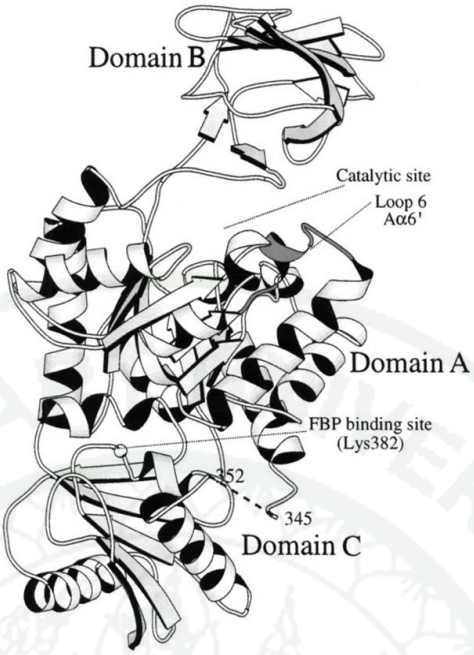

Figure 3 Diagram showing a single subunit of *E. coli* type I PYK. The subunit is divided into three distinct domains which had been labeled as domain A, B and C.

Source: Mettevi *et al.* (1995)

Table 1 List of crystal structures of PYK.

Organisms	**PDB**	**References**
Felis catus, cat	1PKM	(Muirhead *et al.*, 1986; Allen and Muirhead, 1996)
Oryctolagus cuniculus, rabbit	1AQF	(Larsen *et al.*, 1997)
	1A49	(Larsen *et al.*, 1998)
	1F3W	(Wooll *et al.*, 2001)
	1PKN	(Larsen *et al.*, 1994)
Homo sapiens, human, type M1	3SRF	*
Homo sapiens, human, type M2	3ME3	(Anastasiou *et al.*, 2012)
	1T5A	(Dombrauckas *et al.*, 2005)
Homo sapiens, human, type R	2VGG	(Valentini *et al.*, 2002)
Homo sapiens, human, type L	4IP7	(Holyoak *et al.*, 2013)
Toxoplasma gondii	3E0E	(Bakszt *et al.*, 2010)
	3GG8	(Bakszt *et al.*, 2010)
Trypanosoma brucei	3QV9	(Morgan *et al.*, 2011)
	3PP7	(Morgan *et al.*, 2011)
Leishmania mexicana	3KTX	(Morgan *et al.*, 2010)
	3IS4	(Morgan *et al.*, 2010)
	1PKL	(Rigden *et al.*, 1999)
	3E0W	(Tulloch *et al.*, 2008)
Cryptosporidium parvum	4DRS	(Cook *et al.*, 2012)
Saccharomyces cerevisiae	1A3X	(Jurica *et al.*, 1998)
Escherichia coli, type 1	1E0U	(Valentini *et al.*, 2000)
Streptococcus aureus	3T05	(Zoraghi *et al.*, 2011)
	3T0T	(Axerio-Cilies *et al.*, 2012)
Bacillus stearothermophilus	2E28	(Suzuki *et al.*, 2008)
Pylobaculum aerophilum	3QTG	*

*To be published

Each subunit of PYK has been sub-divided into three distinct domains designed as the A, B and C domains, respectively. Domain A is a $(\beta/\alpha)_8$-barral and is the most conserved among the three domains. Domain B is a flexible β-barrel and is most variable. Domain C is a open-sheet and is partial conserved (Munoz and Ponce, 2003). The active and effector sites are always located in pocket between domain A and B, and domain C, respectively. In addition, PYK structures from some organisms have an expanded N-terminus or extra C-terminus domain (Cottam *et al.*, 1969; Tani *et al.*, 1988; Sakai, 2004).

Many PYKs have been shown to be allosteric enzymes that change their conformational ensemble upon binding of effectors. After the effector bound to the enzyme, the binding affinity at the ligand binding site will change. The allosteric enzymes in general can existed in at least two conformations: R state, relaxed or active state, and T state, tensed or inactive state (Changeux and Edelstein, 2005; Monod *et al.*, 1965).

Effectors that bind to PYK may act as either an activator or inhibitor, depending on the source of enzyme (Denton *et al.*, 1996; Mettevi *et al.*, 1996; Morgan *et al.*, 2010; Tanaka *et al.*, 1995). The allosteric and active sites are located at the domain interfaces. In *E. coli*, comparison of the T state with R state revealed the differences in the conformations of the domain B and domain C of each subunit. The subunit rotations observed in T state PYK induce a shift in loop of domain A, leading to distortion of the PEP binding site explanation for the low substrate binding of the T state (Mettevi *et al.*, 1995).

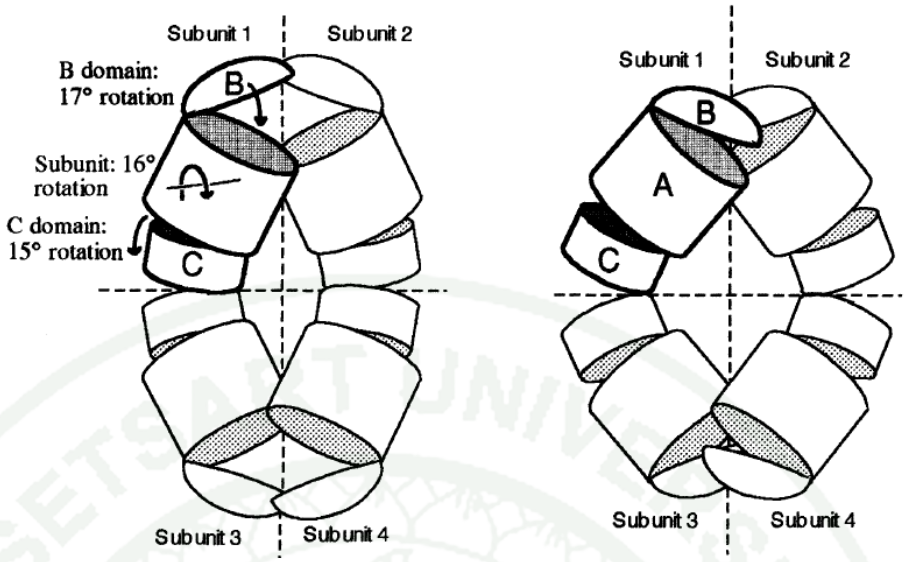

Figure 4 Schematic drawing of the domain and subunit rotation that occurred on transition from the T state which shown on the left hand to the R state which shown on the right hand.

Source: Mettevi *et al.* (1996)

One of the commercial applications of PYK is in the production of ATP. When over-expressed in *E. coli* in large quantity, PYK obtained can be utilized for enzymatic synthesis of ATP from ADP. ATP obtained has a wild range of application such as precursor for synthesis of other commercially important compounds. Other application of PYK is in the diagnosis such as in enzyme assay for measuring the production of ATP. When PYK is coupled to reactions that generated ATP, the production of ATP can be measured with a spectrophotometer at 340 nm as NADH is being converted to NAD^+ (Dolle and Ziegler, 2009; Technikova-Dobrova *et al.*, 1991). In addition, PYK has been targeted as enzyme for development of potent inhibitor. Because PYK is a key regulatory enzyme in glycolytic pathway in many organisms including pathogens, this enzyme has been targeted for the development of antibacterial and antimalarial drugs (Chan *et al.*, 2007; Kumar *et al.*, 2012). In addition, type M2 PYK is important in tumor growth for human. Thus, the type M2 PYK activity is used to indicator for cancer (Haug *et al.*, 2006). Furthermore, PYK can use to non-specific dNDP kinase for dNTPs synthesis (Bao and Ryu, 2007;

Bessman *et al.*, 1957; Ladner and Whitesides, 1985; Lehman *et al.*, 1957; Zinchenko *et al.*, 1990).

2. Synthesis of 2'-deoxynucleoside triphosphates

The amplifications of DNA template in polymerase chain reaction (PCR) require the use of deoxynucleoside triphosphates (dNTP) as precursor (White *et al.*, 1989). The four different dNTP required for synthesis of DNA are deoxyadenosine triphosphate (dATP), deoxycytidine triphosphate (dCTP), deoxyguanosine triphosphate (dGTP) and deoxythymidine triphosphate (dTTP). The commercial usage of dNTP has been shown to be steadily increased due to the increasing application of PCR in the biotechnology, research community and industry (Chen and Janes, 2002; Primrose and Twyman, 2006).

The dNTP can be produced by two different ways, chemical and enzymatic approaches. In many ways, enzymatic synthesis of nucleoside triphosphate (NTP) shares several features with enzymatic synthesis of dNTP. The chemical method involves the reaction of tri-*n*-butylammonium salts of its corresponding dNMP and orthophosphoric acid with dicyclohexylcarbodiimide (DCC) in organic solvents such as pyridine or dimethylformamide (DMF). The chemical method required these toxic solvents and produced yield approximately 40-80% that depended on the specific chemical process used (Moffatt, 1964; Chambers *et al.*, 1957; Chambers *et al.*, 1958; Jocelyn *et al.*, 2008). The purification of individual dNTP component from reaction mixture requires separation of deoxynucleoside monophosphate (dNMP), deoxynucleoside diphosphate (dNDP), DCC and orthophosphoric acid, as well as such byproducts as deoxynucleoside tetra- or penta-phosphates. The separation of dNTP from dNDP is rather difficult and expensive because of the similar molecular properties between the intermediates and products. In addition, the pyridine or DMF solvents must be recovered, separated and recycled due to the stringent involved for waste removal guidelines. Therefore, the chemical method is environmentally harmful (Bao and Ryu, 2007).

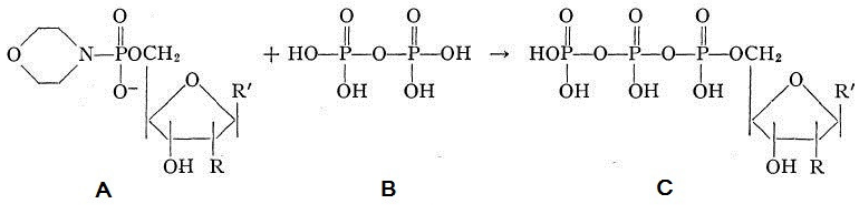

Figure 5 Diagram of NTPs synthesis by chemical process. The attempted extension of the reaction to the direct synthesis through the reaction of nucleoside-5' phosphoromorpholidate (A, R = OH, R' = base) with tributylammonium pyrophosphate in anhydrous pyridine (B). The reaction was produced to nucleoside-5' triphosphate (C, R = OH, R' = base).

Source: modified from previous literature (Moffatt *et al.*, 1964)

Compared to chemical synthesis, the enzymatic synthesis of dNTP is a more convenient, simple and harmless process. The enzymatic method involves the reaction of dNMP kinase which depended on specific base and pyruvate kinase (Lehman *et al.*, 1957; Ladner and Whitesides, 1985; Bessman *et al.*, 1957). The biosynthesis of dNTP involves the use of dNMP as precursors and four different dNMP kinases as the catalytic enzymes. The process consists of two sequential enzymatic phosphorylation reactions, the phosphorylation of dNMP to dNDP in the first step followed by phosphorylation of dNDP to dNTP in the second step (Figure 6).

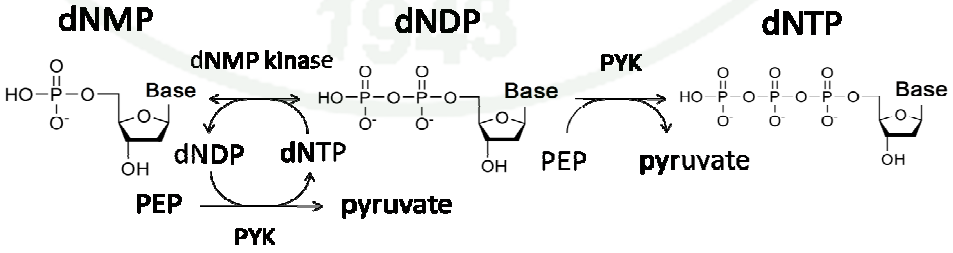

Figure 6 Diagram of biosynthesis reaction for the total dNTP synthesis by enzymatic method from dNMP.

The first step for enzymatic method of synthesis is to convert deoxyadenosine monophosphate (dAMP) to deoxyadenosine diphosphate (dADP) by adenylate kinase (ADK). Similarly, cytidine monophosphate kinase (CMK) for the reaction catalyzed deoxycytidine monophosphate (dCMP) to deoxycytidine diphosphate (dCDP), thymidine monophosphate kinase (TMK) for the reaction converted deoxythymidine monophosphate (dTMP) to deoxythymidine diphosphate (dTDP), and guanosine monophosphate kinase (GMK) for the reaction converted deoxyguanosine monophosphate (dGMP) to deoxyguanosine diphosphate (dGDP), respectively (Singh *et al.*, 2000). Surprisingly, deoxynucleotides kinase (DNK) from bacteriophage T4 can catalyze dTMP and dGMP to dTDP and dGDP which used this enzyme to instead of TMK and GMK for biosynthesis (Duckworth and Bessman, 1967). The dATP is used as the phosphoryl donor for enzymatic reaction for dATP production. Similarly, dCTP, dTTP and dGTP are used as the phosphoryl donor for enzymatic synthesis of dCTP, dTTP and dGTP, respectively (Singh *et al.*, 2000). In the second step, the dNDP intermediate products are further phosphorylated to produce dNTP by using PYK as a nonspecific deoxynucleoside diphosphate kinase enzyme. The phosphoenolpyruvate (PEP) is used as the phosphoryl donor in the second reaction step (Bao and Ryu, 2005; Bao *et al.*, 2005). NMP kinase enzymes for synthesis of dNTP are using in this thesis.

2.1 Adenylate kinase (ADK)

Adenylate kinase (ADK) from *E. coli* was discovered in 1985 (Brune *et al.*, 1985). ADK is an enzyme that converts AMP to ADP reversibly, using ATP as phosphoryl donor (Figure 7). The ADK encoding gene is 648 bp and translated to protein of 216 amino acid residues (Brune *et al.*, 1985).

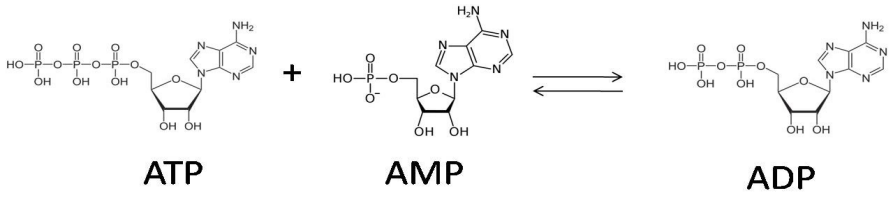

Figure 7 Diagram of ADK activity. AMP, adenosine monophosphate; ADP, adenosine diphosphate; ATP, adenosine triphosphate.

Crystallographic study of ADK from *E. coli* showed that the protein is consisted of two highly flexible domains that close over bound substrates (Figure 8). The LID domain covers ATP and the site of phosphorylation and the LID and the AMP-binding domain closes on AMP when it is bound. Key residues in the domain closure and substrate binding are conserved five arginine in the active site; Arg36, Arg88, Arg123, Arg156 and Arg167. In addition, Arg156 is play an important role in catalysis (Berry *et al.*, 2006).

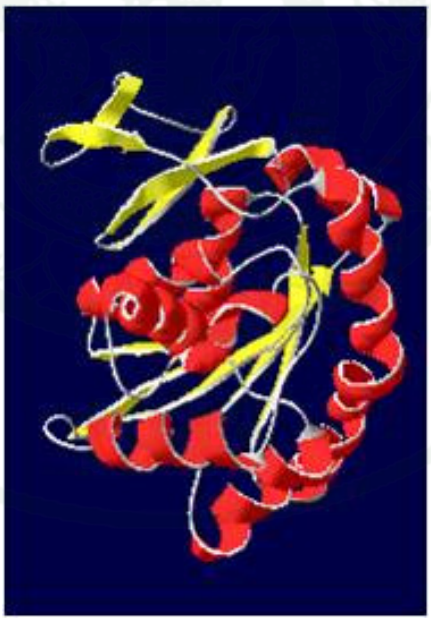

Figure 8 Ribbon diagram of *E. coli* ADK monomeric enzyme (PDB#2ECK). The α-helices and β-sheets were show in red and yellow, respectively.

2.2 Cytidine monophosphate kinase (CMK)

Cytidine monophosphate kinase (CMK) from *E. coli* was first identified in 1995 (Fricke *et al.*, 1995). The CMK encoding gene was translated into a monomeric protein of 225 amino acid residues (Bucurenci *et al.*, 1995). CMK is one of NMP kinases that exhibit substrate specificity toward the base moiety of nucleotides. The phosphorylation of CMP to CDP catalyzed by CMK is a reversible process, using ATP as phosphoryl donor (Figure 9).

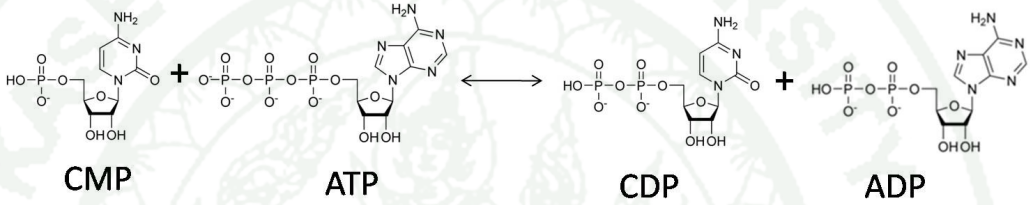

Figure 9 Diagram of CMK activity. ADP, adenosine diphosphate; ATP, adenosine triphosphate; CMP, cytidine monophosphate; CDP, cytidine diphosphate.

The crystal structure of *E. coli* CMK consisted of central parallel β-sheet, the strands of which are connected by α-helices (Briozzo *et al.*, 1998) (Figure 10).

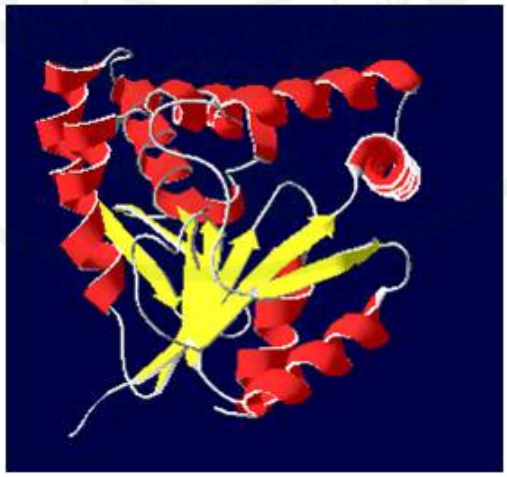

Figure 10 Ribbon diagram of the monomer of *E. coli* CMK (PDB#2CMK). The α-helices and β-sheets are shown in red and yellow, respectively.

2.3 Deoxynucleotide kinase (DNK)

Nucleoside monophosphate (NMP) kinases catalyzed the phosphorylation of the nucleoside monophosphate to the nucleoside diphosphate using ATP as a phosphoryl donor. The enzymes belong to this family generally shows high specificity toward their substrates, with the exception of deoxynucleotide kinase (DNK) from bacteriophage T4. DNK is the only member of this family of the enzymes that recognizes three nucleotides: dGMP, dTMP and 5-hydroxymethyl-dCMP (dHMP) (Duckworth and Bessman, 1967) (Figure 11). Only deoxynucleotides were phosphorylated, by the enzyme, indicating that the enzyme recognizes the sugar moiety of the substrate as well as the base. Kinetic study of the enzyme showed that one active site is responsible for all three activities (Table 2).

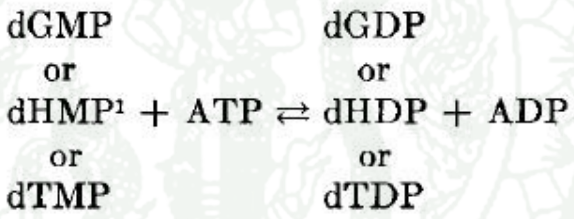

Figure 11 Diagram of DNK activity. ADP, adenosine diphosphate; ATP, adenosine triphosphate; dGMP, deoxyguanosine monophosphate; dGDP, deoxyguanosine diphoaphate; dTMP, deoxythymidine monophosphate; dTDP, deoxythymidine diphosphate; dHMP, 5-hydroxymethyl-dCMP; dHDP, 5-hydroxymethyl-dCDP.

Source: Duckworth and Bessman, (1967)

Table 2 The specificity of DNK for nucleoside monophosphate

Substrate	Concentration (mM)	Activity (U/ml)
dTMP	1.8	780
dGMP	1.0	780
dHMP	0.5	640
dAMP	1.8	0
dCMP	1.8	8
dCMP	4.0	16
dUMP	1.8	80
dUMP	4.0	196
5-CH3-dCMP	2.1	16
5-Br-dUMP	1.0	420
UMP	4.0	32
GMP	4.0	8

Source: Duckworth and Bessman, (1967)

The DNK gene was sequenced since 1985 (Broida and Abelson, 1985; Koch *et al.*, 1989) and protein over-expressed and purified (Brush *et al.*, 1990). The polypeptide chain consisted of 241 amino acid residues. The sequence comparisons were shown no significant homology, 12-18% identity, between DNK and other NMP kinase. On the other hand, the triphosphate binding site had conserve sequence GXXXXGK, where X as any amino acid, observed in many nucleotide binding proteins is also present in DNK. The crystal structure of DNK was shown the polypeptide chain was folded into two domain of equal size, one of resembles the mononucleotide binding motif with the glycine-rich P-loop (PDB#1DEL). The second domain consisted of five α-helices to form the NMP binding packet (Teplyakov *et al.*, 1996).

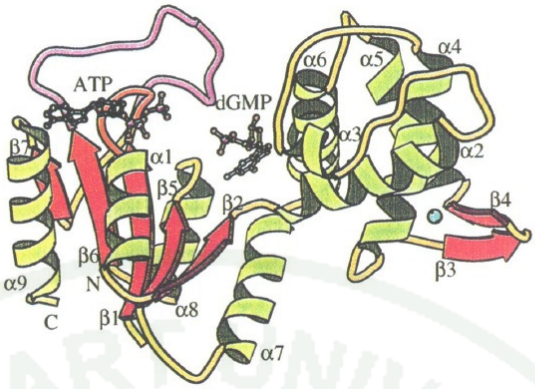

Figure 12 Ribbon diagram of the bacteriophage T_4 DNK monomer. Ball-and-stick models of ATP and dGMP indicated the corresponding binding sites. The P-loop was shown in orange, the LID loop in purple. The Mg^{2+} was shown as a cyan ball. The α-helices and β-sheets were show in yellow and red, respectively.

Source: Teplyakov *et al.* (1996)

Figure 13 Ribbon diagram of the bacteriophage T_4 DNK homodimer in native form. Secondary structure elements involved in the subunit interface were labeled. The α-helices and β-sheets were show in yellow and red, respectively.

Source: Teplyakov *et al.* (1996)

3. *Streptomyces* sp.

The genus *Streptomyces* was proposed in 1943 (Waskman and Henrici, 1943) and classified in the family Streptomycetaceae on the basis of morphology and subsequently cell wall chemotype. Streptomycetes are Gram-positive aerobic members of the order Actinomycetales within the class Actinobacteria and have high G + C content (Figure 14). Species describe within the genus *Streptomyces* increased from approximately 40 to over 3000. Many of these strains were considered to be synonyms. Standard identification criteria and type strains were needed to prevent overspeciation.

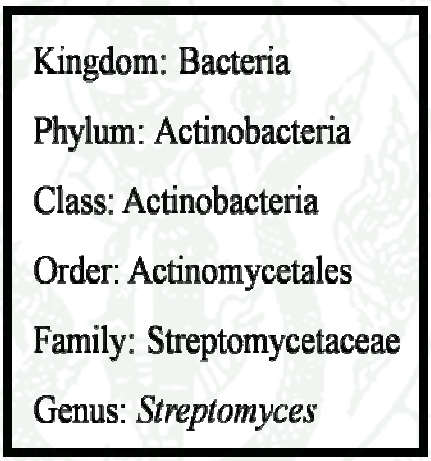

Figure 14 Scientific classification of *Streptomyces* spp.

In 1964, the International *Streptomyces* Project (ISP) was initiated to introduce standard criteria for the determination of species so as to reduce the number of poorly re-described synonymous species. Currently, more than 450 *Streptomyces* species were redescribed and type strains were selected and deposited in internationally recognized culture collections (Anderson and Wellington, 2001).

Streptomycetes produce an extensive branching substrate and aerial mycelium. Growth occurs at the hyphal apices and is accompanied by branching, thus producing a complex tightly woven matrix of hyphae during the vegetative growth phase. As the colony ages, aerial mycelia (sporophores) are produced which develop into chains of

spores (conidia) by the formation of cross-walls in the multinucleate aerial filaments. This is followed by separation of individual cells directly into spores (Wildermuth and Hopwood, 1970; McGregor, 1954).

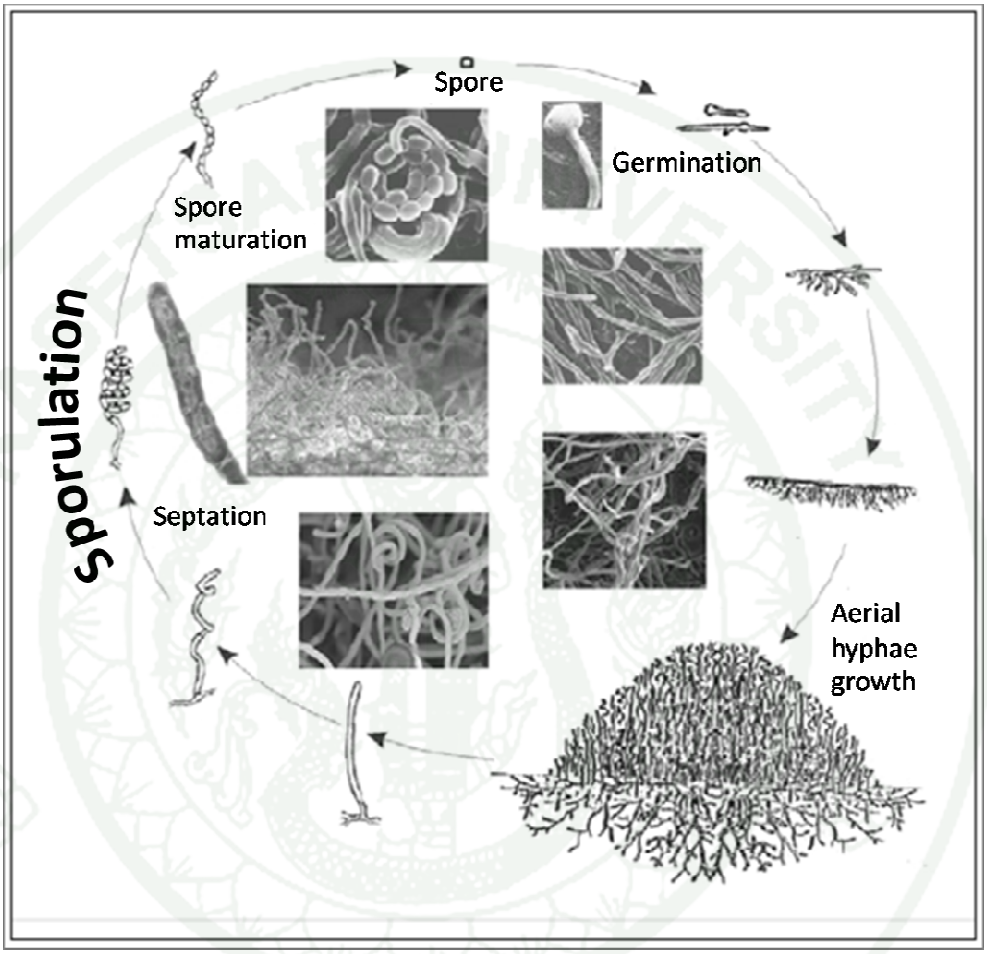

Figure 15 Life cycle of *Streptomyces* spp.

Source: Jakimowicz (2007)

Streptomyces was found predominant in soil and decaying vegetation. In addition, these can found in hot spring and ocean. Most of these have characterized to produce of natural antibiotic that human used for treat patients, but some species of *Streptomyces* have characterized for pathogen in living such as *S. somaliensis* and *S. albus* were pathogen in human (Mishra *et al.*, 1980). Therefore, investigation of

Streptomyces has many literatures in many files. Recently, genetic information was interested to study in researchers.

And now, complete genome was discovered from several species of *Streptomyces*, such as *S. coelicolor* (Bentley *et al.*, 2002), *S. lividans* (Lin *et al.*, 2006), *S. avermitilis* (Ikeda *et al.*, 2003), *S. griseus* (Ohnishi *et al.*, 2008), *S. hygroscopicus* (Pang *et al.*, 2002) and *S. rimosus* (Pandza *et al.*, 1997).

1.1 *Streptomyces antibioticus*

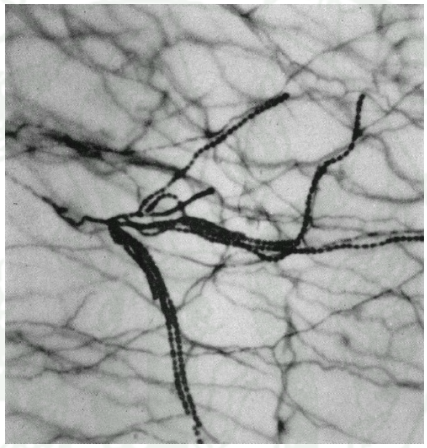

Figure 16 Morphology of vegetative mycelium and sporulating hyphae of *S. antibioticus.*

Source: Waskman and Woodruff (1941)

S. antibioticus (*Actinomyces antibioticus*) is a soil-inhabiting bacteria which was first isolate in 1941 (Waskman and Woodruff, 1941). *S. antibioticus* exhibits morphology of a spore-bearing hyphea produced in the form of straight aerial mycelium. The sporophores are arranged in cluster rather than spiral. *S. antibioticus* can germinated in 35-47.5 ˚C and is classified as facultative thermophilic bacteria (Bergey, 1919), pH 6.0-9.5 (Hardisson *et al.*, 1978).

1.2 *Streptomyces coelicolor*

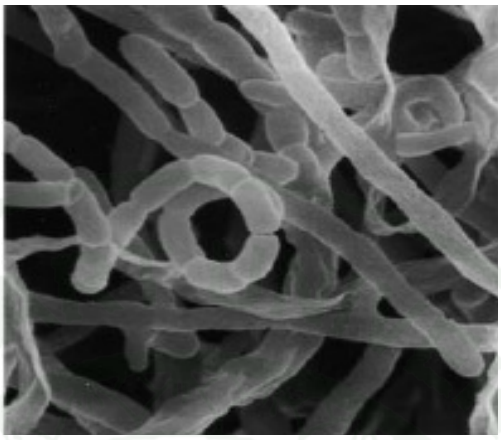

Figure 17 Sporulation hyphae of *S. coelicolor*.

Source: Umeyama *et al.* (2000); Tanaka *et al.* (1995)

S. coelicolor is also a soil-inhibiting, facultative thermophilic bacteria that was first isolated in 1908 (Muller *et al.*, 1908). Although the morphology of *S. coelicolor* is in many ways similar to that of *S. antibioticus,* however the sporophore of *S. coelicolor* is spiral form (Wildermuth and Hopwood, 1970). Genome sequence of *S. coelicolor* had been completely sequenced, is consisted of a linear chromosome with 8,667,507 bp and contains 7,825 predicted genes (Bentley *et al.*, 2002).

MATERIALS AND METHODS

1. Bacteria strains and growth conditions

Streptomyces antibioticus and *S. coelicolor* were grown in yeast extract-malt extract (YEME) liquid medium (Hopwood *et al.*, 1985) which composed of 34% sucrose, 1% glucose, 5% peptone, 3% yeast extract and 0.5% $MgCl_2$. Cell cultures were shaken vigorous at 250 rpm for 48 hours at 30˚C. *E. coli* BL21(DE3) [F^- ompT gal dcm lon $hsdS_B(r_B^- m_B^-)$ λ(DE3 [lacI lacUV5-T7 gene 1 ind1 sam7 nin5])] and *E. coli* DH5α [F^- endA1 glnV44 thi-1 recA1 relA1 gyrA96 deoR nupG Φ80d*lacZ*ΔM15 Δ(*lacZYA-argF*)U169, $hsdR17(r_K^- m_K^+)$, λ–] were grown in 1 liter flask containing Luria-Bertain (LB) liquid medium (Sambrook *et al.*, 1989) with shaking at 220 rpm overnight at 37˚C. Cells were collected by centrifuge at 5,000 rpm for 15 minutes at 4˚C. Solid LB media was prepared by the addition of 1.8% agar.

2. Isolation of genomic DNA from *Streptomyces antibioticus* and *Streptomyces coelicolor*

Genomic DNA of *S. antibioticus* and *S. coelicolor* were isolated by method as previously described (Hopwood *et al.*, 1985). Briefly, two grams of cells were suspended in 5 ml of TE buffer containing 10 mg of lysozyme and incubated at 30˚C for 1 hour. EDTA was added to a final concentration of 100 mM and incubated for 5 minutes at 30˚C. SDS was added to final concentration of 0.1% (v/v) and incubated further at 37˚C for 2 hours. The contaminated proteins in the mixture were removed by phenol-chloroform extraction. The RNA remained in the mixture was removed by addition 30µg/ml RNaseA and incubated further at 37˚C for 1 hour. Genomic DNA was precipitated from the reaction mixture by addition of 0.25 volumes of 5 M NaCl and 10% PEG. The genomic DNA precipitated was dissolved in 5 ml TE buffer and precipitated again by addition of sodium acetate and absolute ethanol. Genomic DNA was pooled and dissolved in TE buffer. The amount of DNA was determined by absorption at 260 nm with spectrophotometer.

Table 3 List of oligonucleotide primers.

Primer name	Sequences (5' to 3')	Primer length (nt)	T_m (°C)	% GC
Degenerated primers for amplification of central region of putative *pyk* gene of *S. antibioticus*				
Sapyk-F	TCT CCG ACM ACA AGG GCM TSA A	22	58	45
Sapyk-R	CGR TAG CGS GAG AGS CGV	18	59	56
Primers for determination of putative *pyk* gene of *S. antibioticus* by chromosomal walking PCR				
Sapyk-3F	TCC AAG GGT CTG CAG CCG CT	20	58	65
Sapyk-5R	CTC CTC GTC CAT GAC GCG GT	20	58	65
Primers for determination of full-length of putative *pyk* type I gene of *S. antibioticus*				
SapykIR	TCA TGG ACA CCC ACG TGG GG	20	58	65
Primers for amplification of *pyk* type I gene of *S. coelicolor*				
Scpyk-F	AAA **CAT ATG** CGC CGA GCA AAG ATC GTC TGC A	31	63	48
Scpyk-R	AAA <u>CTC GAG</u> CTT GGG AAT GTC GTC CTC CCC GAT	33	67	55

Melting temperature (T_m) is calculated using the equation $T_m = 2(A+T) + 4(G+C)$

Degenerate primer Symbol M = A or C, S = C or G, R = A or G and V = A or C or G

Bold and underlined were indicated recognition site of *Nde*I, and *Xho*I, respectively.

3. Amplification of central region of putative *pyk* gene from *S. antibioticus*

Nucleotide sequences of *pyk* genes from various species of *Streptomyces* sp. (Table 4), were aligned by the ClustalW2 program (Thompson *et al.*, 1994). The highly conserved regions of the gene were used for designing the degenerated primers (Table 3). The reaction mixture for degenerated PCR contained to 100 ng of *S.*

antibioticus genomic DNA, 1x *Taq* buffer (Invitrogen), 0.5 µM of each degenerated primers named Sapyk-F and Sapyk-R (Table 3), 0.2 mM dNTP, 0.2U *Taq* DNA polymerase (Invitrogen) 1.5 mM $MgCl_2$ and 5% DMSO. The condition for amplification: the initial denaturation at 94°C for 5 minutes, 3 steps cycling for 35 cycles; denaturation at 94°C for 1 minute, annealing at 53°C for 1 minute and extension at 72°C for 1 minute and 45 seconds, and final extension at 72°C for 10 minutes. The PCR product was analyzed by 1% agarose gel electrophoresis.

Table 4 The nucleotide sequences of *pyk* gene from various species of *Streptomyces* sp. for designing degenerated primers.

GeneID	Gene	Source	Reference
1097448	*pyk* I	*S. coelicolor*	(Bentley *et al.*, 2002)
1100863	*pyk* II	*S. coelicolor*	(Bentley *et al.*, 2002)
8843636	*pyk* I	*S. scabiei*	(Loria *et al.*, 2006)
8845851	*pyk* II	*S. scabiei*	(Loria *et al.*, 2006)
1210560	*pyk* A1	*S. avermitilis*	(Ikeda *et al.*, 2003)
1211436	*pyk* A2	*S. avermitilis*	(Ikeda *et al.*, 2003)
6212002	putative *pyk* SGR_2113	*S. griseus*	(Ohnishi *et al.*, 2008)
6212091	putative *pyk* SGR_5516	*S. griseus*	(Ohnishi *et al.*, 2008)

4. Amplification of upstream region of putative *pyk* gene from *S. antibioticus*

The primers for amplification of the upstream and downstream regions of *pyk* gene were designed from the known highly conserved region franking the central region of the gene. In addition, Scpyk-F for amplified type I *pyk* gene of *S. coelicolor* was used to find the upstream region. The reaction mixture contained 50 ng of *S. antibioticus* genomic DNA, 1X *Taq* buffer (Invitrogen), 0.5 µM of Scpyk-F and Sapyk-5R (Table 3), 0.2 mM dNTP, 0.2U *Taq* DNA polymerase (Invitrogen), 1.5 mM $MgCl_2$ and 5% DMSO. The condition for amplification was as follow: initial denaturation at 94°C for 5 minutes, 3 steps cycling for 35 cycles; denaturation at 94°C for 1 minute, annealing at 50°C for 1 minute and extension at 72°C for 3 minutes, and

final extension at 72°C for 10 minutes. The PCR product was analyzed by 1% agarose gel electrophoresis.

5. Amplification of downstream region of putative *pyk* gene from *S. antibioticus*

The downstream region was determined by semi-random PCR methodology (Ge and Charon, 1997). The reaction mixture contained 50 ng of fragments of *S. antibioticus* genomic DNA that digested with *Nde*I, 1X *Taq* buffer (Invitrogen), 0.5 µM of each primers (random primer from Promega and Sapyk-3F, Table 3), 0.2 mM dNTP, 0.2U *Taq* DNA polymerase (Invitrogen), 1.5 mM $MgCl_2$ and 5% DMSO. The condition for amplification was as follow: initial denaturation at 94°C for 5 minutes, 3 steps cycling for 30 cycles; denaturation at 94°C for 1 minute, annealing at 50.7°C for 30 seconds and extension at 72°C for 4 minutes, and final extension at 72°C for 10 minutes. The PCR product was analyzed by 1% agarose gel electrophoresis.

6. Amplification of overlapping site of putative *pyk* gene from *S. antibioticus* for checking the recombinant plasmids

The PCR products from amplification of downstream region had two bands. Thus, the verification of PCR fragments had necessary by amplification of overlapping site. The reaction mixture contained 50 ng of fragments of *S. antibioticus* genomic DNA that digested with *Nde*I, 1X *Taq* buffer (Invitrogen), 0.5 µM of Sapyk-R and Sapyk-3F (Table 3), 0.2 mM dNTP, 0.2U *Taq* DNA polymerase (Invitrogen), 1.5 mM $MgCl_2$ and 5% DMSO. The condition for amplification was as follow: initial denaturation at 94°C for 5 minutes, 3 steps cycling for 30 cycles; denaturation at 94°C for 1 minute, annealing at 50.7°C for 30 seconds and extension at 72°C for 4 minutes, and final extension at 72°C for 10 minutes. The PCR product was analyzed by 1% agarose gel electrophoresis.

Figure 18 Outline for strategy of overlapping site of putative *pyk* gene. The primers used for amplification of central region (Sapyk-F and Sapyk-R) and primers used for amplification of upstream and downstream regions (Sapyk-3F and Sapyk-5R).

7. Amplification of full-length of putative type I *pyk* gene from *S. antibioticus*

After the downstream region was analyzed nucleotide sequence, the reverse primer was designed for amplification of full-length of type I *pyk* gene. The reaction mixture contained 50 ng of *S. antibioticus* genomic DNA, 1X *Taq* buffer (Invitrogen), 0.5 µM of Scpyk-F and SapykIR (Table 3), 0.2 mM dNTP, 0.2U *Taq* DNA polymerase (Invitrogen), 1.5 mM $MgCl_2$ and 5% DMSO. The condition for amplification was as follow: initial denaturation at 94°C for 5 minutes, 3 steps cycling for 30 cycles; denaturation at 94°C for 1 minute, annealing at 60.2°C for 1 minute and extension at 72°C for 1 minute and 30 seconds, and final extension at 72°C for 10 minutes. The PCR product was analyzed by 1% agarose gel electrophoresis.

8. Amplification of type I *pyk* gene from *S. coelicolor*

The type I *pyk* gene from *S. coelicolor* was amplified by specific primers (GeneID: 1097448) (Bentley *et al.*, 2002). The reaction mixture contained 150 ng of *S. coelicolor* genomic DNA, 1X *Taq* buffer (Invitrogen), 0.5 µM of Scpyk-F and Scpyk-R (Table 3), 0.2 mM dNTP, 0.2U *Taq* DNA polymerase (Invitrogen), 1.5 mM $MgCl_2$ and 5% DMSO. The condition for amplification was as the following: initial denaturation at 94°C for 5 minutes, 3 steps cycling for 35 cycles; denaturation at 94°C for 1 minute, annealing at 60°C for 1 minute and extension at 72°C for 2 minutes, and final extension at 72°C for 10 minutes. The PCR product was analyzed by 1% agarose gel electrophoresis.

9. Construction of recombinant plasmid for cloning and sequencing

PCR fragments from amplification reaction was analyzed on 1% agarose gel, ligated into pGEM®-T-Easy vector (Promega) (Figure 19) and transformed into *E. coli* DH5α. The transformed clones carrying recombinant plasmids were screened by blue-white colonies. Plasmids were subsequently purified by the alkaline lysis method (Sambrook *et al.*, 1989), the positive clones were sent to sequencing by Macrogen, Korea.

10. Construction of recombinant plasmid for overexpression of type I PYK from *S. coelicolor*

The type I *pyk* gene of *S. coelicolor* was separated from pGEM®-T-Easy vector by double digestion with *Nde*I and *Xho*I. Then, isolated gene was ligated with pET-26b vector (Novagen) (Figure 20), overexpression vector, and transformed into *E. coli* BL21 (DE3) for overexpression. *E. coli* BL21 (DE3) carrying pET-26b which ligated with type I *pyk* gene from *S. coelicolor*, named pET-Scpyk, was cultured in LB contained 50 µg/ml kanamycin.

11. Computation of secondary structure and phylogenetic tree of PYK from *S. antibioticus* (SaPYK) and *S. coelicolor* (ScPYK)

The amino acid sequences of SaPYK and ScPYK were analyzed by multiple sequence alignment, phosphorylation site, phylogenetic tree construction and protein modeling. The multiple sequences alignment were constructed based on the known amino acid sequences of PYK from various organisms by ClustalW2 (Thompson *et al.*, 1994) and MUSCLE program (Edgar, 2004), and phylogenetic trees was constructed using the PhyML program (Guindon and Gascuel, 2003). The phosphorylation sites of the pyruvate kinase were determined by KinasePhos program (Huang *et al.*, 2005). The secondary and tertiary structures of the pyruvate kinase were predicted by the SWISS-MODEL program (Arnold *et al.*, 2006).

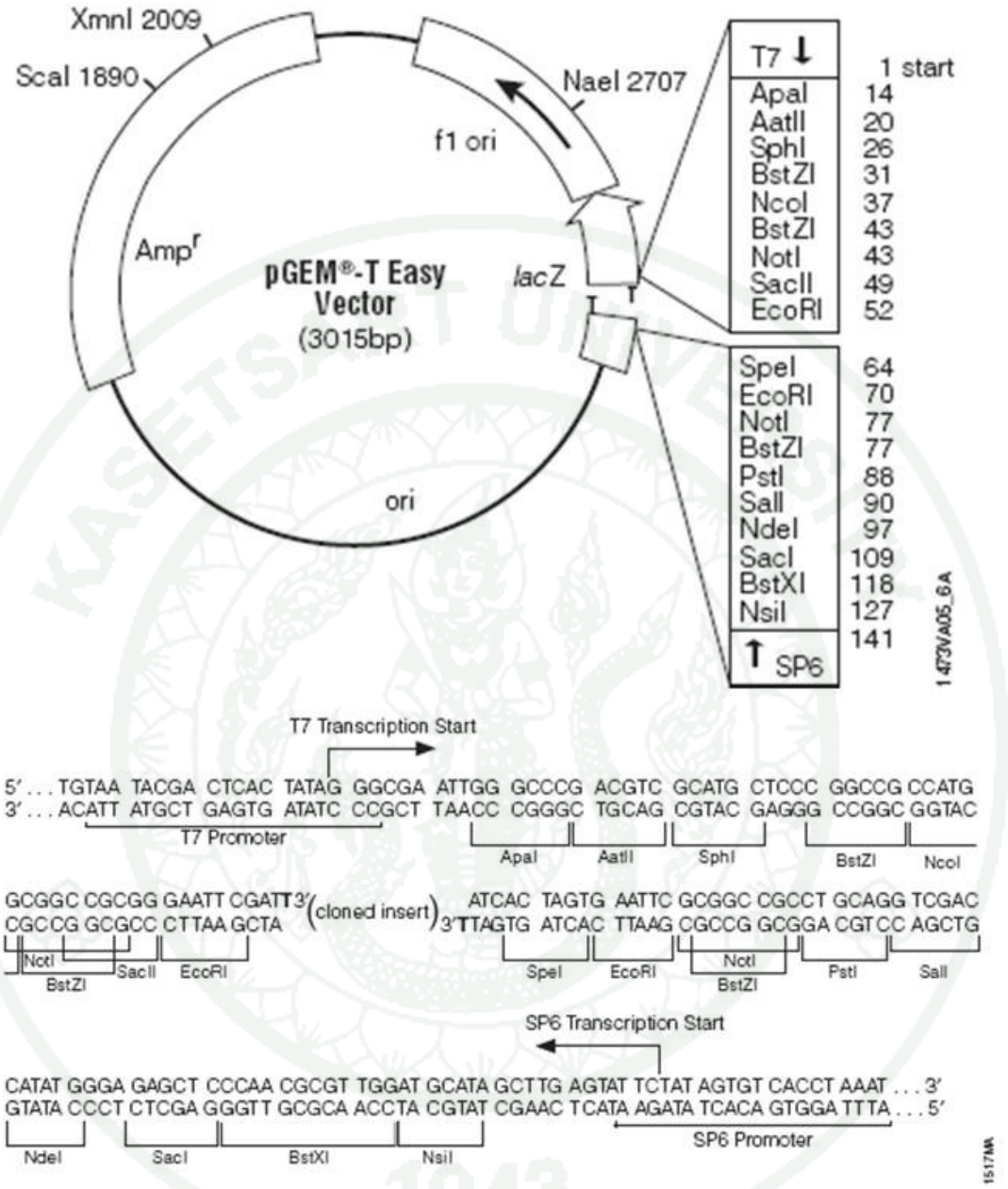

Figure 19 The plasmid map of pGEM®-T-Easy vector

Source: Promega (2010)

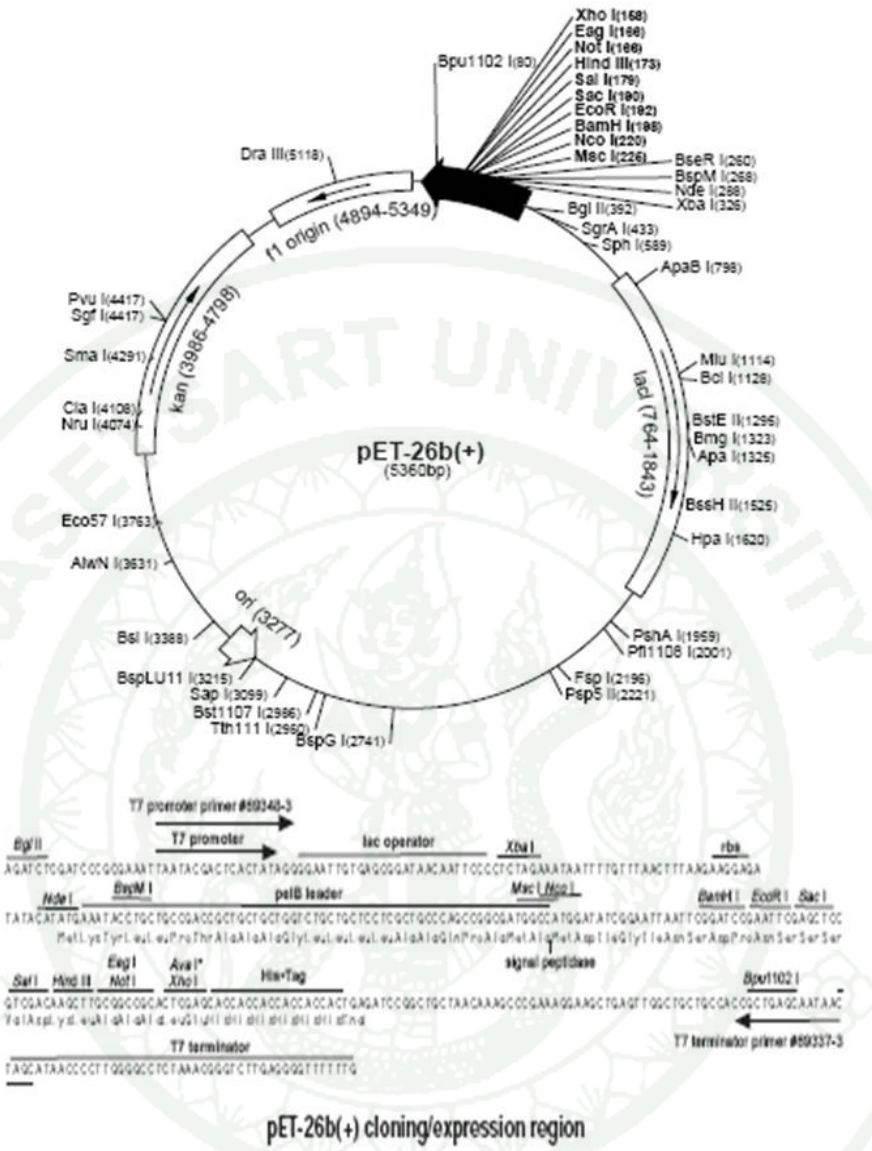

Figure 20 The plasmid map of pET-26b(+)

Source: Novagen (1992)

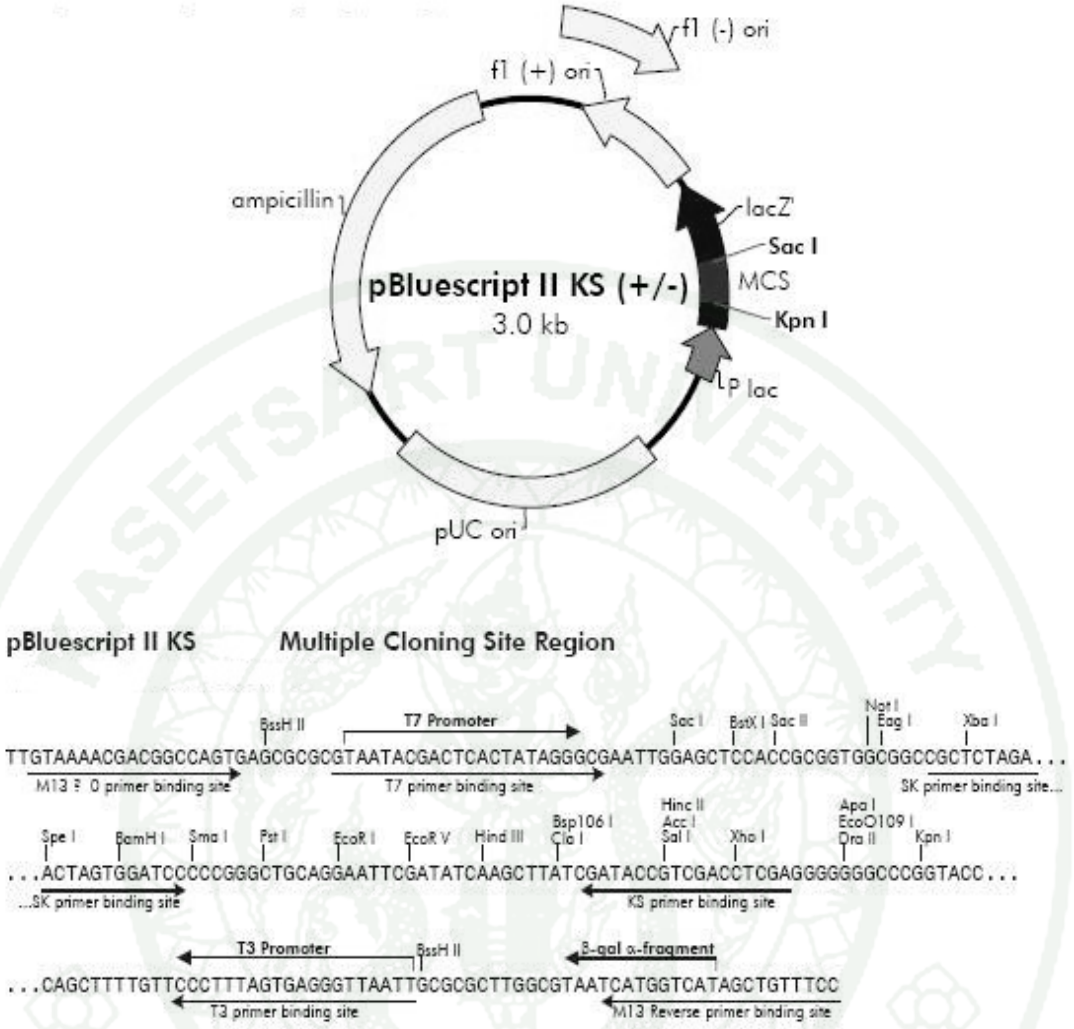

Figure 21 The plasmid map of pBluescript II KS

Source: Stratagene (2008)

12. Overexpression and purification of ADK of *E. coli* from *E. coli* BL21 (DE3) carrying pET-*adk*

E. coli BL21 (DE3) carrying pET-*adk*, a plasmid that over-expressed adenylate kinase (*adk* gene ligated with pET-26b(+)), constructed by member from our laboratory (Poopanitpan, 2005), was cultured in 50 ml of LB containing 50 µg/ml of kanamycin at 220 rpm, 37°C for overnight. After that, the cell culture was inoculated into 1 liter of fresh LB contained 50 µg/ml kanamycin and shaken at 220 rpm, 37°C. When OD_{600} reached 0.5, 1 mM lactose was added to induce the expression of recombinant ADK which had a polyhistidine tag at C-terminus of protein. After 5 hours of incubation, the induced cell was harvested by centrifugation at 5,000 rpm and stored at -20°C. All purification steps were carried out at 4°C. Cell pellets were resuspended in lysis buffer (20 mM Tris-HCl pH 8.0, 50 mM KCl, 0.5% Tween 20, 0.1% Triton X-100, 1 mM EDTA, 1 mM PMSF and 2 mM β-mercaptoethanol or BME). The suspension was sonicated for complete lyzed cell and centrifuged for 15 minutes at 10,000 rpm to separated supernatant. Streptomycin sulfate was added to the supernatant to the final concentration of 1% and the mixture was incubated on ice for 1-2 hours to precipitate DNA. The recombinant protein was isolate by DEAE column which equilibrated with buffer A (50 mM Tris-HCl pH 8.0 and 2 mM BME) and eluted with buffer A containing 20-100 mM KCl. The ADK was eluted by 50-70 mM KCl (Lu and Inouye, 1996). Purified protein was measured by Bradford method (Bradford, 1976) and analyzed by SDS-PAGE.

13. Overexpression and purification of CMK of *E. coli* from *E. coli* BL21 (DE3) carrying pET-*cmk*

E. coli BL21 (DE3) carrying pET-*cmk*, a plasmid that over-expressed cytidine monophosphate kinase (*cmk* gene ligated with pET-26b(+)), constructed by member from our laboratory (Howhan, 2004), was cultured in 50 ml LB containing 50 µg/ml of kanamycin at 220 rpm, 37°C for overnight. After overnight growth, this culture was inoculated into 1 liter of fresh LB containing 50 µg/ml of kanamycin and shaken at 220 rpm, 37°C. When OD_{600} reaches 0.5, lactose at the final concentration of 5 mM

was added to induce the expression of the polyhistidine tagged CMK. Cells were harvested after 4 hours by centrifugation at 5,000 rpm and storage at -20°C. All purification steps were carried out at 4 ^{o}C. The cell pellets were resuspended in lysis buffer (20 mM Tris-HCl pH 8.0, 50 mM KCl, 0.5% Tween 20, 0.1% Triton X-100, 1 mM EDTA, 1 mM PMSF and 2 mM BME). The suspension was sonicated for complete lyzed cell and centrifuged for 15 minutes at 10,000 rpm to separated supernatant. Streptomycin sulfate was added to the supernatant to the final concentration of 1% and the mixture was incubated on ice for 1-2 hours to precipitate DNA. The recombinant protein was isolated by Ni^{2+}-NTA column (Qiagen) which had been equilibrated with buffer B (20 mM Tris-HCl pH 8.0, 500 mM NaCl and 10 mM BME). The recombinant CMK was eluted with buffer B containing 100 mM imidazole. Purified protein was measured by Bradford method (Bradford, 1976) and analyzed by SDS-PAGE.

14. Overexpression and purification of DNK of bacteriophage T_4 from *E. coli* BL21 (DE3) carrying pET-T4dnk

E. coli BL21 (DE3) carrying pET-T4*dnk*, a plasmid that over-expressed deoxynucleoside monophosphate kinase (*dnk* gene ligated with pET-26b(+)), was constructed by member from our laboratory (Poopanitpan, 2005), was cultured in 50 ml of LB containing 50 µg/ml of kanamycin at 220 rpm, 37°C for overnight. After that, the cell culture was inoculated into 1 liter of fresh LB contained 50 µg/ml kanamycin and shaken at 220 rpm, 37°C. When OD_{600} reached 0.5, 1 mM lactose was added to induce the expression of recombinant DNK which had a polyhistidine tag at C-terminus of protein. After 5 hours of incubation, the induced cell was harvested by centrifugation at 5,000 rpm and stored at -20°C. All purification steps were carried out at 4°C. Cell pellets were resuspended in lysis buffer (20 mM Tris-HCl pH 8.0, 50 mM KCl, 0.5% Tween 20, 0.1% Triton X-100, 1 mM EDTA, 1 mM PMSF and 2 mM BME). The suspension was sonicated for complete lyzed cell and centrifuged for 15 minutes at 10,000 rpm to separated supernatant. The recombinant protein was isolate by Ni^{2+}-NTA column (Qiagen) which equilibrated with buffer C (20 mM Tris-HCl pH 8.0, 300 mM KCl and 10 mM BME). The recombinant DNK was eluted with buffer C

containing 100 mM imidazole. Purified protein was measured by Bradford method (Bradford, 1976) and analyzed by SDS-PAGE.

15. Overexpression and purification of type I PYK of *E. coli* from *E. coli* BL21 (DE3) carrying pGV5A

E. coli BL21 (DE3) carrying pGV5A, a plasmid that over-expressed *E. coli* type I pyruvate kinase (*pyk* gene ligated with pBluescript II KS), constructed by (Valentini *et al.*, 1997), was cultured in 50 ml LB containing 100 µg/ml of amplicillin at 220 rpm, 37°C for overnight. After overnight growth, this culture was inoculated into 1 liter of fresh LB containing 100 µg/ml of ampicillin and shaken at 220 rpm at 37°C. When OD_{600} reached 0.7, 0.6 mM IPTG was added to induce the expression of recombinant PYK. After 4 hours of incubation, the induced cell was harvested by centrifugation at 5,000 rpm and stored at -20°C. All purification steps were carried out at 4°C. Cell pellets were resuspended in lysis buffer (10 mM Tris-HCl pH 7.5, 100 mM KCl, 10 mM $MgCl_2$, 1 mM EDTA, 1 mM PMSF and 2 mM BME). The suspension was sonicated for complete lyzed cell and centrifuged for 15 minutes at 10,000 rpm to separated supernatant. Streptomycin sulfate was added to the supernatant to the final concentration of 1% and the mixture was incubated on ice for 1-2 hours to precipitate DNA. The recombinant protein was isolate by DEAE column which equilibrated with buffer D (50 mM Tris-HCl pH 7.5 and 2 mM BME) and eluted with buffer D containing 100-200 mM KCl. The pyruvate kinase was eluted by 150 mM KCl. Purified protein was measured by Bradford method (Bradford, 1976) and analyzed by SDS-PAGE.

16. Overexpression, purification and refolding of type I PYK of *S. coelicolor* from *E. coli* BL21 (DE3) carrying pET-Scpyk

E. coli BL21 (DE3) carrying pET-Scpyk cultured in 50 ml LB containing 50 µg/ml of kanamycin at 220 rpm, 37°C for overnight. After overnight growth, this culture was inoculated into 1 liter of fresh LB containing 50 µg/ml of kanamycin and shaken at 220 rpm at 37°C. When OD_{600} reached 0.7, 0.6 mM IPTG was added to

induce the expression of recombinant PYK. After 3 hours of incubation, the induced cell was harvested by centrifugation at 5,000 rpm and stored at -20°C. All purification steps were carried out at 4°C. Cell pellets were resuspended in lysis buffer (20 mM Tris-HCl pH 8.0, 50 mM KCl, 0.5% Tween 20, 0.1% Triton X-100, 1 mM EDTA, 1 mM PMSF and 2 mM BME). The suspension was sonicated for complete lyzed cell and centrifuged for 15 minutes at 10,000 rpm to separated Inclusion bodies. Inclusion bodies were washed five times with 50 mM Tris-HCl, pH 7.5, and 5 mM β-mercaptoethanol. The inclusion bodies were denatured with 4 M urea and incubated at 4°C for overnight. The denatured recombinant ScPYK was isolated by Ni^{2+}-NTA column. The denatured enzyme was refolded by dilution with buffer without urea (50 mM Tris-HCl pH 7.5, 100 mM KCl, 5 mM $MgCl_2$ and 5 mM BME) and incubated on ice for 3 hours (Price and Stevens, 1983). Purified protein was measured by Bradford method (Bradford, 1976) and analyzed by SDS-PAGE.

17. Assay activity of ADK

The activity of purified ADK was assayed by coupling to LDH and PYK (Figure 22). The reaction was initiated by the addition of purified ADK to the reaction mixture containing 50 mM Tris-HCl (pH 7.5), 50 mM KCl, 2 mM $MgCl_2$, 2 mM PEP, 1 mM ATP, 1 mM dAMP, 0.2 mM NADH, 1 U of LDH and PYK. The activity was monitored by measuring the decrease in absorbance at 340 nm on conversion of NADH to NAD^+ with UV-visible spectrophotometer.

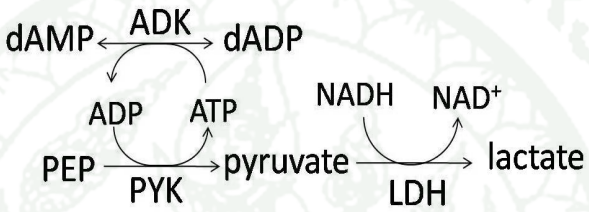

Figure 22 Diagram of assay activity of ADK. ADK, adenylate kinase; ADP, adenosine diphosphate; ATP, adenosine triphosphate; dAMP, deoxyadenosine monophosphate, dADP, deoxyadenosine diphosphate; LDH, lactate dehydrogenase; NAD^+, nicotinamide adenine dinucletide; NADH, nicotinamide adenine dinucleotide, reduced form; PEP, phosphoenolpyruvate; PYK, pyruvate kinase.

18. Assay activity of CMK

The activity of purified CMK was assayed by coupling to LDH and PYK (Figure 23). The reaction was initiated by the addition of purified CMK to the reaction mixture containing 50 mM Tris-HCl (pH 7.5), 50 mM KCl, 2 mM $MgCl_2$, 2 mM PEP, 1 mM ATP, 1 mM dCMP, 0.2 mM NADH, 1 U of LDH and PYK. The activity was monitored by measuring the decrease in absorbance at 340 nm on conversion of NADH to NAD^+ with UV-visible spectrophotometer.

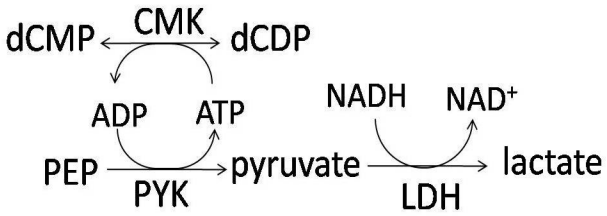

Figure 23 Diagram of assay activity of CMK. ADP, adenosine diphosphate; ATP, adenosine triphosphate; CMK, cytidine monophosphate kinase; dCMP, deoxycytidine monophosphate; dCDP, deoxycytidine diphosphate; LDH, lactate dehydrogenase; NAD^+, nicotinamide adenine dinucletide; NADH, nicotinamide adenine dinucleotide, reduced form; PEP, phosphoenolpyruvate; PYK, pyruvate kinase.

19. Assay activity of DNK

The activity of purified DNK was assayed by coupling to LDH and PYK (Figure 24). The reaction was initiated by the addition of purified DNK to the reaction mixture containing 100 mM Tris-HCl (pH 7.5), 100 mM KCl, 20 mM $MgCl_2$, 2 mM PEP, 1 mM ATP, 1.5 mM dGMP, 0.2 mM NADH, 1 U of LDH and PYK. The activity was monitored by measuring the decrease in absorbance at 340 nm on conversion of NADH to NAD^+ with UV-visible spectrophotometer.

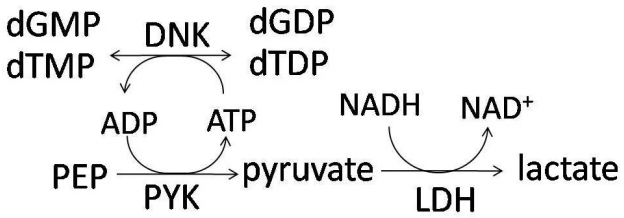

Figure 24 Diagram of assay activity of DNK. ADP, adenosine diphosphate; ATP, adenosine triphosphate; DNK, deoxynucleotides kinase; dGMP, deoxyguanosine monophosphate; dGDP, deoxyguanosine diphoaphate; dTMP, deoxythymidine monophosphate; dTDP, deoxythymidine diphosphate; LDH, lactate dehydrogenase; NAD^+, nicotinamide adenine dinucletide; NADH, nicotinamide adenine dinucleotide, reduced form; PEP, phosphoenolpyruvate; PYK, pyruvate kinase.

20. Assay activity of PYK

The activity of purified PYK was assayed by coupling to LDH (Figure 25). The reaction was initiated by the addition of purified PYK to the reaction mixture containing 50 mM Tris-HCl (pH 7.5), 50 mM KCl, 2 mM $MgCl_2$, 2 mM PEP, 2 mM ADP, 0.2 mM NADH, 1 U of LDH and PYK. The activity was monitored by measuring the decrease in absorbance at 340 nm on conversion of NADH to NAD^+ with UV-visible spectrophotometer.

Figure 25 Diagram of assay activity of PYK. ADP, adenosine diphosphate; ATP, adenosine triphosphate; LDH, lactate dehydrogenase; NAD^+, nicotinamide adenine dinucletide; NADH, nicotinamide adenine dinucleotide, reduced form; PEP, phosphoenolpyruvate; PYK, pyruvate kinase.

21. Enzymatic synthesis of dATP

Enzymatic synthesis of dATP from dAMP involves the use of two essential recombinant enzymes, ADK and PYK. The composition of buffer, salt, precursors and recombinant enzymes used in the synthesis are outlined in Figure 26. To determine which condition can be used to completely convert dAMP to dATP, enzymatic synthesis of dATP was performed at 10 mM, 20 mM, 60 mM and 100 mM dAMP in a total volume of 100 µl. As shown in the diagram, because two molecules of PEP are required to phosphorylate one molecule of dAMP to dATP, therefore, the stoichiometry of dAMP to PEP used in the reaction was maintained at a ratio of 1:2 (Figure 26). In addition, when higher concentration of dAMP was used in the synthesis, the amount of enzyme used in the synthesis also increased. Conditions used for synthesis of dATP starting with 10 mM, 20 mM, 60 mM and 100 mM dAMP were outlined in Table 5.

Table 5 The condition of enzymatic synthesis of dATP.

	10 mM-scale	20 mM-scale	60 mM-scale	100 mM-scale
Tris-HCl pH8.0 (mM)	100	100	100	100
KCl (mM)	50	50	200	200
$MgCl_2$ (mM)	20	20	100	100
PEP (mM)	20	40	120	200
dATP (mM)	0.3	0.3	0.5	0.5
dAMP (mM)	10	20	60	100
PYK (U)	5	6	8	10
ADK (U)	2	3	3.5	4

For instance, to synthesize dATP at 10 mM scale, 10 mM dAMP, 0.3 mM dATP, 20 mM PEP, PYK (5 U) and ADK (2 U) were added to buffer containing 100 mM Tris-HCl pH 8.0, 50 mM KCl, 20 mM $MgCl_2$ (total volume = 100 µl) and

incubated at 37°C for 3 hours. The products formed were analyzed on TLC and DEAE-cellulose column.

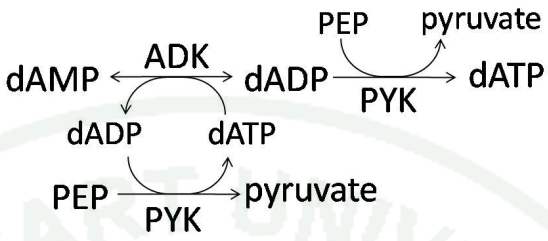

Figure 26 Diagram of dATP synthesis. ADK, adenylate kinase ; dAMP, deoxyadenosine monophosphate; dADP, deoxyadenosine diphosphate; dATP, deoxyadenosine triphosphate; PEP, phosphoenolpyruvate; PYK, pyruvate kinase

22. Enzymatic synthesis of dCTP

Enzymatic synthesis of dCTP from dCMP involves the use of two essential recombinant enzymes, CMK and PYK. The composition of buffer, salt, precursors and recombinant enzymes used in the synthesis are outlined in Figure 27. To determine which condition can be used to completely convert dCMP to dCTP, enzymatic synthesis of dCTP was performed at 10 mM, 20 mM, 60 mM and 100 mM dCMP in a total volume of 100 µl. As shown in the diagram, because two molecules of PEP are required to phosphorylate one molecule of dCMP to dCTP, therefore, the stoichiometry of CAMP to PEP used in the reaction was maintained at a ratio of 1:2 (Figure 27). In addition, when higher concentration of dCMP was used in the synthesis, the amount of enzyme used in the synthesis also increased. Conditions used for synthesis of dCTP starting with 10 mM, 20 mM, 60 mM and 100 mM dCMP were outlined in Table 6.

Table 6 The condition of enzymatic synthesis of dCTP.

	10 mM-scale	20 mM-scale	60 mM-scale	100 mM-scale
Tris-HCl pH8.0 (mM)	100	100	100	100
KCl (mM)	50	50	200	200
$MgCl_2$ (mM)	20	20	100	100
PEP (mM)	20	40	120	200
dCTP (mM)	0.3	0.3	0.3	0.5
dCMP (mM)	10	20	60	100
PYK (U)	5	6	9	10
CMK (U)	2	3	4.5	5

For instance, to synthesize dCTP at 10 mM scale, 10 mM dCMP, 0.3 mM dCTP, 20 mM PEP, PYK (5 U) and ADK (2 U) were added to buffer containing 100 mM Tris-HCl pH 8.0, 50 mM KCl, 20 mM $MgCl_2$ (total volume = 100 µl) and incubated at 37°C for 7 hours. The products formed were analyzed on TLC and DEAE-cellulose column.

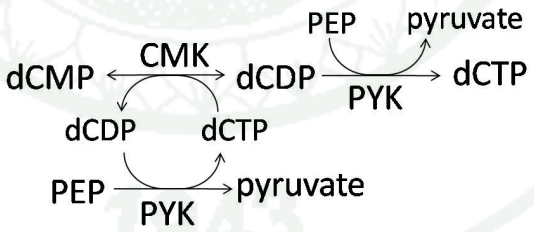

Figure 27 Diagram of dCTP synthesis. CMK, cytidine monophosphate kinase; dCMP, deoxycytidine monophosphate; dCDP, deoxycytidine diphosphate; dCTP, deoxycytidine triphosphate; PEP, phosphoenolpyruvate; PYK, pyruvate kinase.

23. Enzymatic synthesis of dGTP

Enzymatic synthesis of dGTP from dGMP involves the use of two essential recombinant enzymes, DNK and PYK, which had been purified from *E. coli* BL21 carrying the appropriated plasmid. The necessary precursors and recombinant enzymes used in the synthesis are outlined in Figure 28. To determine which condition can be used to completely convert dGMP to dGTP, enzymatic synthesis of dGTP was performed at 10 mM, 20 mM and 50 mM dGMP in a total volume of 100 µl. As shown in the diagram, because two molecules of PEP are required to phosphorylate one molecule of dGMP to dGTP, therefore, the stoichiometry of dGMP to PEP used in the reaction was maintained at a ratio of 1:2 (Figure 28). In addition, when a higher concentration of dGMP was used in the synthesis, a larger amount of enzyme was used. Conditions used for synthesis of dGTP starting with 10 mM, 20 mM and 50 mM dGMP were summarized in Table 7.

Table 7 The condition of enzymatic synthesis of dGTP.

	10 mM-scale	20 mM-scale	50 mM-scale
Tris-HCl pH8.0 (mM)	100	100	100
KCl (mM)	100	100	100
$MgCl_2$ (mM)	20	20	20
ATP (mM)	0.3	0.3	0.3
PEP (mM)	20	40	100
dGMP (mM)	10	20	50
PYK (U)	5	6	8
DNK (U)	2	3	4

For instance, to synthesize dGTP at 10 mM scale, 10 mM dGMP, 0.3 mM dGTP, 20 mM PEP, PYK (5 U) and DNK (2 U) were added to buffer containing 100 mM Tris-HCl pH 8.0, 100 mM KCl, 20 mM $MgCl_2$ (total volume = 100 µl) and incubated at 37°C for 24 hours. The products formed were analyzed on TLC and DEAE-cellulose column.

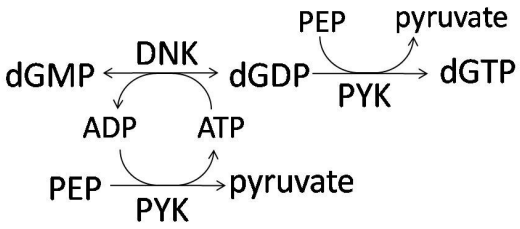

Figure 28 Diagram of dGTP synthesis. ADP, adenosine diphosphate ; ATP, adenosine triphosphate ; DNK, deoxynucleotides kinase; dGMP, deoxyguanosine monophosphate; dGDP, deoxyguanosine diphoaphate; dGTP, deoxyguanosine triphosphate; PEP, phosphoenolpyruvate; PYK, pyruvate kinase.

24. Enzymatic synthesis of dTTP in 10 mM-scale

Enzymatic synthesis of dTTP from dTMP, similar with enzymatic synthesis of dGTP, involves the use of two essential recombinant enzymes, DNK and PYK, which had been purified from *E. coli* BL21 carrying the appropriated plasmid. The necessary precursors and recombinant enzymes used in the synthesis are outlined in Figure 29. To determine which condition can be used to completely convert dTMP to dTTP, enzymatic synthesis of dTTP was performed at 10 mM dTMP in a total volume of 100 µl. The reaction mixture containing 10 mM dTMP, 0.3 mM dTTP, 20 mM PEP, 5 U of purified PYK and 2 U of purified DNK was incubated in 100 mM Tris-HCl pH 8.0, 100 mM KCl, 20 mM $MgCl_2$ (total volume = 100 µl) at 37°C for 24 hours. The products formed were analyzed on TLC and DEAE-cellulose column. As shown in the diagram, because two molecules of PEP are required to phosphorylate one molecule of dGMP to dGTP, therefore, the stoichiometry of dGMP to PEP used in the reaction was maintained at a ratio of 1:2 (Figure 29).

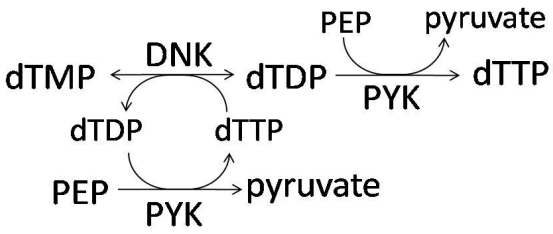

Figure 29 Diagram of dTTP synthesis. DNK, deoxynucleotides kinase; dTMP, deoxythymidine monophosphate; dTDP, deoxythymidine diphosphate; dTTP, deoxythymidine triphosphate; PEP, phosphoenolpyruvate; PYK, pyruvate kinase.

25. Separation of enzymatic synthesis of dNTP by chromatography

25.1 Anion exchange chromatography

After incubation, nucleotides in the reaction mixture were separated by DEAE-cellulose anion exchange chromatography. DEAE-cellulose column (1 cm diameter x 5 cm length) was washed with 10 ml of 1 M ammonium bicarbonate and 30 ml of water. The reaction was loaded onto the column and washed with 10 ml of water. After that, elution was carried out using 50, 100 and 150 mM triethylammonium bicarbonate (TEAB). Fraction of 1.5 ml was collected. And then, fractions were detected in absorbance at 260 nm.

25.2 Thin-layer chromatography (TLC)

PEI-cellulose plates were used to separate dNTPs. The 20 nmole of the samples were used applied in volumes of 1-3 µl approximately 1 cm apart and distance from the edge, and 1-1.5 cm above the bottom. The plates were dried by hot air and run vertically in close chambers with 0.3-0.5 cm of 0.7 M LiCl. The plates were identified under UV light at 254 nm and photographed.

RESULTS AND DISCUSSION

Pyruvate kinase (PYK) is an essential enzyme in metabolic pathway which is necessary for the survival of most organisms. Therefore, the physical properties of PYK, its catalytic mechanism and three-dimensional structure have been extensively studied by researchers over the decades. Many *pyk* genes had been identified and their sequences published. Although the nucleotide sequence of the *pyk* gene from *S. coelicolor* is available in the Genbank, the sequence of *pyk* gene from *S. antibioticus* remains unknown. Thus, one of the objectives in this study is to determine the nucleotide sequence of the *pyk* gene from *S. antibioticus*. The identification of unknown gene can be determined by various techniques depending on sources: genomic DNA or protein. Chromosomal walking techniques based on the PCR have been proved to be more successful as they are simple, less time consuming and low cost. Thus, putative *pyk* gene from *S. antibioticus* was determined by chromosomal walking PCR in this study. PYK is not only key enzyme in metabolism but also a significant enzyme used in the enzymatic synthesis of dNTP.

1. PYK from *S. antibioticus*

1.1 Determination of the putative *pyk* gene from *S. antibioticus*

In the first step, central region was determined by degenerate PCR. To amplify the *pyk* gene by PCR, a pair of degenerated primers was designed based on conserved regions of known *pyk* genes from various *Streptomyces* spp. After that, the DNA sequence encoding central region was sequenced. Base on the nucleotide sequence of known central region, two pairs of primers were designed and used to amplify the downstream and upstream regions of the *pyk* gene (Figure 30).

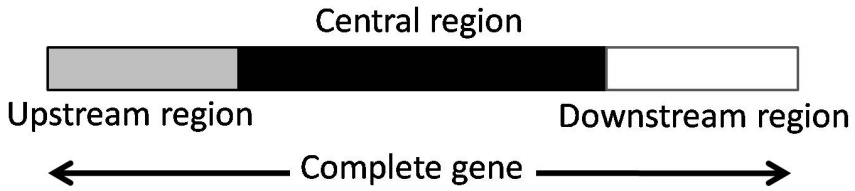

Figure 30 Outline for strategy of determination of complete encoding gene of putative *pyk* gene. Diagram shows three parts of putative *pyk* gene; upstream region (gray box), central region (black box) and downstream region (white box).

1.1.1 Determination of central region of putative *pyk* gene from *S. antibioticus* by degenerate PCR

The central region of putative *pyk* gene from *S. antibioticus* was amplified by PCR, using a pair of degenerated primers Sapyk-F and Sapyk-R, respectively. PCR product was separated on 1% agarose gel electrophoresis (Figure 31A). The 725 bp fragment was gel purified and ligated into pGEM-T-Easy vector. The obtained recombinant 3.7 kb plasmid, named pGEM-cenSapyk, was sequenced (Figure 31B). The nucleotide sequence of central region of putative *pyk* gene was the highest similar with *pyk* gene in region 7.39 Mb from *S. hygroscopicus* subsp. *jinggangensis* 5008 (GenBank Accession Number#YP_006247639) (94% identity) and type II *pyk* gene from *S. coelicolor* (GenBank Accession Nuber#NP_629562) (92% identity) (Figure 32).

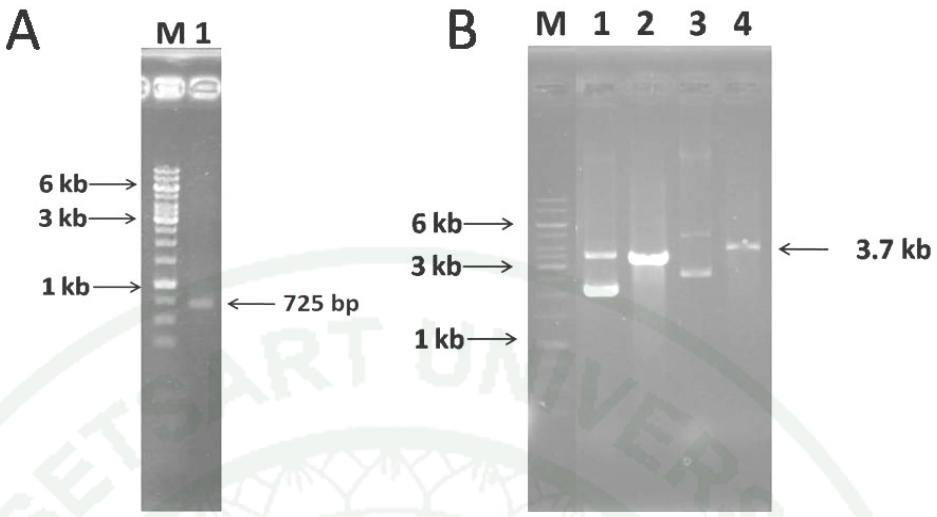

Figure 31 Agarose gel electrophoresis of determination of central region of putative *pyk* gene from *S. antibioticus*. (A) The PCR amplicon after amplification of central region of putative *pyk* gene from *S. antibioticus* by Sapyk-F and Sapyk-R. Lane M, DNA ladder; lane 1, PCR amplicon after amplification of central region of putative *pyk* gene. (B) The digestion of recombinant pGEM-cenSapyk. Lane M, DNA ladder; lane 1, undigested pGEM-T-Easy vector; lane 2, digested pGEM-T-Easy vector with *Nde*I; lane 3, undigested pGEM-cenSapyk; lane 4, digested pGEM-cenSapyk with *Nde*I.

```
  1   TCTCCGACCACAAGGGCCTCAACCTGCCCGGCGCGGCCGTGAACGTGCCCGCGCTGAGCG
  1     S  D  H  K  G  L  N  L  P  G  A  A  V  N  V  P  A  L  S  E
 61   AGAAGGACGTCGAGGACCTGCGCTTCGCCCTCCGCATGGGCTGCGACATGGTCGCGCTGT
 21     K  D  V  E  D  L  R  F  A  L  R  M  G  C  D  M  V  A  L  S
121   CCTTCGTCCGGGACGCCAAGGACATCCAGGACGTGCACCGCGTCATGGACGAGGAGGGCC
 41     F  V  R  D  A  K  D  I  Q  D  V  H  R  V  M  D  E  E  G  R
181   GCCGCGTCCCCGTCATCGCCAAGGTGGAGAAGCCGCAGGCGGTGGAGAACATGGAGGACG
 61     R  V  P  V  I  A  K  V  E  K  P  Q  A  V  E  N  M  E  D  V
241   TCGTCGCGGCGTTCGACGCGGTGATGGTCGCCCGTGGTGACCTCGCCGTCGAGTACCCGC
 81     V  A  A  F  D  A  V  M  V  A  R  G  D  L  A  V  E  Y  P  L
301   TCGAAAAGGTCCCCATGGTGCAGAAGCGCCTGATCGAGCTGTGCCGGCGCAACGCCAAGC
101     E  K  V  P  M  V  Q  K  R  L  I  E  L  C  R  R  N  A  K  P
361   CCGTGATCGTCGCGACCCAGATGATGGAGTCGATGATCACCAACTCCCGGCCGACCCGCG
121     V  I  V  A  T  Q  M  M  E  S  M  I  T  N  S  R  P  T  R  A
421   CCGAGGCCTCGGACGTGGCCAACGCGATCCTGGACGGCGCCGACGCGGTCATGCTGTCGG
141     E  A  S  D  V  A  N  A  I  L  D  G  A  D  A  V  M  L  S  A
481   CCGAGTCCTCGGTGGGCGCGTACCCGGTCGAGACGGTCAAGACCATGTCGAAGATCGTCA
161     E  S  S  V  G  A  Y  P  V  E  T  V  K  T  M  S  K  I  V  T
541   CCGCGGCCGAGCAGGAGCTGCTGTCCAAGGGTCTGCAGCCGCTGGTGCCGGGCAAGAAGC
181     A  A  E  Q  E  L  L  S  K  G  L  Q  P  L  V  P  G  K  K  P
601   CGCGCACCCAGGGCGGTTCGGTGGCCCGCGCGGCCTGCGAGATCGCCGACTTCCTCGGCG
201     R  T  Q  G  G  S  V  A  R  A  A  C  E  I  A  D  F  L  G  G
661   GCAAGGGCCTGATCGCGTTCACCAAGTCCGGTGACACCGCGCGCCGGCTCTCCCGCTATC
221     K  G  L  I  A  F  T  K  S  G  D  T  A  R  R  L  S  R  Y  R
721   GAATC
241     I
```

Figure 32 The nucleotide and deduced amino acid sequence of central region of putative *pyk* gene from *S. antibioticus*. Left column; nucleotide and deduced amino acid sequence number.

1.1.2 Determination of upstream region of putative *pyk* gene from *S. antibioticus*

Based on known nucleotide sequence of the central region of putative *pyk* gene from previous experiment, four specific primers were designed accordingly and used to amplify upstream and downstream regions of the *pyk* gene. For upstream region, nucleotide sequence of 5'-terminal region of putative *pyk* gene is conservation. Thus, amplification of upstream region of putative *pyk* gene was used forward primer for amplify *pyk* gene from *S. coelicolor* or Scpyk-F for amplified with reverse primer that was based on nucleotide sequence from central region or Sapyk-5R. The obtained PCR product was a single band of approximately 624 bp (Figure 33A). The PCR product was ligated with pGEM-T-Easy vector, named pGEM-SapykN with the size of approximately 3.6 kb (Figure 33B). The nucleotide sequence of upstream region of

pyk gene was the highest similar with *pyk* gene in region 7.39 Mb from *S. hygroscopicus* subsp. *jinggangensis* 5008 (GenBank Accession Number#YP_006247639) (95% identity) and type II *pyk* gene from *S. coelicolor* (GenBank Accession Nuber#NP_629562) (90% identity) (Figure 34).

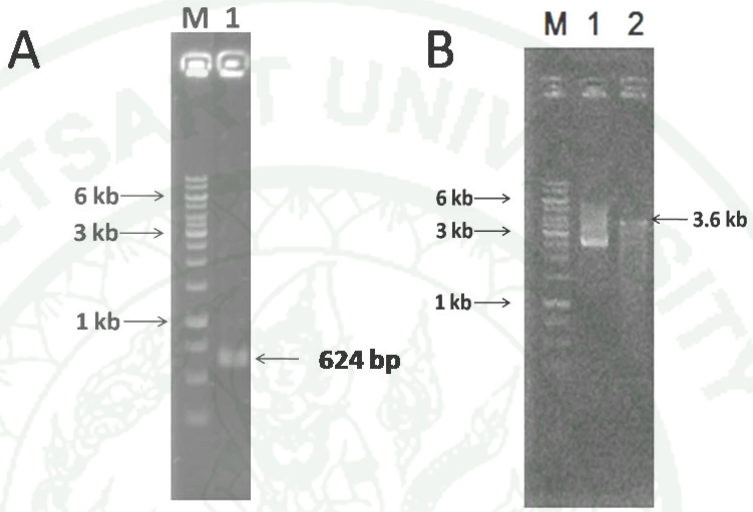

Figure 33 Agarose gel electrophoresis of determination of upstream region of putative *pyk* gene from *S. antibioticus.* (A) The PCR amplicon after amplification of upstream region of the putative *pyk* gene from *S. antibioticus*. Lane M, DNA ladder; lane 1, PCR product from amplification using specific Scpyk-F and Sapyk-5R primers. (B) The digestion of recombinant pGEM-SapykN. Lane M, DNA ladder; lane 1, undigested pGEM-SapykN; lane 2, digested pGEM-SapykN with *Nde*I.

```
   1  ATGCGCCGAGCAAAGATCGTCTGCACTCTCGGCCCCGCGGTCGACTCCCACGAGATGCTC
   1  M  R  R  A  K  I  V  C  T  L  G  P  A  V  D  S  H  E  M  L
  61  GTCGCCATGATCGAGGCGGGCATGAACGTAGCCCGCTTCAACTTCAGCCACGGCACCCAC
  21  V  A  M  I  E  A  G  M  N  V  A  R  F  N  F  S  H  G  T  H
 121  GCTGAGCACCAGGCGCGGTACGACCGCGTCCGGGCCGCGTCCAAGGAGACCGGCCGCCCC
  41  A  E  H  Q  A  R  Y  D  R  V  R  A  A  S  K  E  T  G  R  P
 181  ATCGGCGTCCTCGCCGACCTCCAGGGCCCGAAGATCCGTCTGGAGACCTTCGCCGAGGGT
  61  I  G  V  L  A  D  L  Q  G  P  K  I  R  L  E  T  F  A  E  G
 241  CCGGTCGAGCTGGAGCGCGGTGACGAGTTCGTCATCACGACCGAGGACGTGCCGGGCGAC
  81  P  V  E  L  E  R  G  D  E  F  V  I  T  T  E  D  V  P  G  D
 301  AAGCACATCTGCGGTACGACGTACAAGGGGCTGCCGGGCGATGTCTCGCGCGGCGACCAG
 101  K  H  I  C  G  T  T  Y  K  G  L  P  G  D  V  S  R  G  D  Q
 361  GTCCTGATCAACGACGGCAACGTCGAACTGAAGGTCCTGGACGTCGAGGGCCCGCGGGTG
 121  V  L  I  N  D  G  N  V  E  L  K  V  L  D  V  E  G  P  R  V
 421  CGGACGATCGTCATCGAGGGCGGTGTCGTCTCCGACCACAAGGGCATCAACCTGCCCGGC
 141  R  T  I  V  I  E  G  G  V  V  S  D  H  K  G  I  N  L  P  G
 481  GCGGCCGTGAACGTGCCCGCGCTGAGCGAGAAGGACGTCGAGGACCTGCGCTTCGCCCTC
 161  A  A  V  N  V  P  A  L  S  E  K  D  V  E  D  L  R  F  A  L
 541  CGCATGGGCTGCGACATGGTCGCGCTGTCCTTCGTCCGGGACGCCAAGGACATCCAGGAC
 181  R  M  G  C  D  M  V  A  L  S  F  V  R  D  A  K  D  I  Q  D
 601  GTGCACCGCGTCATGGACGAGGAG
 201  V  H  R  V  M  D  E  E
```

Figure 34 The nucleotide and deduced amino acid sequence of upstream region of putative *pyk* gene from *S. antibioticus*. Left column; nucleotide and deduced amino acid sequence number.

1.1.3 Determination of downstream region of putative *pyk* gene from *S. antibioticus*

The downstream region of the putative *pyk* gene was determined by semi-random PCR chromosomal walking. Because multiple sequence alignment showed that the C-ternimus of *pyk* gene is not conserved, therefore the reverse primer which designed according to the *pyk* sequence *S. coelicolor* cannot be used for amplification of the *pyk* gene from *S. antibioticus*. Thus, the *pyk* gene from *S. antibioticus* was amplified by PCR, using random primer from Promega and forward primer designed from central region of putative *pyk* gene. When the PCR products were analyzed on agarose gel, two bands of approximately 0.8 kb and 1.5 kb were observed (Figure 35).

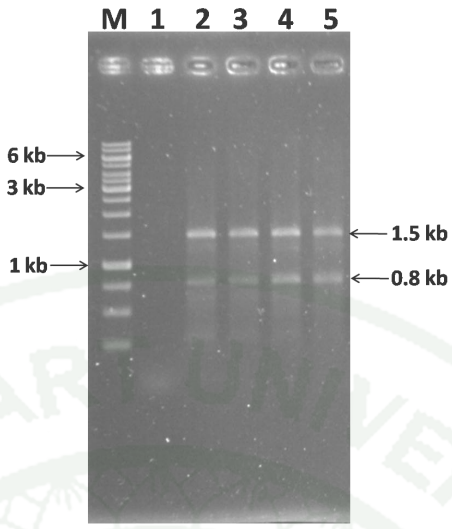

Figure 35 Agarose gel electrophoresis of PCR amplicon after amplification of downstream region of putative *pyk* gene from *S. antibioticus* by Sapyk-3F and random primer. Lane M, DNA ladder; lane 1, non template as negative control, lane 2-5, PCR products from annealing temperatures in PCR condition as 50.7°C, 52.9°C, 56.4°C and 58.7°C, respectively.

These two fragments were gel purified and ligated into pGEM-T-Easy vector, resulting in two new recombinant plasmids with the 0.8 kb and 1.5 kb inserts. These recombinant plasmids were designated as pGEM-Sapyk0.8kb and pGEM-Sapyk1.5kb, respectively. The recombinant plasmids were length of approximately 3.8 kb and 4.5 kb for pGEM-Sapyk0.8kb and pGEM-Sapyk1.5kb, respectively (Figure 36).

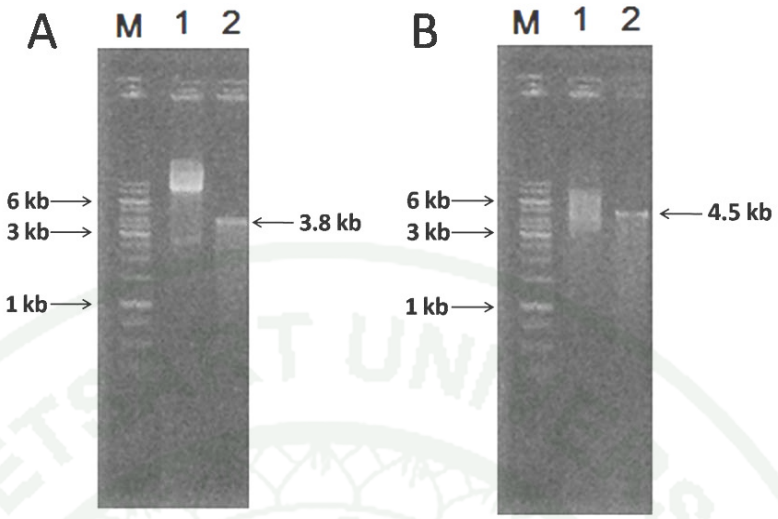

Figure 36 Agarose gel electrophoresis of digestion of recombinant (A) pGEM-Sapyk0.8kb and (B) pGEM-Sapyk1.5kb. Lane M, DNA ladder; lane 1, undigested recombinant plasmids; lane 2, digested recombinant plasmids with *Nde*I.

The nucleotide sequence of the putative *pyk* gene in the recombinant plasmids was determined by amplification of overlapping region region with Sapyk-3F and Sapyk-R as forward and reverse primers. The recombinant pGEM-Sapyk1.5kb was given PCR product in single band of approximately 150 bp (Figure 37, lane 5).

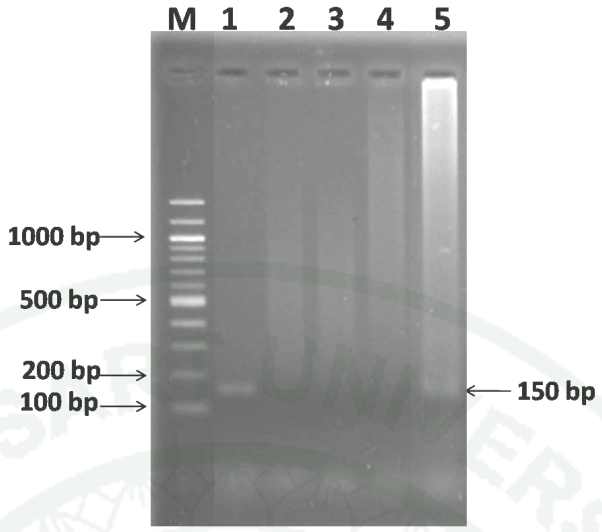

Figure 37 Agarose gel electrophoresis of PCR amplicon after amplification of overlapping site from recombinant plasmids for checking. Lane M, DNA ladder; lane 1, positive control by gDNA from *S. antibioticus* as template; lane 2, negative control by pGEM-T-Easy vector as template; lane 3, pGEM-Sapyk0.8kb as template; lane 4, negative control by pGEM-T-Easy vector as template; lane 5, pGEM-Sapyk1.5kb as template

Thus, pGEM-Sapyk1.5 was sequenced and the obtained nucleotide sequence was analyzed using BLAST program. The result showed that DNA fragment contained three different genes; an incomplete downstream region of the putative *pyk* gene (1-418 nucleotide residues), conserved hypothetical gene (419-953 nucleotide residues) and two-component system response regulator gene (954-1,500 nucleotide residues) (Figure 38).

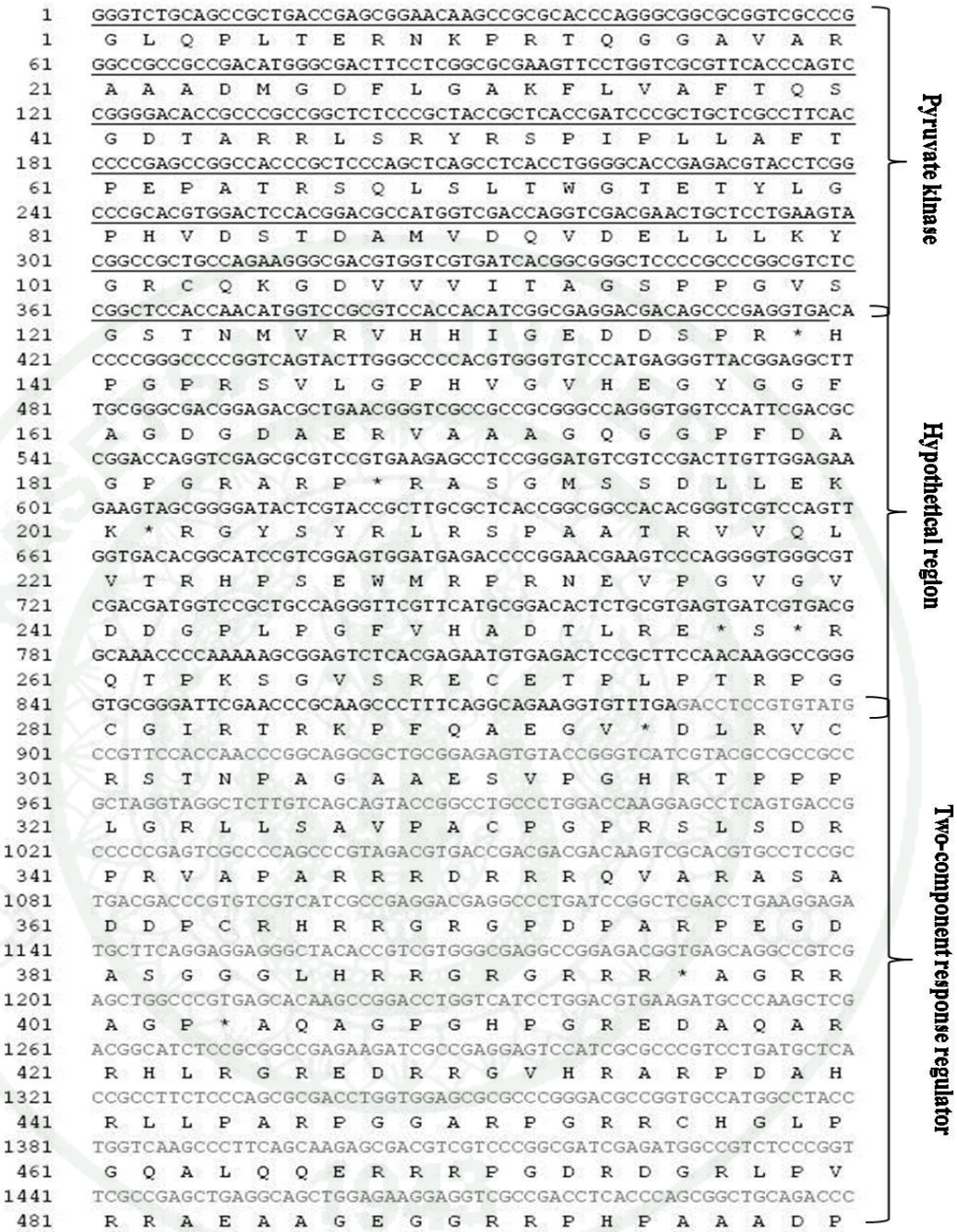

Figure 38 The nucleotide and deduced amino acid sequence of PCR fragment from amplification of downstream region of putative *pyk* gene from *S. antibioticus*. Underline showed the coding region of putative type I *pyk* gene. The hypothetical gene and two-component response regulator gene are black and gray alphabets, respectively. Left column; nucleotide and deduced amino acid sequence number.

Surprisingly, downstream region of putative *pyk* gene from pGEM-Sapyk1.5kb was not combined with central and upstream regions in previous experiments (Figure 39). The analyzed nucleotide sequence showed that putative *pyk* gene from downstream region was different type with central and upstream regions. The putative *pyk* genes from *S. antibioticus* were identified based on *pyk* genes from *S. coelicolor*. The downstream region is putative type I *pyk* gene, but central and upstream regions are putative type II *pyk* gene (Figure 40).

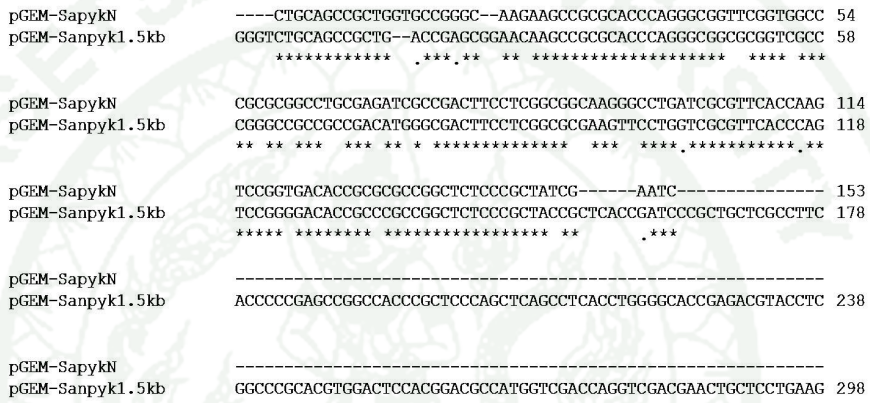

Figure 39 Analysis of comparison of nucleotide sequence of downstream region and central region for putative *pyk* gene from *S. antibioticus* by nucleotide sequences alignment. pGEM-SapykN as nucleotide sequence of central region and pGEM-Sapyk1.5kb as nucleotide sequence of downstream region.

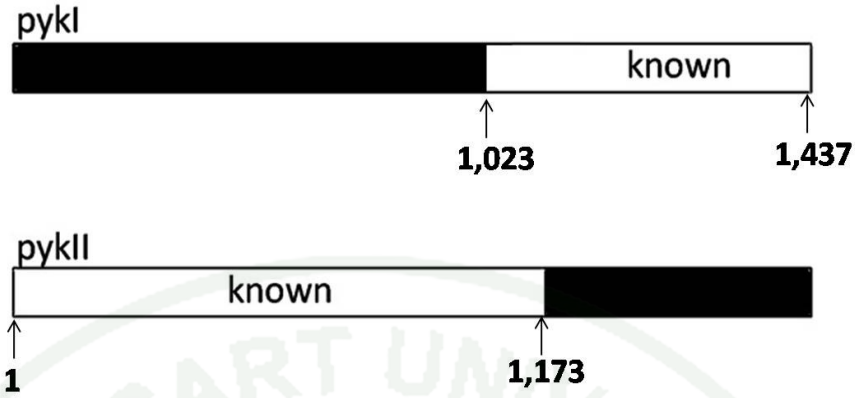

Figure 40 Diagram of known gene sequences for putative *pyk* genes from *S. antibioticus*. The putative type I *pyk* gene is known 1,023 to 1,437 nucleotides residues and putative type II *pyk* gene is know 1 to 1,173 nucleotide residues. The black box represents region where the nucleotide sequence had been determined and the white box was known region.

The full-length of putative type I *pyk* gene was identified by amplification using forward primer for amplify *pyk* gene from *S. coelicolor* or Scpyk-F for amplified with reverse primer that was based on nucleotide sequence from downstream region or SapykIR. On the other hand, the full-length of putative type II *pyk* gene cannot be identified because the 3'-terminal region is not conserved. And we tried to find the downstream region of putative type II *pyk* gene from *S. antibioticus* by inverse PCR (Ochman *et al.*, 1988) and two-step gene walking method (Pilhofer *et al.*, 2007), but this was unsuccessful (data not shown). Thus, the putative type II *pyk* gene from *S. antibioticus* can identified only to the partial sequence, was 1,173 nucleotides and 208 deduced amino acid residues (Figure 41).

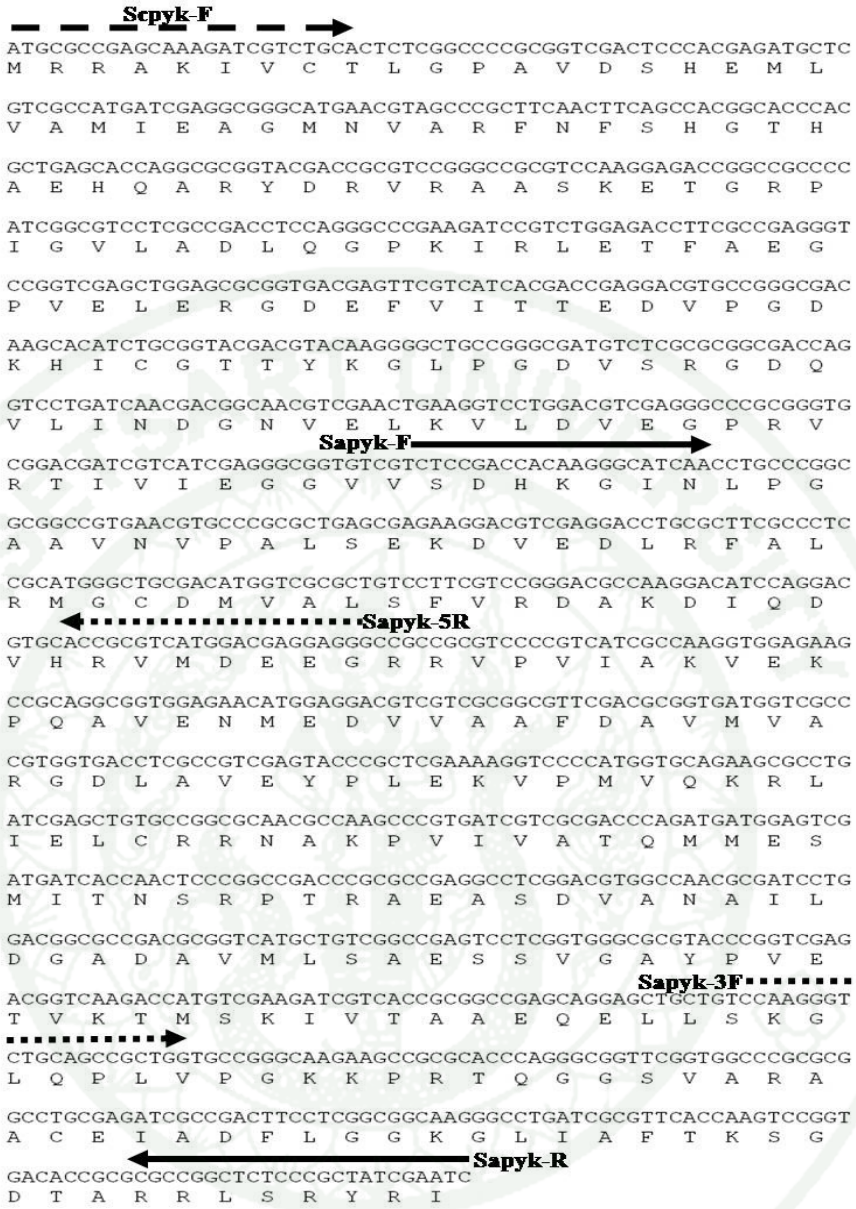

Figure 41 The partial nucleotide and deduced amino acid sequence of the putative type II *pyk* gene from *S. antibioticus*. The arrows above the sequences show the position where complementary primers will anneal during amplifications. Primers that anneal to the central region are shown as solid arrows; primers that will anneal to the upstream and downstream regions are shown as round dot arrows; primer that will anneal to the upstream region shows dash arrow. Left column; nucleotide and deduced amino acid sequence number.

1.1.4 Determination of full-length of putative type I *pyk* gene from *S. antibioticus*

Based on the known nucleotide sequence of downstream region of putative *pyk* gene, the reverse primer was subsequently synthesized and used to amplify the complete *pyk* gene. The forward primer used for amplification was the same primer used in amplification of the *pyk* gene from *S. coelicolor*, namely Scpyk-F. When PCR products were analyzed by 1% agarose gel, a single band that migrated with size of approximately 1.5 kb was observed (Figure 42A).

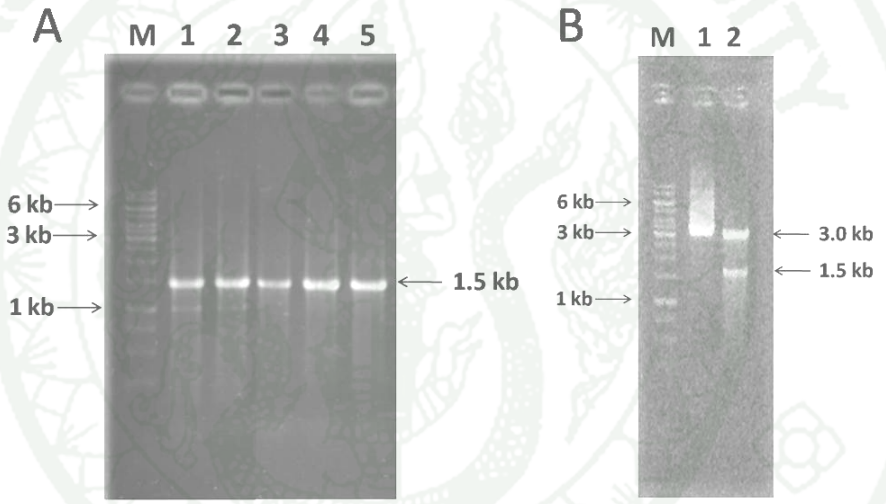

Figure 42 Agarose gel electrophoresis of determination of full-length of putative type I *pyk* gene from *S. antibioticus*. (A) The PCR amplicon after amplification of full-length of putative type I *pyk* gene from *S. antibioticus* by using Scpyk-F and SapykIR. Lane M, DNA ladder; lane 1-5, PCR products from 53.7°C, 54.3°C, 57.7°C, 59.4°C and 60.2°C as annealing temperatures, respectively. (B) The digestion of recombinant pGEM-SapykI. Lane M, DNA ladder; lane 1, undigested pGEM-SapykI; lane 2, digested pGEM-SapykI with *Nde*I.

After the PCR product was ligated with pGEM-T-Easy vector, the obtained 4.5 kb recombinant plasmid was designated as pGEM-SapykI. In Figure 46, digestion of recombinant pGEM-SapykI by *Nde*I observed two DNA bands on 1% agarose gel, 3.0 kb and 1.5 kb (Figure 42B), because both of insert gene and pGEM-T-Easy contain restriction site for *Nde*I. The nucleotide sequence of putative type I *pyk* gene from *S. antibioticus* was the highest similar with *pyk* gene in region 10.14 Mb from *S. hygroscopicus* subsp. *jinggangensis* 5008 (GenBank Accession Number #YP_006244633) and type I *pyk* gene from *S. coelicolor* (GenBank Accession Number#NP_626275) which had 96% and 88% identity, respectively. The encoding of putative type I *pyk* gene of *S. antibioticus* was 1,437 nucleotides and deduced amino acid sequence was 478 residues (Figure 43).

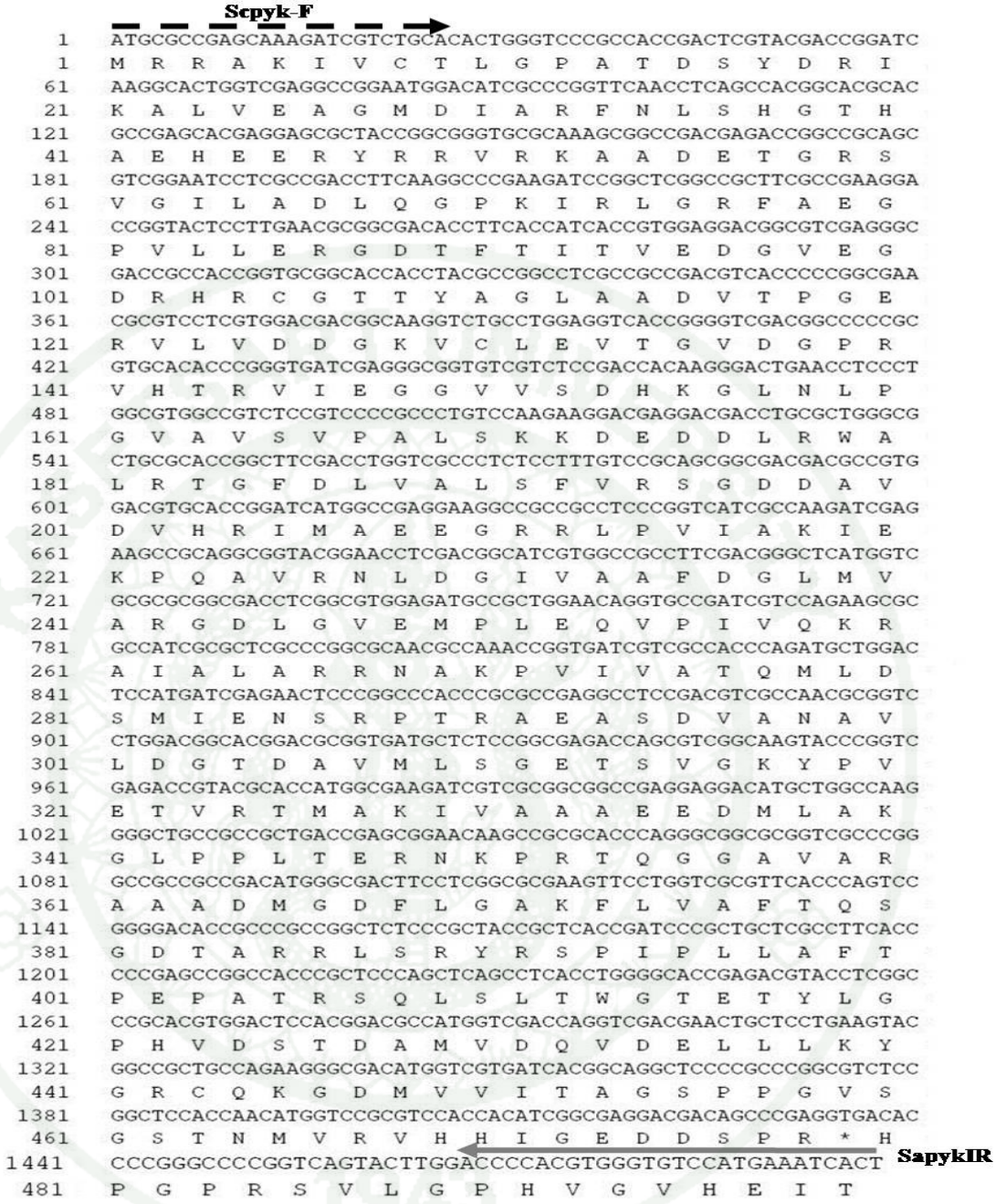

Figure 43 The nucleotide and deduced amino acid sequence of the putative type I *pyk* gene from *S. antibioticus*. The arrows above the sequences show the position where complementary primers anneal during amplifications. Forward and reverse primers that will anneal to the putative type I *pyk* gene are shown as black dash and gray solid arrow, respectively. Left column; nucleotide and deduced amino acid sequence number.

1.2 The prediction of secondary structure of type I PYK from *S. antibioticus*

The deduced amino acid sequence of type I PYK from *S. antibioticus* (SaPYK) contained 478 residues. Three-dimensional modeling of type I SaPYK monomer based on deduced amino acid sequence by SWISS-MODEL was showed in Figure 48. The predicted structure modeling of type I SaPYK is highly structural homology with PYK from *B. stearothermophilus* (PDB#2E28) which had 43% identity (C-alpha root mean square deviation, 0.48 Å). The structure contained to three domains: A, B and C domains. Domain A was formed by two separated stretches of amino acids, residues 1–69 and 166–335, that fold together to form a TIM barrel motif with two additional α helices. This domain was supposed to contain the catalytic site. Domain B was formed a small seven-stranded β-barrel motif with a additional α helix, comprising residues 70-165, that formed a cap over the active site at domain A. Domain C was formed to open-sheet motif, and included residues 335–478 (Figure 44 and 45). In addition, kinetic studies of PYK from *B. stearothermophilus* was activated by AMP and amino acid residues which effector binding sites were indicated that Trp416 and His425, corresponding to Trp413 and His422 in SaPYK, are important for effector specificity (Munoz and Ponce, 2003; Suzuki *et al.*, 2008). The type I SaPYK may be activated by AMP.

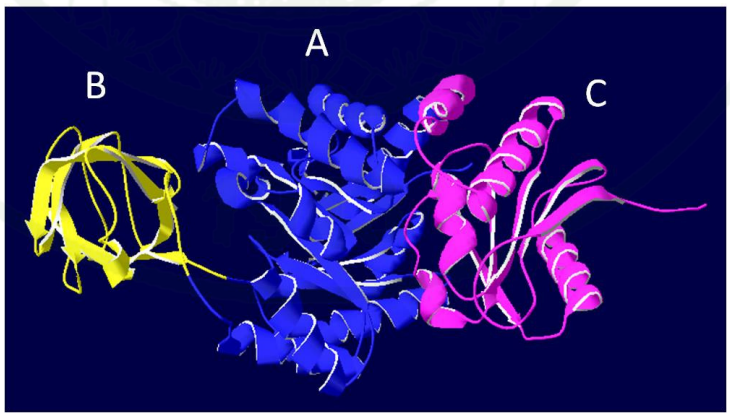

Figure 44 Cartoon diagram of the predicted structure model of type I SaPYK. The structure was similar to PYK from *B. stearothermophilus* (PDB#2E28). Domains A, B and C are shown in blue, yellow and magenta, respectively.

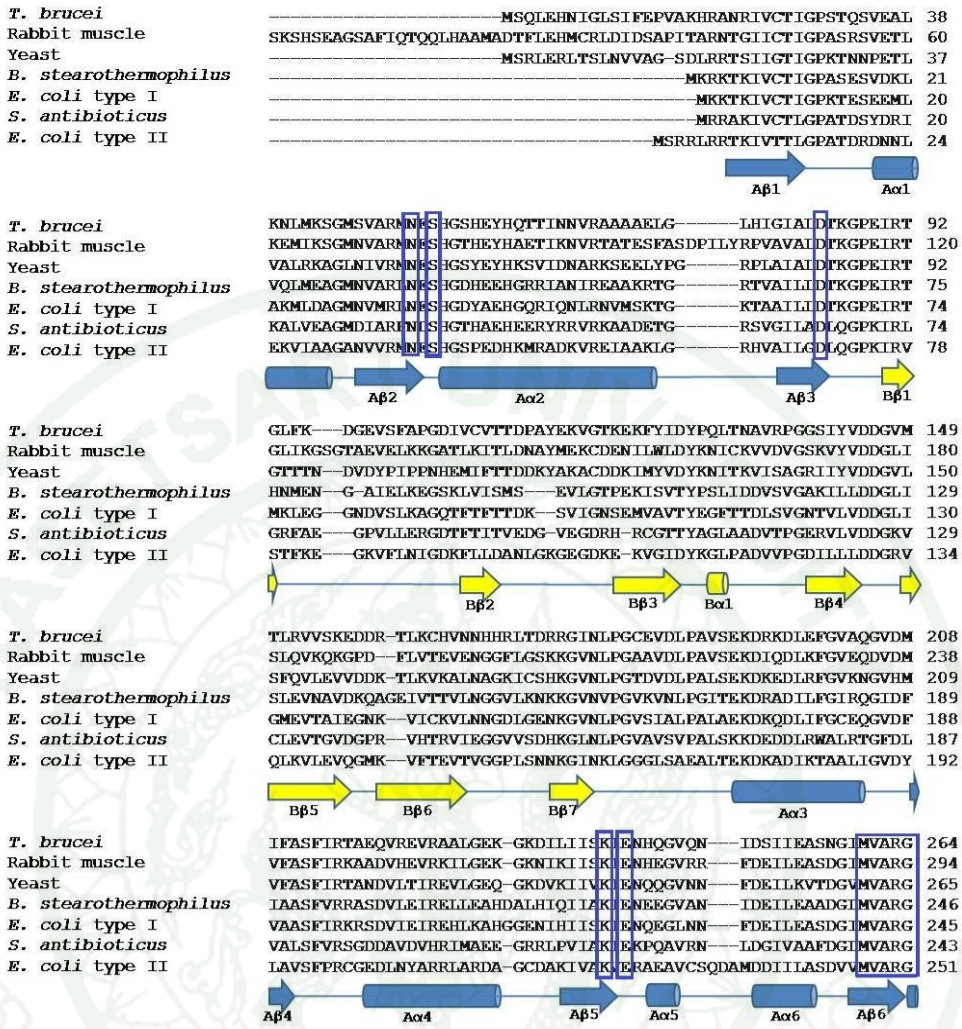

Figure 45 The multiple sequence alignment and predicted secondary structure of type I SaPYK. The organisms and accession numbers for the amino acid sequences are: *B. stearothermophilus* (BAA02406), *E. coli*, type I (AAB47952), *E. coli*, type II (YP_490116), *Oryctolagus cuniculus*, rabbit muscle (AAC48536), *Saccharomyces cerevisiae*, yeast (CAA24631) and *T. brucei* (CAA41018). The α-helice, β-sheets and lines were shown as rolls, arrows and loops, respectively. The domain A, B and C of were shown as blue, yellow and magenta, respectively. The substrate and metal binding sites were shown in blue boxes and effector binding sites were shown in orange boxes. The amino acid residues of type I SaPYK were corresponding with effector binding sites of PYK from *B. stearothermophilus* which are showed as orange arrows.

Figure 45 (Continued)

2. PYK from *S. coelicolor*

2.1 Determination of type I *pyk* gene from *S. coelicolor*

The type I *pyk* from *S. coelicolor* (GenBank Accession Number#NP_626275) was amplified by specific primers, Scpyk-F and Scpyk-R. When the obtained PCR product was analyzed by 1% agarose gel electrophoresis, a single band of approximately 1.4 kb was observed (Figure 46A). This PCR product was gel purified and ligated into pGEM-T-Easy vector, resulting in a 4.4 kb recombinant plasmid designated as pGEM-Scpyk. The spacer region was closely distance between two *Nde*I sites. Insert gene and vector were not separated (Figure 46B, lane 4). Then, the insert gene in recombinant plasmid was sequenced (Figure 47).

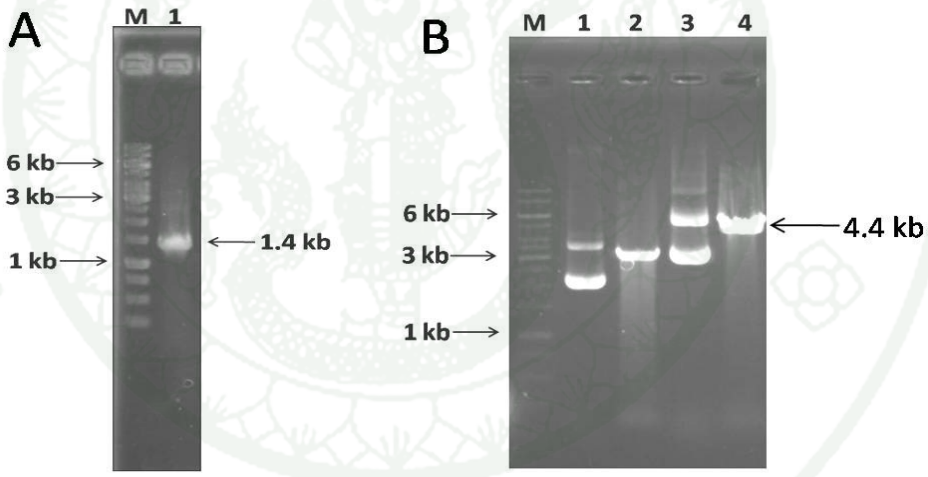

Figure 46 Agarose gel electrophoresis of determination of type I *pyk* gene from *S. coelicolor*. (A) The PCR amplicon after amplification of type I *pyk* gene from *S. coelicolor*. Lane M, DNA ladder; lane 1, PCR product. (B) The digestion of recombinant pGEM-Scpyk. Lane M, DNA ladder; lane 1, undigested pGEM-T-Easy vector as negative control; lane 2, digested pGEM-T-Easy vector with *Nde*I as negative control; lane 3, undigested pGEM-Scpyk; lane 4, digested pGEM-Scpyk with *Nde*I.

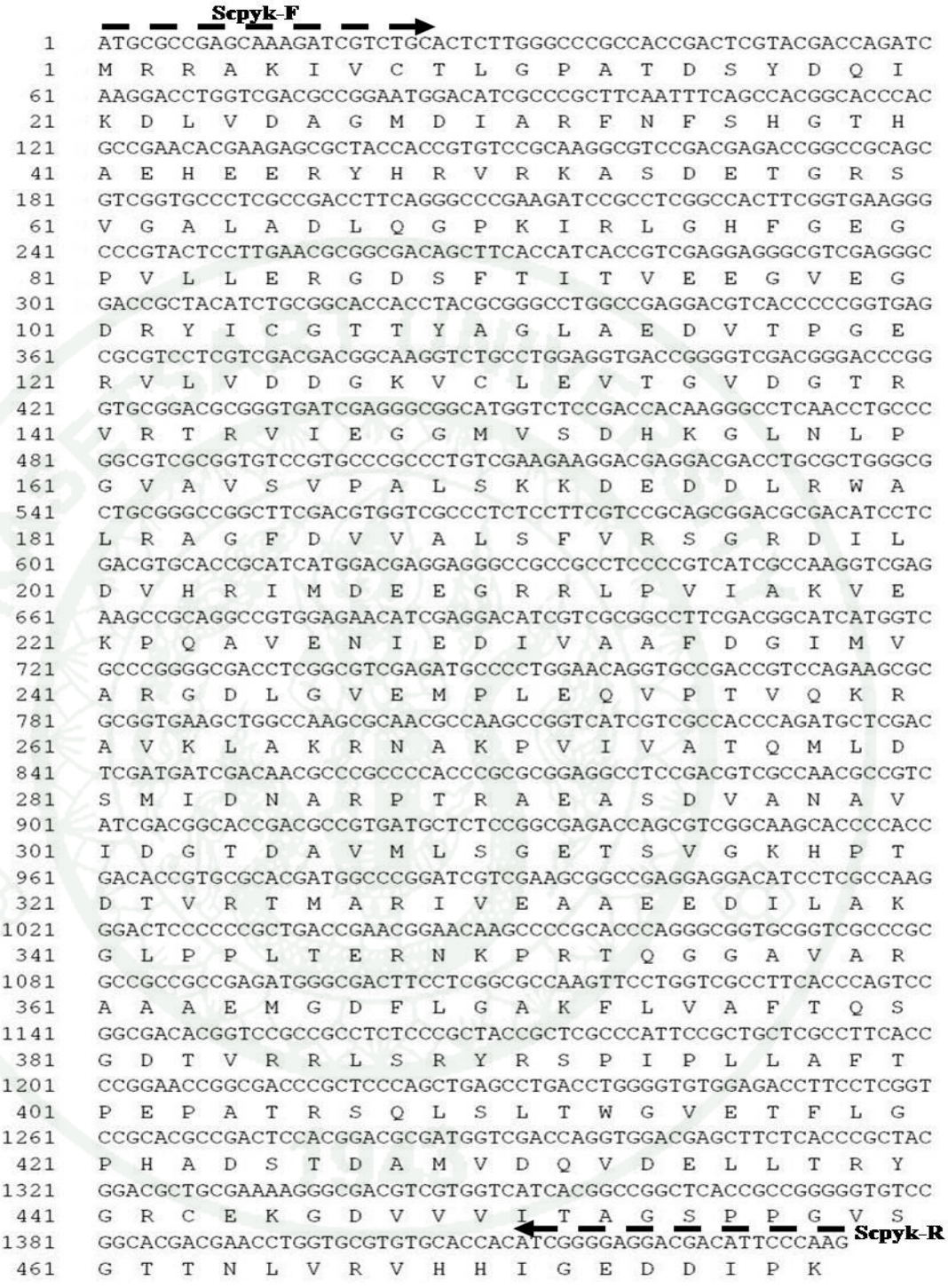

Figure 47 The nucleotide and amino acid sequence of type I *pyk* gene from *S. coelicolor*. The dash arrows show the location where specific primers were annealed in amplification. Left column; nucleotide and deduced amino acid sequence number.

2.2 Construction of recombinant pET-Scpyk for overexpression

The type I *pyk* gene from *S. coelicolor* was separated from pGEM-Scpyk by double digestion with *Nde*I and *Xho*I, ligated with pET-26b and transformed into *E. coli* BL21 (DE3). Since the reverse primer used to amplify the type I *pyk* gene from *S. coelicolor* did not contain a stop codon, cells carrying pET-Scpyk will express the recombinant PYK as polyhistidine-tag protein at C-terminus upon induction with IPTG. The recombinant pET-Scpyk was obtained recombinant 6.8 kb (Figure 48) and confirmed by sequencing.

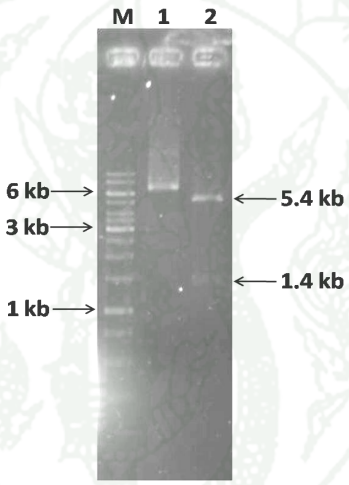

Figure 48 Agarose gel electrophoresis of double digestion of recombinant pET-Scpyk with *Nde*I and *Xho*I. Lane M, DNA ladder; lane 1, undigested pET-Scpyk; lane 2, double digested pET-Scpyk with *Nde*I and *Xho*I.

2.3 Overexpression and determination of solubility of type I PYK of *S. coelicolor* (ScPYK) from *E. coli* carrying pET-Scpyk

The recombinant pET-Scpyk was transformed to *E. coli* BL21 (DE3) for overexpression. *E. coli* carrying pET-Scpyk was induced by IPTG or lactose for final concentration to 0.5 mM at 37°C, 220 rpm. After 1-5 hours of induction, the 1 ml of cell cultures was collected for analyze on 12% SDS-PAGE. The results show *E. coli* carrying pET-Scpyk which expressed with 0.5 mM IPTG less time than 0.5 mM

lactose (Figure 49). Because of lactose can be used as a carbon source for cell growth. Additionally, lactose must be converted to allolactose by β-galatosidase before using as inducer for lac operon in recombinant plasmid. Thus, *E. coli* carrying pET-Scpyk, using 0.5 mM lactose as inducer, wanted more time for express the recombinant protein (Weng *et al.*, 2006). Unfortunately, proteins had two bands in SDS-PAGE; estimated molecular weight of recombinant enzyme was approximately 51 and 60 kDa.

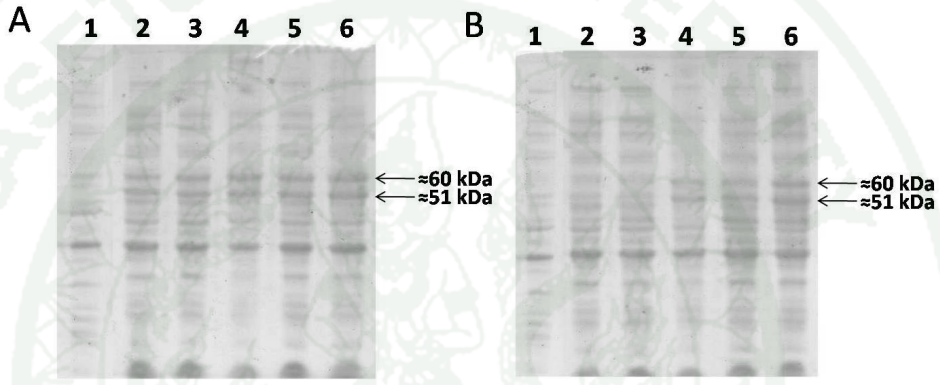

Figure 49 SDS-PAGE of overexpression level of *E. coli* BL21 (DE3) carrying pET-Scpyk that produced recombinant ScPYK with (A) 0.5 mM IPTG or (B) 0.5 mM lactose at 37°C . Lane 1-6, total protein after induction 0-5 hours, respectively.

When cells were disrupted by sonication and the supernatant was separated from the cell pellet by centrifugation, the recombinant protein was found in the pellet fraction, indicating that the protein formed insoluble inclusion bodies. Proteins in these so-called "inclusion bodies" are mostly inactive and denatured (Figure 50). Several approaches have been currently used to prevent the expressed proteins from forming inclusion bodies. These approaches include decrease the growth rate by lowing the temperature or speed of shaking (Boulé *et al.*, 1998; Shirano and Shibata, 1990; Vasina and Baneyx, 1997; Narawongsanont, 2010), decrease the expression rate by decreasing the concentration of inducer (Weng *et al.*, 2006), enhance the protein folding by co-expression with chaperon (Liu and Chang, 2003; Machida *et al.*, 2000;

Ou *et al.*, 2001) and *in vitro* unfolding and refolding of the protein (Wang *et al.*, 2002; Akbari *et al.*, 2010; Price and Stevens, 1983).

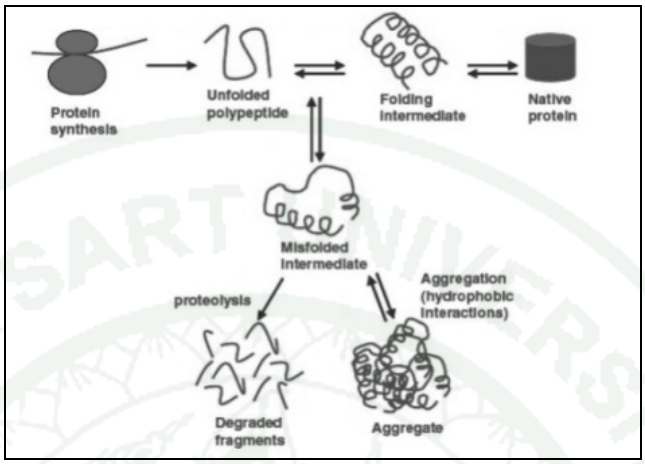

Figure 50 Schematic drawing of inclusion bodies process in recombinant protein technology.

Source: Garcìa-Fruitòs *et al.* (2009)

To prevent the expressed ScPYK from forming inclusion bodies, *E. coli* carrying pET-Scpyk was grown at 37 °C and then the temperature was decreased to 30°C, 25°C or 16°C after induction with IPTG. Analysis of the expressed protein on SDS-PAGE showed that the recombinant protein still formed inclusion bodies even the temperature was lower (Figure 51). To further decrease the growth rate, growth conditions were modified by (i) lowering the speed of shaking, (ii) diluting LB (data not show) and (iii) inducing the expression with lower concentration of inducer (Figure 52), the recombinant protein still formed inclusion bodies. Therefore, *in vitro* denaturation and refolding of inclusion bodies were solubilized the recombinant solubilized ScPYK.

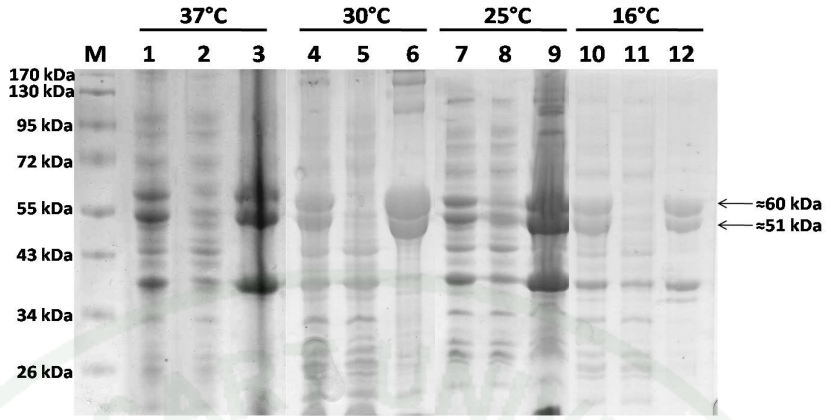

Figure 51 SDS-PAGE of solubility of recombinant ScPYK from *E. coli* BL21 (DE3) carrying pET-Scpyk when induction with 0.5 mM IPTG in 37°C (lane 1-3), 30°C (lane 4-6), 25°C (lane 7-9) and 16°C (lane 10-12). Lane M, protein ladder; lane 1, 4, 7 and 10, cell-free extract; lane 2, 5, 8, and 11, supernatant after separeated from cell-free extract by centrifugation ; lane 3, 6, 9 and 12, pellet after separated from cell-free extract by centrifugation.

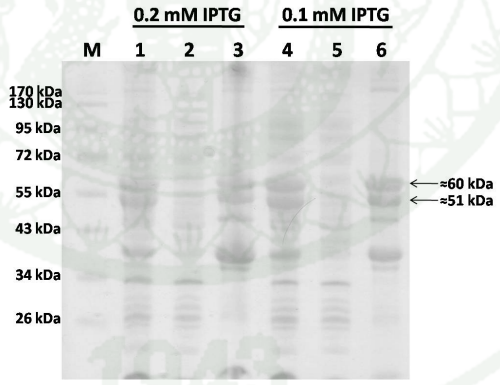

Figure 52 SDS-PAGE of solubility of recombinant ScPYK from *E. coli* BL21 (DE3) carrying pET-Scpyk when induction with 0.2 mM (lane 1-3) and 0.1 mM IPTG (lane 4-6) in 25°C. Lane M, protein ladder; lane 1 and 4, cell-free extract; lane 2 and 5, supernatant after separeated from cell-free extract by centrifugation ; lane 3 and 6, pellet after separated from cell-free extract by centrifugation.

There are several possible reasons why two bands instead of one were observed on SDS-PAGE after the protein had been purified by Ni-affinity chromatography. First, it is possible that one of the bands may be corresponded to a phosphorylated form of PYK (Cytrynska *et al.*, 2001; Portela *et al.*, 2002, *et al.*, 2006). PYK catalyzes a sequential order bi-substrate (PEP and ADP) and bi-product (pyruvate and ATP) reaction. In the first half of the reaction, the phosphate group from PEP was transfer to the enzyme to form a phosphorylated enzyme, releasing pyruvate in the reaction (Cytrynska *et al.*, 2001). In the second half of the reaction, the phosphoryl group on the enzyme is transferred to ADP, forming ATP. The phosphorylation sites on ScPYK were predicted by KinasePhos program (Huang *et al.*, 2005). The deduced amino acid sequence of ScPYK contained 11 possible phosphorylation sites: 6 serine residues, 3 threonine residues and 2 tyrosine residues (Figure 53). In the overexpression system, the ratio between recombinant PYK and phosphate group from the host cell may be different. And phosphate groups may be bound to a portion of the enzyme to affect the protein's migration on SDS-PAGE (Portela *et al.*, 2002, *et al.*, 2006). One of the several existing methods of detecting the present of phosphoryl group is the use of phosphor-specific antibody (Portela *et al.*, 2006), western blotting (Portela *et al.*, 2002; Cytrynska *et al.*, 2001) or isoelectric focusing for perform (Anderson and Peck, 2008).

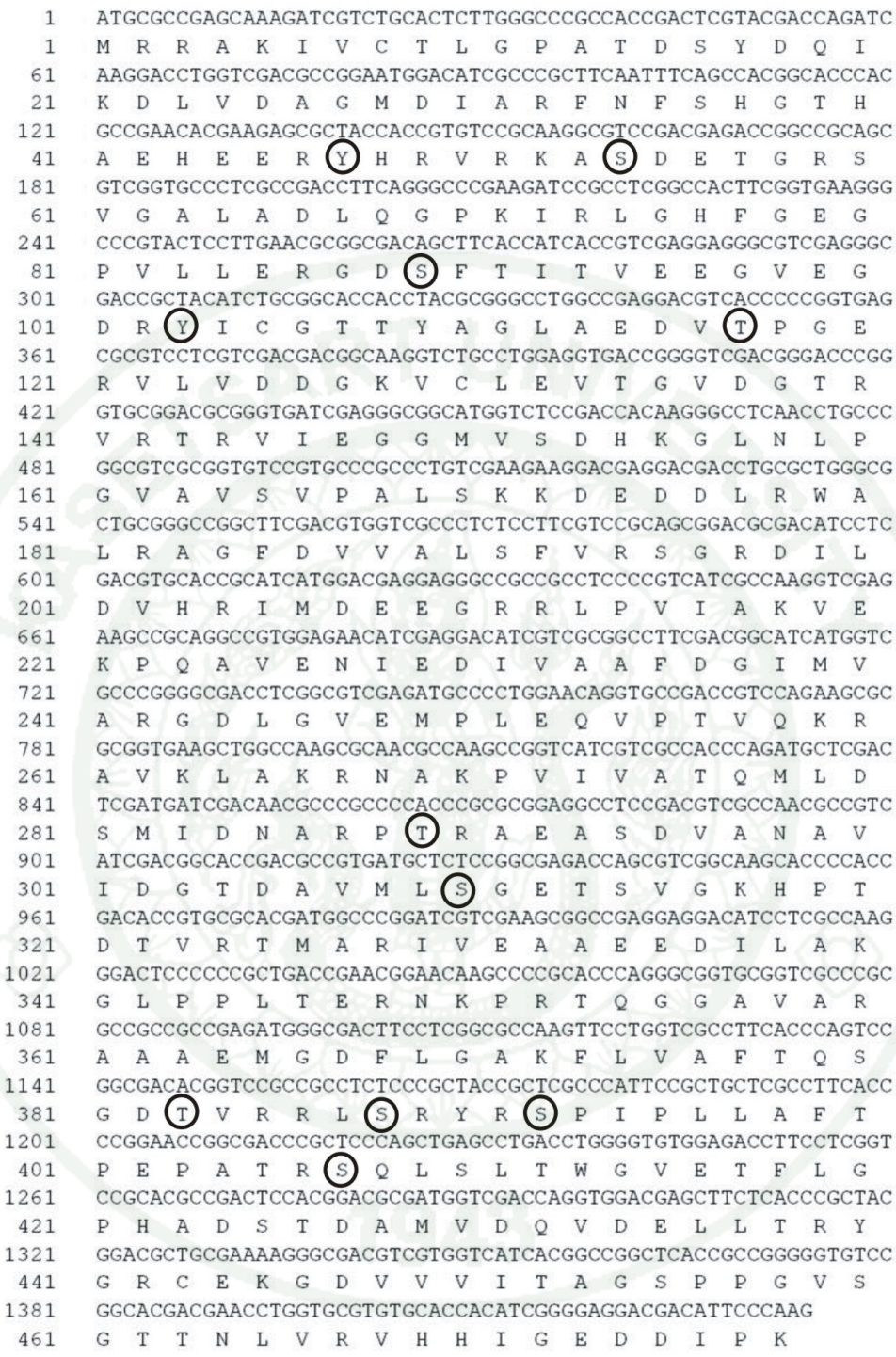

Figure 53 Phosphorylation sites in deduced amino acid sequence of ScPYK. The phosphorylation sites were labelled in black circles. Left column; nucleotide and deduced amino acid sequence number.

The second possible reason of observing two bands of the purified protein on SDS-PAGE is due to an inefficient translation stop at the stop codon during translation. In inefficient translational stop, the nucleotide sequence at the 3' terminal region of the type I *pyk* gene in pET-26b vector showed TGAG stop signal present in the vector which not good termination efficiency in *E. coli* (Björnsson and Isaksson, 1993). This can explain for the observed translation misreading in expression system. The downstream region shows the presence of a highly efficient TAA stop signal in frame with the original TGA but 20 codons downstream, before the T7 transcriptional terminator (Figure 54). The sequence context could be expressed the recombinant ScPYK with additional 21 amino acid fused at C-terminal end (Gonzalez *et al.*, 2003). However, the molecular weight of recombinant ScPYK was predicted by ExPASy, the phosphorytlate form and inefficient translational stop could be expressed the recombinant ScPYK with additional molecular weight approximately 2 kDa (data not show).

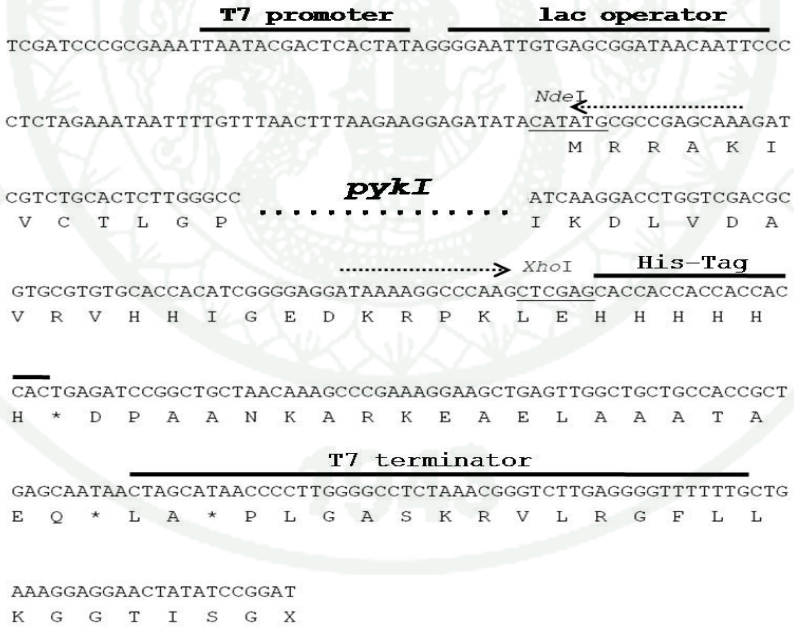

Figure 54 Scheme of the type I *pyk* gene from *S. coelicolor* inserted into pET-26b(+) vector. The dot arrows indicated the region of type I *pyk* gene in recombinant pET-Scpyk. The solid lines indicated the region of T7 promoter, lac operator, His-Tag and T7 terminator in vector.

Glutathione (sulfur) import system ATP-binding protein (GsiA) from *E. coli* had been cloned and over-expressed by Wang and coworkers (Wang *et al.*, 2011). had been cloned and over-expressed by Wang and coworkers (Wang *et al.*, 2011). When *E. coli* cells carrying recombinant plasmid with *gsiA* gene were induced with IPTG, analysis of the expressed proteins on SDS-PAGE showed that two bands were strongly induced: one being the recombinant GsiA protein and another an unknown protein with molecular weight 10 kDa larger than GsiA protein. This phenomenon is similar to that observed with the expression of recombinant ScPYK in *E. coli* in this study. Surprisingly, when *E. coli* Rosetta (DE3) was used as host cell for expression of recombinant GsiA, the level of the unknown high molecular weight protein appear to decrease. *E. coli* Rosetta (DE3) is BL21 derivatives which is designed to enhance the expression of eukaryotic proteins that contain codons rarely used in *E. coli*. Wang *et al*, 2011 do not offer any explanation for the decrease in the level of higher molecular weight expression when *E. coli* Rosetta (DE3) was used as the host. Nevertheless, the likelihood of the codon context may be affected the level of expression. The nucleotide sequence of the type I *pyk* gene from *S. coelicolor* contained high G+C content (72%) (Bentley *et al.*, 2002). Figure 55 shows the map of average codon usage of the genomes from eight commonly studied organisms. Compared to eight organisms, *Streptomyces coelicolor* has the most extreme codon usage profile (Figure 55). The GC rich content of *Streptomcyes* genes might have a strong bias that resulted in an error of protein translation (Gustafsson *et al.*, 2004) (Table 8).

The error of protein translation could be assay by peptide mass mapping, liquid chromatography-mass spectrometry (LC-MS) (Tanaka *et al.*, 1995).

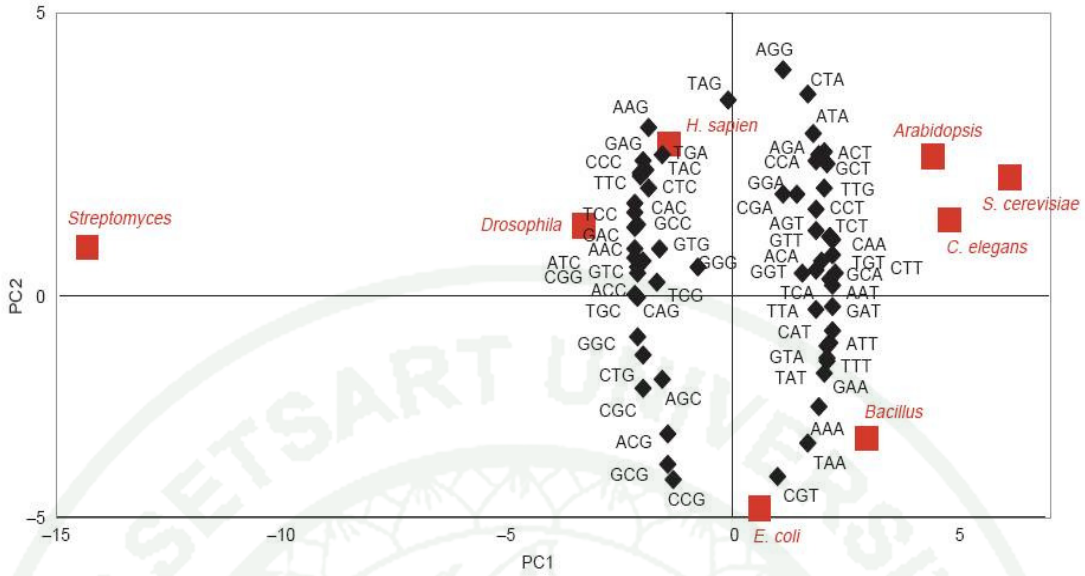

Figure 55 The average codon preferences of the genomes from eight commonly studied organisms. Two dimensions were identified that explained for 70% (PC1) and 12% (PC2) of the total codon variability information, respectively. The black diamonds indicated the loads. The values of the codon loads have been normalized to that of the organism spreading. The red squares represent the preferences of each organism plotted within this space.

Source: Gustafsson *et al.* (2004)

Table 8 Summary of codon usage for *E. coli* (upper table) and *S. coelicolor* (lower table)

Escherichia coli K12 **[gbbct]: 14 CDS's (5122 codons)**

fields: [triplet] [frequency: **per thousand**] ([number])

UUU 19.7(101)	UCU 5.7(29)	UAU 16.8(86)	UGU 5.9(30)
UUC 15.0(77)	UCC 5.5(28)	UAC 14.6(75)	UGC 8.0(41)
UUA 15.2(78)	UCA 7.8(40)	UAA 1.8(9)	UGA 1.0(5)
UUG 11.9(61)	UCG 8.0(41)	UAG 0.0(0)	UGG 10.7(55)
CUU 11.9(61)	CCU 8.4(43)	CAU 15.8(81)	CGU 21.1(108)
CUC 10.5(54)	CCC 6.4(33)	CAC 13.1(67)	CGC 26.0(133)
CUA 5.3(27)	CCA 6.6(34)	CAA 12.1(62)	CGA 4.3(22)
CUG 46.9(240)	CCG 26.7(137)	CAG 27.7(142)	CGG 4.1(21)
AUU 30.5(156)	ACU 8.0(41)	AAU 21.9(112)	AGU 7.2(37)
AUC 18.2(93)	ACC 22.8(117)	AAC 24.4(125)	AGC 16.6(85)
AUA 3.7(19)	ACA 6.4(33)	AAA 33.2(170)	AGA 1.4(7)
AUG 24.8(127)	ACG 11.5(59)	AAG 12.1(62)	AGG 1.6(8)
GUU 16.8(86)	GCU 10.7(55)	GAU 37.9(194)	GGU 21.3(109)
GUC 11.7(60)	GCC 31.6(162)	GAC 20.5(105)	GGC 33.4(171)
GUA 11.5(59)	GCA 21.1(108)	GAA 43.7(224)	GGA 9.2(47)
GUG 26.4(135)	GCG 38.5(197)	GAG 18.4(94)	GGG 8.6(44)

Coding GC 52.35% 1st letter GC 60.82% 2nd letter GC 40.61% 3rd letter GC 55.62%

Streptomyces coelicolor A3(2) **[gbbct]: 8375 CDS's (2743050 codons)**

fields: [triplet] [frequency: **per thousand**] ([number])

UUU 0.4(1222)	UCU 0.6(1781)	UAU 1.0(2696)	UGU 0.7(1986)
UUC 25.9(71022)	UCC 20.2(55452)	UAC 19.5(53525)	UGC 7.1(19435)
UUA 0.1(175)	UCA 1.1(2987)	UAA 0.1(383)	UGA 2.4(6523)
UUG 2.4(6706)	UCG 13.7(37630)	UAG 0.5(1468)	UGG 15.2(41567)
CUU 1.6(4399)	CCU 1.6(4261)	CAU 1.7(4680)	CGU 5.5(15031)
CUC 36.5(100256)	CCC 25.5(69887)	CAC 21.8(59920)	CGC 39.1(107385)
CUA 0.4(981)	CCA 1.4(3706)	CAA 1.4(3708)	CGA 2.6(7101)
CUG 60.9(167041)	CCG 33.4(91515)	CAG 25.2(69255)	CGG 31.9(87371)
AUU 0.6(1736)	ACU 1.2(3276)	AAU 0.7(1985)	AGU 1.5(4180)
AUC 27.5(75512)	ACC 39.8(109099)	AAC 16.3(44627)	AGC 12.5(34157)
AUA 0.7(1811)	ACA 1.7(4528)	AAA 1.1(2921)	AGA 0.8(2129)
AUG 15.8(43327)	ACG 19.0(52030)	AAG 19.6(53671)	AGG 3.7(10061)
GUU 1.5(4008)	GCU 3.1(8453)	GAU 3.1(8438)	GGU 9.2(25257)
GUC 46.9(128649)	GCC 78.4(215055)	GAC 58.2(159730)	GGC 60.9(167167)
GUA 2.7(7306)	GCA 5.6(15417)	GAA 8.7(23997)	GGA 7.2(19677)
GUG 35.0(95906)	GCG 49.5(135712)	GAG 48.2(132351)	GGG 18.2(49822)

Coding GC 72.30% 1st letter GC 72.67% 2nd letter GC 51.39% 3rd letter GC 92.83%

Source: http://www.kazusa.or.jp/codon

2.4 Purification and refolding of ScPYK from *E. coli* carrying pET-Scpyk

The recombinant ScPYK expressed in *E. coli* carrying pET-Scpyk formed inclusion bodies. The inclusion bodies can be solubilized by denaturating with strong detergents such as urea or guadinine-HCl. In this experiment, inclusion body was solubilized by addition of 4 M urea and refolding to its native formed by dilution with buffer (Price and Stevens, 1983; Porter *et al.*, 1980) (Figure 56). Unfortunately, after unfolded and refolded, PYK lost most of its activity and not very stable (Table 9). The problem with *in vitro* unfolding/refolding ScPYK may due to the fact that PYKs found in most organisms are multi-domain protein and form tetramer in solution. Proteins forming monomer are generally easier to unfold and refold than protein forming multimer. Because, the renaturation mechanism of PYK have two steps; polypeptide was folded to subunit and subunit was association to native conformation (Figure 57) (Bornmann *et al.*, 1974). In each step, additives may be influence or necessary to renaturation, for example, sucrose, L-valine or metal ions (Bornmann *et al.*, 1974; Chang *et al.*, 2001; Lilie *et al.*, 1998; Vallejo and Rinas, 2004). The refolding buffers were supplement with additives, such as sucrose, lactose, glycerol, Triton X-100 or glycine, which cannot improve activity (data not show).

The process of unfolding/refolding of recombinant ScPYK can be followed by fluorescence spectroscopy (Swain *et al.*, 1997; Weiss, 2000; Yan and Marriott, 2003) or circular dichroism spectroscopy (Corrêa and Ramos, 2009; Matsuo *et al.*, 2004; Wallace and Janes, 2001). The conformation of the native protein possessing catalytic activity can be analyzed by size exclusion chromatography for determined the molecular weight (Pornbanlualap and Chalopagorn, 2011) or x-ray crystallography to determine the subunit interaction in the quaternary structure of PYK (Mettevi *et al.*, 1995; Suzuki *et al.*, 2008; Wooll *et al.*, 2001).

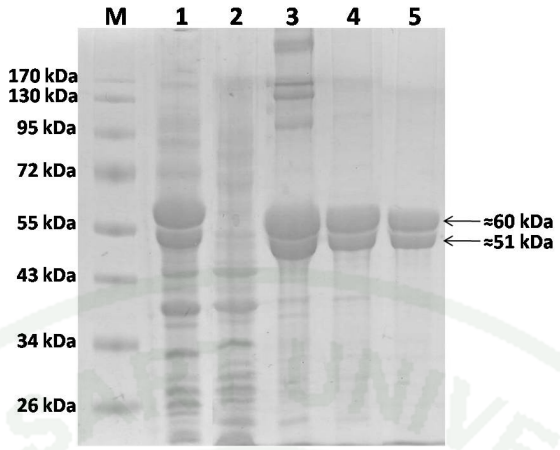

Figure 56 SDS-PAGE of purification and refolding of ScPYK from *E. coli* BL21 (DE3) carrying pET-Scpyk. Lane M, protein ladder; lane 1, cell-free extract; lane 2, supernatant after separeated from cell-free extract by centrifugation; lane 3, pellet after separeated from cell-free extract by centrifugation; lane 4, denatured ScPYK; lane 5, purified ScPYK by Ni^{2+}-NTA column.

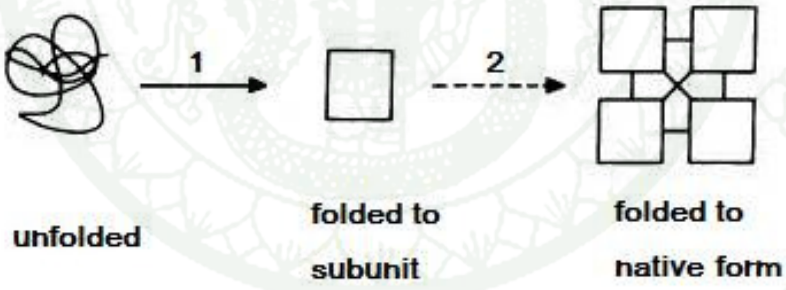

Figure 57 Schematic drawing of renaturation of PYK. The unfolded protein was folded to subunit (1) and subunits were folded to native conformation (2).

Source: Bornmann *et al.* (1974)

Table 9 Summary table of purification of type I ScPYK from *E. coli* BL21 (DE3) carrying pET-Scpyk

Steps	Total volume (ml)	Total protein (mg)	Total activity (U)	Specific activity (U/mg)	% Recovery
Cell-free extract	15	56.2	nd	nd	100
Ni^{2+}-NTA	10	0.5	nd	nd	1
Refolding by dilution method	5	0.4	0.3	0.7	0.9

One unit of enzyme is the amount which catalyzed the phosphorylation of 1 µmole of ADP per minute at 25°C.

nd, not determined

2.5 The prediction of secondary structure of type I ScPYK

The deduced amino acid of type I ScPYK is 478 residues. Three-dimensional modeling of type I ScPYK monomer based on deduced amino acid sequence by SWISS-MODEL is shown in Figure 61. The predicted three-dimensional structure of of type I ScPYK based on molecular modeling is most similar to that of PYK from *B. stearothermophilus* (Suzuki *et al.*, 2008) 42% identity (C-alpha root mean square deviation, 0.41 Å). The structure contained 3 domains, A, B and C. Domain A is formed by two separated stretches of amino acids, residues 1–69 and 164–336, that fold together to form a TIM barrel motif with two additional α helices. This domain is proposed to contain the catalytic site. Domain B formed a small seven-stranded β-barrel motif with a additional α-helic, comprising residues 70-163, that formed a cap over the active site at domain A. Domain C formed open-sheet motif, and included residues 337–478, similar with type I SaPYK (Figure 58 and 59). When the predicted structure modeling of type I ScPYK was compared with type I SaPYK, the Aα4 of type I ScPYK is additional one amino acid residue.

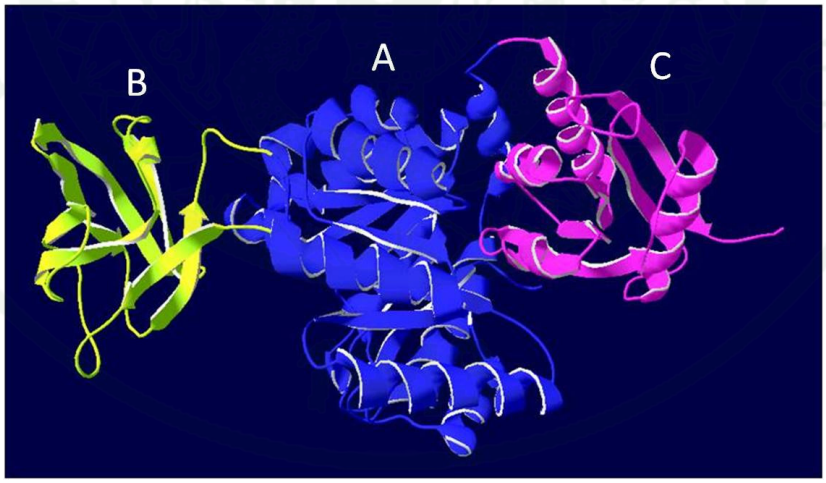

Figure 58 Cartoon diagram of the predicted structure model of type I ScPYK. The structure was similar to PYK from *B. stearothermophilus* (PDB#2E28). Domains A, B and C are shown in blue, yellow and magenta, respectively.

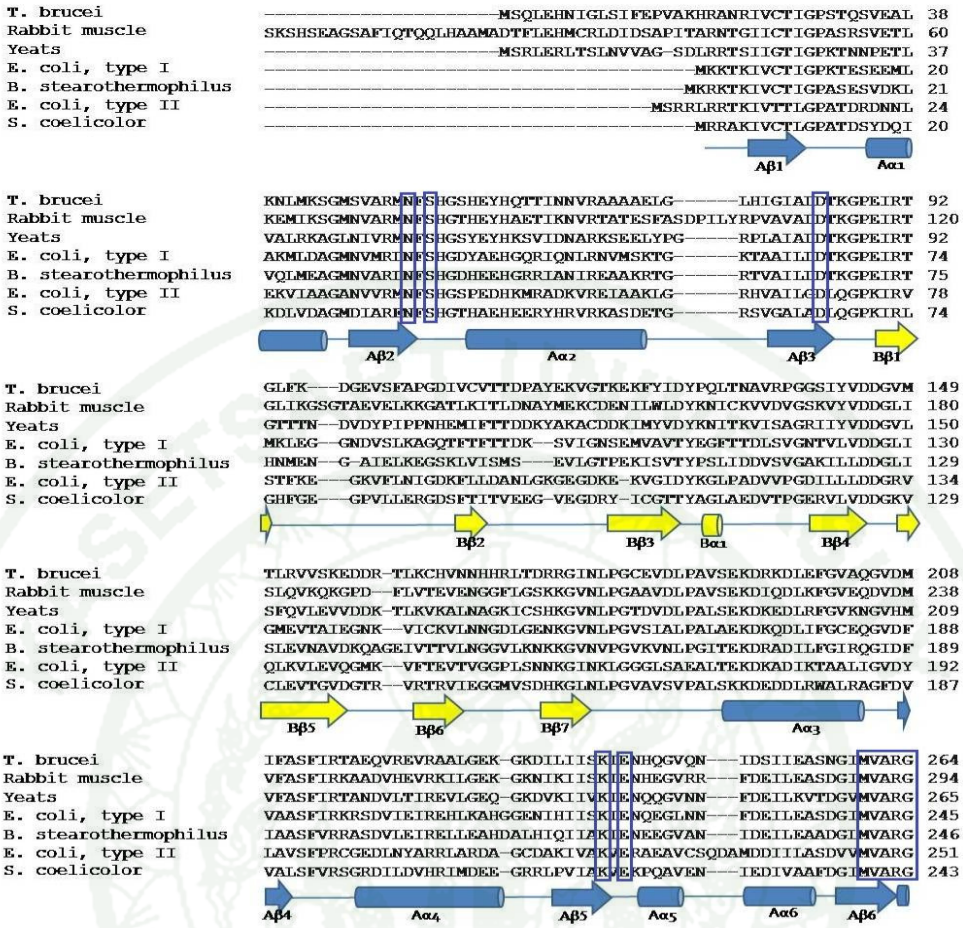

Figure 59 The multiple sequence alignment and predicted secondary structure of type I ScPYK. The organisms and accession numbers for the amino acid sequences are: *B. stearothermophilus* (BAA02406), *E. coli*, type I (AAB47952), *E. coli*, type II (YP_490116), *Oryctolagus cuniculus*, rabbit muscle (AAC48536), *Saccharomyces cerevisiae*, *Streptomyces coelicolor* (NP_626275), yeast (CAA24631) and *T. brucei* (CAA41018). The α-helice, β-sheets and lines were shown as rolls, arrows and loops, respectively. The domain A, B and C of were shown as blue, yellow and magenta, respectively. The substrate and metal binding sites were shown in blue boxes and effector binding sites were shown in orange boxes. The amino acid residues of type I ScPYK were corresponding with effector binding sites of PYK from *B. stearothermophilus* which shown as orange arrows.

Figure 59 (Continued)

2.6 Phylogenetic tree of type I SaPYK and type I ScPYK

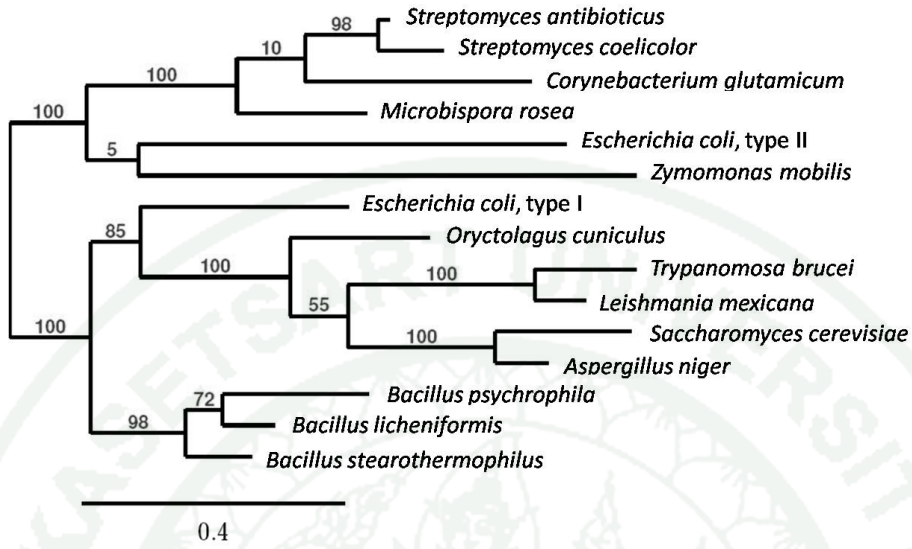

Figure 60 Phylogenetic tree of PYK. The tree was constructed by the maximum likehood method based on the sequence alignment the PhyML program (expressed as percentages of 100 replications). The numbers at nodes are bootstrap value. The organisms and accession numbers for the amino acid sequences are: *Aspergillus niger* (AAB22392) (fungi), *Bacillus licheniformis* (BBA06727) (bacteria), *B. phychrophila* (BAA06725) (bacteria), *B. stearothermophilus* (BAA02406) (bacteria), *Corynebacterium glutamicum* (AAA56793) (bacteria), *Escherichai coli*, type I (AAB47952) (bacteria), *E. coli*, type II (YP_490116) (bacteria), *Leishmania mexicana* (CAA52898) (protozoa), *Microbispora rosea* (BAC76684) (bacteria), *Oryctolagus cuniculus* (AAC48536) (animal), *Saccharomyces cerevisiae* (CAA24631) (yeast), *Streptomyces antibioticus* (bacteria), *Streptomyces coelicolor* (NP_626275) (bacteria), *Trypanosoma brucei* (CAA41018) (protozoa), and *Zymomonas mobilis* (AAC28104) (bacteria).

The deduced amino acid sequences of type I SaPYK and type I ScPYK shown highest similarities with PYK from *Microbispora rosea* or *M. thermodiastatica* (Arai *et al.*, 1998) (64% and 61% identities, respectively) and *Corynebacterium glutamicum*

(Jetten *et al.*, 1994) (62% and 58% identities, respectively). PYK from *M. rosea* and *C. glutamicum*, actinomycetes have been shown to be activated by AMP. Phylogenetic relationship shows that the SaPYK and ScPYK fall within the type II group and is similar to *E. coli* type II PYK (Somani *et al.*, 1977) (Figure 60), which is activated by AMP (Bourniquel *et al.*, 2002). Three-dimensional structure modeling and phylogenetic tree clearly showed that both type I SaPYK and ScPYK may be activated by AMP.

3. Synthesis of dNTP

In this study, enzymatic synthesis of dNTPs was accomplishing using NMP kinases to convert dNMP to dNDP and pyruvate kinase to convert dNDP to dNTP (Bao and Ryu, 2007; Lehman *et al.*, 1957). First, ADK, CMK and DNK were purified and used as dNMP kinases to convert dNMPs to dNDPs. These enzymes show high specificity toward the base moiety of the dNMP. Next, PYK was expressed and purified and used as the kinase to convert dNDP to dNTP. Previous attempts to synthesize dNMP to dNTP by Howhan, Poopanipan and Narawongsanont from our laboratory did succeed but at 1 mM-scale because they used *E. coli* type II PYK in the synthesis (Howhan , 2004; Narawongsanont, 2010; Poopanitpan, 2005). *E. coli* type I PYK was found to be unstable and easily aggregated when incubated at 37°C (Somani *et al.*, 1977). In addition, PYK from *S. antibioticus* and *S. coelicolor* are not yet available. Hence, we used PYK type I of *E. coli*, which is stable and not aggregated at 37°C (Malcovati and Valentini, 1982; Valentini *et al.*, 1997), for dNDP kinase in synthesis. After synthesis, products were analyzed by TLC and DEAE chromatography. Finally, dNTP were used to amplify DNA fragment for proving that they actually function in molecular research.

3.1 Overexpression and purification of *E. coli* ADK from *E. coli* BL21 (DE3) carrying pET-*adk*

ADK from *E. coli* carrying pET-*adk* which induced 1 mM lactose at 37°C has total activity of 9,730 U and specific activity approximately 113.8 U/mg (Table 10). The recombinant ADK was fused polyhistidine tagged at C-terminus but it's not bind with Ni^{2+}-NTA column. The C-terminus of ADK may be buried into the structure (Berry *et al.*, 2006; Poopanitpan *et al.*, 2005). Thus, Ni^{2+}-NTA column can't bind with polyhistidine tag. The recombinant ADK can be eluted from DEAE-cellulose column with buffer A contained 50 mM KCl The purified ADK show a single band of approximately 27 kDa on 12% SDS-PAGE (Figure 61, lane 5).

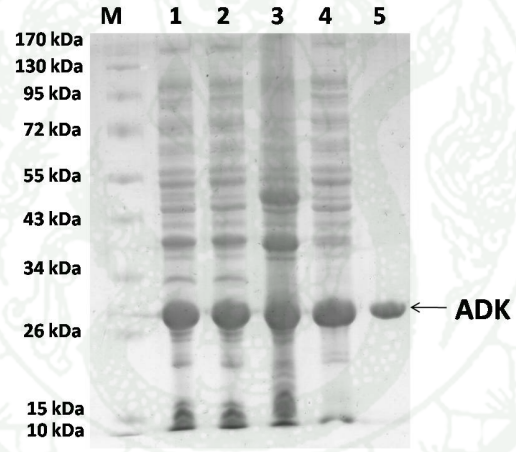

Figure 61 SDS-PAGE of purification steps of ADK from *E. coli* BL21 (DE3) carrying pET-*adk*. Lane M, protein ladder; lane 1, cell-free extract; lane 2, supernatant after centrifuged from cell-free extract; lane 3, pellet after centrifuged from cell-free extract; lane 4, supernatant after remove DNA by Streptomycin sulfate; lane 5, purified ADK eluted from DEAE-cellulose.

Table 10 Table summarizing the purification of *E. coli* ADK from one liter culture

Steps	Total volumn (ml)	Total protein (mg)	Total activity (U)	Specific activity (U/mg)	% Recovery
Cell-free extract	29	229	20321	88.7	100
Supernatant after removed DNA by Streptomycin sulfate	30	171	18870	110.3	74.7
DEAE-cellulose	3	85.5	9730	113.8	37.3

One unit of ADK activity is the amount of enzyme required to phosphorylate 1 µmole of dAMP to dADP in one minute at 25°C.

3.2 Overexpression and purification of *E. coli* CMK from *E. coli* BL21 (DE3) carrying pET-*cmk*

CMK purified from one liter of *E. coli* carrying pET-*cmk* induced with 5 mM lactose has the total activity of 3,106 U and specific activity approximately 63.5 U/mg (Table 11). The recombinant CMK can be eluted from Ni-affinity column with buffer B contained 100 mM imidazole (Howhan *et al.*, 2004). The purified CMK show a single band of approximately 27 kDa on 12% SDS-PAGE (Figure 62, lane 5).

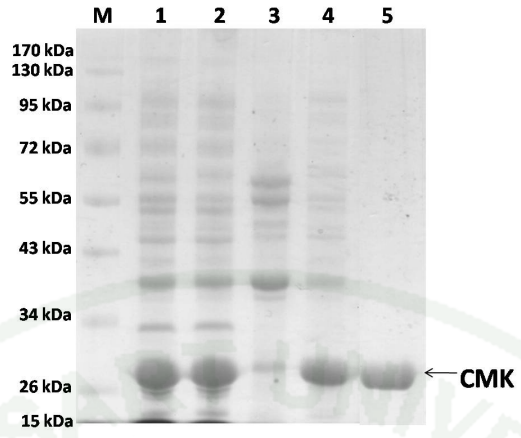

Figure 62 SDS-PAGE of purification steps of *E. coli* CMK from *E. coli* BL21 (DE3) carrying pET-*cmk*. lane M, protein ladder; lane 1, cell-free extract; lane 2, supernatant after centrifuged from cell-free extract; lane 3, pellet after centrifuged from cell-free extract; lane 4, DNA precipitated by Streptomycin sulfate; lane 5, purified CMK eluted from Ni^{2+}-NTA column.

Table 11 Table summarizing the purification of *E. coli* CMK from one liter culture

Steps	Total volumn (ml)	Total protein (mg)	Total activity (U)	Specific activity (U/mg)	% Recovery
Cell-free extract	18	216	3492	16.2	100
Supernatant after removed DNA by Streptomycin sulfate	18	174	3121	17.9	80.5
Ni^{2+}-NTA column	1.7	48.9	3106	63.5	22.6

One unit of CMK activity activity is the amount of enzyme required to phosphorylate 1 µmole of dCMP to dCDP in one minute at 25°C.

3.3 Overexpression and purification of bacteriophage T_4 DNK from *E. coli* BL21 (DE3) carrying pET-T4*dnk*

DNK from *E. coli* carrying pET-*dnk* which induced 1 mM lactose at 37°C has total activity of 4,840 U and specific activity approximately 47.8 U/mg (Table 12). The recombinant DNK can be eluted with buffer C contained 100 mM imidazole (Poopanitpan *et al.*, 2005). The purified DNK show a single band of approximately 25 kDa on 12% SDS-PAGE (Figure 63).

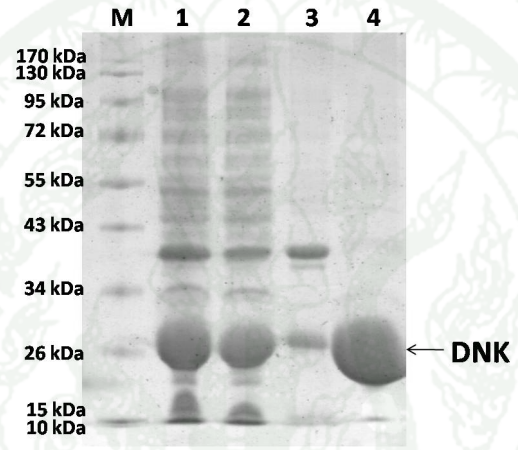

Figure 63 SDS-PAGE of purification steps of bacteriophage T_4 DNK from *E. coli* BL21 (DE3) carrying pET-T4*dnk*. lane M, protein ladder; lane 1, cell-free extract; lane 2, supernatant after centrifuged from cell-free extract; lane 3, pellet after centrifuged from cell-free extract; lane 4, purified DNK eluted from Ni^{2+}-NTA column.

Table 12 Table summarizing the purification of bacteriophage T_4 DNK from one liter culture

Steps	Total volumn (ml)	Total protein (mg)	Total activity (U)	Specific activity (U/mg)	% Recovery
Cell-free extract	18	162	15912	98.2	100
Ni^{2+}-NTA column	4	101.2	4840	47.8	62.5

One unit of DNK activity is the amount of enzyme required to phosphorylate 1 nmole of dGMP to dGDP in one minute at 25°C.

3.4 Overexpression and purification of *E. coli* type I PYK from *E. coli* BL21 (DE3) carrying pGV5A

The purified PYK from *E. coli* carrying pGV5A which induced 0.6 mM IPTG at 37°C (1 liter) by DEAE-cellulose column has total activity and specific activity approximately 875 U and 67.6 U/mg, respectively (Table 13). The pyruvate kinase was eluted by 150 mM KCl. (Valentini *et al.*, 1997). The purified *E. coli* type I PYK show a single band of approximately 60 kDa on 12% SDS-PAGE (Figure 64).

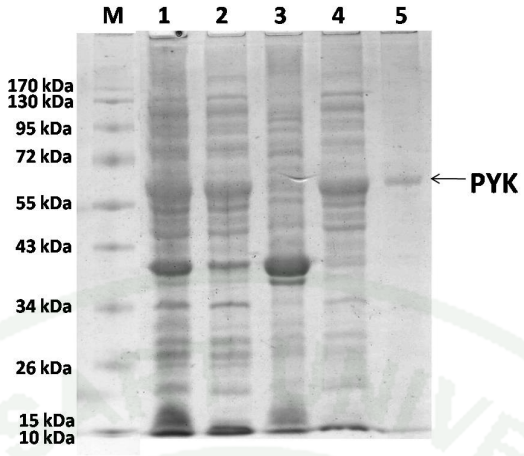

Figure 64 SDS-PAGE of purification steps of *E. coli* type I PYK from *E. coli* BL21 (DE3) carrying pGV5A. Lane M, protein ladder; lane 1, cell-free extract; lane 2, supernatant after centrifuged from cell-free extract; lane 3, pellet after centrifuged from cell-free extract; lane 4, DNA precipitated by Streptomycin sulfate; lane 5, purified PYK eluted from DEAE.

Table 13 Table summarizing the purification of *E. coli* type I PYK from one liter culture

Steps	Total volumn (ml)	Total protein (mg)	Total activity (U)	Specific activity (U/mg)	% Recovery
Cell-free extract	20	58	1126	19.4	100
DNA precipitation by Streptomycin sulfate	21.5	46.4	988	21.3	80
DEAE-cellulose	3.5	12.9	875	67.6	22.3

One unit of enzyme is the amount which catalyzed the phosphorylation of 1 µmole of ADP per minute at 25°C.

3.5 Enzymatic synthesis of dNTP

The dNTP was synthesized using dNMP kinase that depended on base; dATP using ADK, dCTP using CMK and dGTP and dTTP using DNK; and PYK as dNDP kinase. These reactions were incubated at 37°C, collected every hour and analyzed on PEI-cellulose TLC. The PEI-cellulose TLC has been described for measurement of deoxyribonucleoside mono-, di- and triphosphates with charged solvents in anion exchange chromatography. The results of synthesis of dATP show that reaction for 10 mM-scale was completely converted dAMP to dATP (Figure 65). In contrast, these reactions for 20 mM, 60 mM and 100 mM-scale were appeared dADP (6%) and dATP (94%) as products (Figure 65, 66 and 72, Table 14), as presented in the synthesis of dCTP which appeared dCDP (10%) and dCTP (90%) as products (Figure 67, 68 and 73, Table 14). The results indicated that ADK and CMK may rapidly complete formation of dADP and dCDP by dATP and dCTP as phosphoryl donor, respectively (one unit of ADK and CMK activity is catalyzed 1µmole of substrate to product in one minute). dADP and dCDP may accumulated in the reactions. However, PYK was not complete formation of dATP and dCTP in high concentration of substrates. The high concentration of substrate may inhibit activity of PYK, substrate inhibition (Waygood and Sanwal, 1974; Waygood *et al.*, 1975).

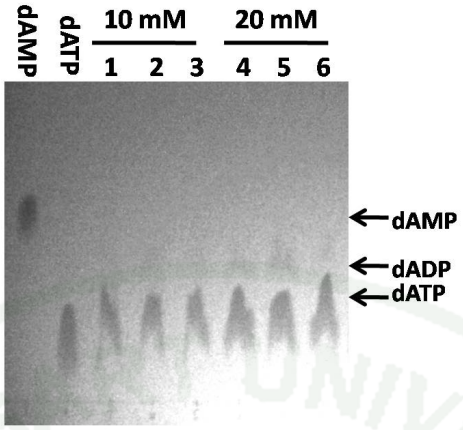

Figure 65 Analysis of dATP synthesis in 10 mM (lane 1-3) and 20 mM-scale (lane 4-6) by PEI-cellulose TLC. Lane dAMP and dATP, standards; lane 1 and 4, reaction after incubated for 1 hour; lane 2 and 5, reaction after incubated for 2 hours; lane 3 and 6, reaction after incubated for 3 hours. The 3 µl of samples were separated by TLC in 0.7 M LiCl.

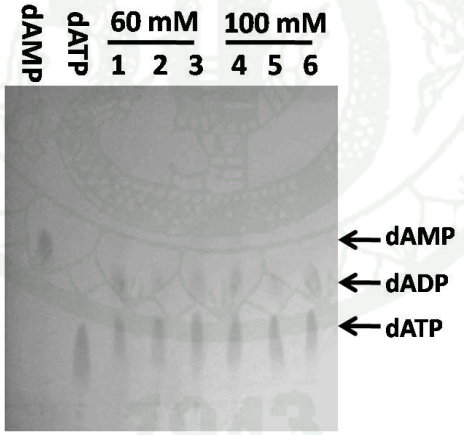

Figure 66 Analysis of dATP synthesis in 60 mM (lane 1-3) and 100 mM-scale (lane 4-6) by PEI-cellulose TLC. Lane dAMP and dATP, standards; lane 1 and 4, reaction after incubated for 1 hour; lane 2 and 5, reaction after incubated for 2 hours; lane 3 and 6, reaction after incubated for 3 hours. The 3 µl of diluted samples (20nmole) were separated by TLC in 0.7 M LiCl.

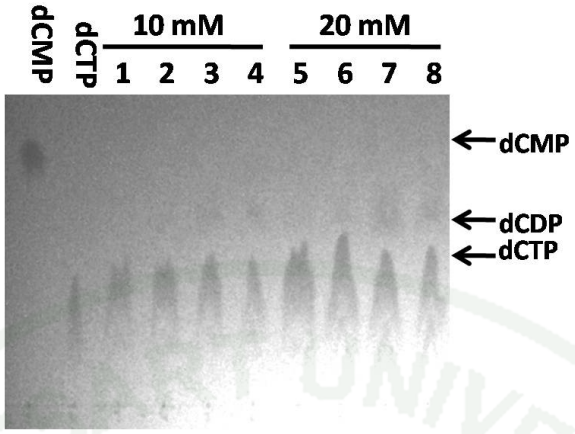

Figure 67 Analysis of dCTP synthesis in 10 mM (lane 1-4) and 20 mM-scale (lane 5-8) by PEI-cellulose TLC. Lane dCMP and dCTP, standards; lane 1 and 5, reaction after incubated for 1 hour; lane 2 and 6, reaction after incubated for 3 hours; lane 3 and 7, reaction after incubated for 5 hours; lane 4 and 8, reaction after incubated for 7 hours. The 3 µl of samples were separated by TLC in 0.7 M LiCl.

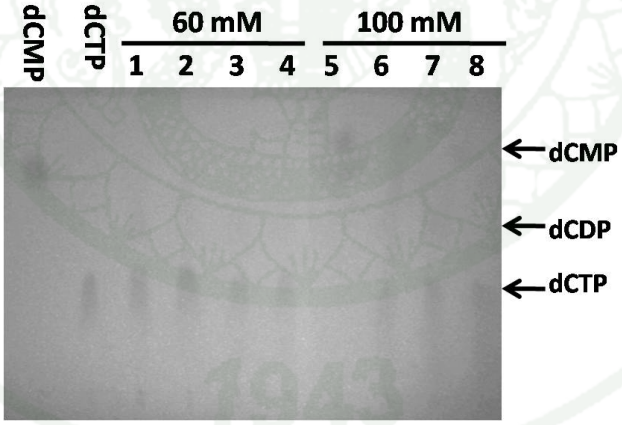

Figure 68 Analysis of dCTP synthesis in 60 mM (lane 1-4) and 100 mM-scale (lane 5-8) by PEI-cellulose TLC. Lane dCMP and dCTP, standards; lane 1 and 5, reaction after incubated for 1 hour; lane 2 and 6, reaction after incubated for 3 hours; lane 3 and 7, reaction after incubated for 5 hours; lane 4 and 8, reaction after incubated for 7 hours. The 3 µl of diluted samples (20nmole) were separated by TLC in 0.7 M LiCl.

On the other hand, the results of synthesis of dGTP and dTTP show that completely converted dGMP and dTMP to dGTP and dTTP, respectively, in all conditions (Figure 69-71, 74 and 75, Table 14). The results considered that velocity of DNK activity was slow (one unit of DNK activity is catalyzed 1 nmole of substrate to product in one minute). dGDP and dTDP were not accumulated in reaction, substrate inhibition of PYK was disappeared. In addition, the synthesis of dGTP was used different phosphoryl donor, ATP, contrast with synthesis of dTTP which using dTTP as phosphoryl donor (Figure 69). This indicated that DNK may weakly bound with dGTP, similar with dTTP. Moreover, K^+ may be prevented formation of dGDP for function of dGMP kinase, no dTMP kinase (Bello and Bessmab, 1963).

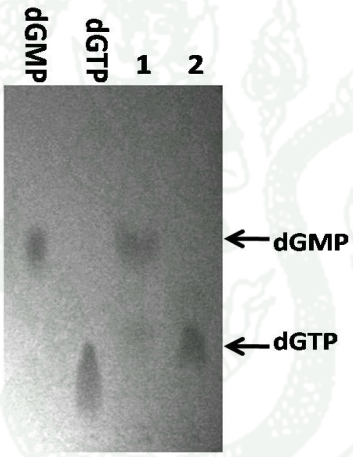

Figure 69 Analysis of dGTP synthesis by using different phosphoryl donors by PEI-cellulose TLC. Lane dGMP and dGTP, standards; lane 1, dGTP synthesis by using dGTP as phosphoryl donor; lane 2, dGTP synthesis by using ATP as phosphoryl donor. The 3 µl of samples were separated by TLC in 0.7 M LiCl.

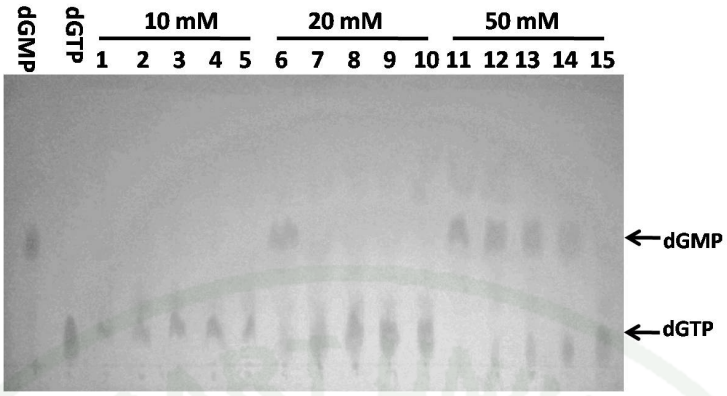

Figure 70 Analysis of dGTP synthesis in 10 mM (lane 1-5), 20 mM (lane 6-10) and 50 mM-scales(lane 11-15) by PEI-cellulose TLC. Lane dGMP and dGTP, standards; lane 1, 6 and 11, reaction after incubate for 1 hour; lane 2, 7 and 12, reaction after incubated for 3 hours; lane 3, 8 and 13, reaction after incubated for 5 hours; lane 4, 9 and 14, reaction after incubated for 7 hours; lane 5, 10 and 15, reaction after incubated for overnight. The 3 µl of diluted samples (20nmole) were separated by TLC in 0.7 M LiCl.

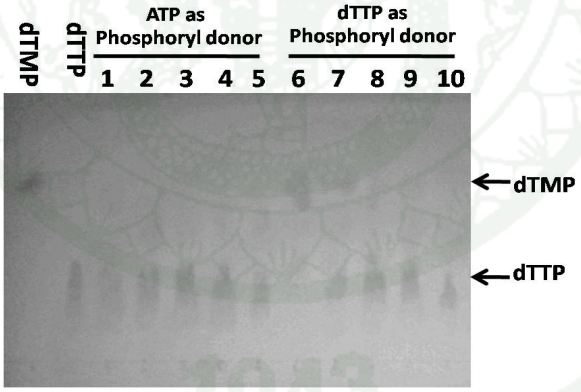

Figure 71 Analysis of dTTP synthesis by using ATP (lane 1-5) and dTTP (lane 6-10) as phosphoryl donor by PEI-cellulose TLC. Lane dTMP and dTTP, standards; lane 1 and 6, reaction after incubated for 1 hour; lane 2 and 7, reaction after incubated for 3 hours; lane 3 and 8, reaction after incubated for 5 hours; lane 4 and 9, reaction after incubated for 7 hours; lane 5 and 10, reaction after incubated for overnight. The 3 µl of samples were separated by TLC in 0.7 M LiCl.

Table 14 The production of enzymatic synthesis of dNTP

Types of dNTP	mM-scale (maximum rate)	% yield
dATP	100 mM	96%
dCTP	100 mM	90%
dGTP	50 mM	100%
dTTP	10 mM	100%

The quality of products was analyzed by DEAE chromatography. The DEAE chromatography has similar concept with PEI-cellulose TLC. The deoxyribonucleotides bound with DEAE beads and separated with different concentration of TEAB buffer; 50 mM, 100 mM and 150 mM were eluted deoxyribonucleoside mono-, di- and triphosphates, respectively (Figure 72-75). The fractions were analyzed by measurement of absorbance at 260 nm and determined wavelength of maximum absorption or λmax; 260, 271, 251 and 269 nm for adenosine, cytidine, guanosine and thymidine, respectively.

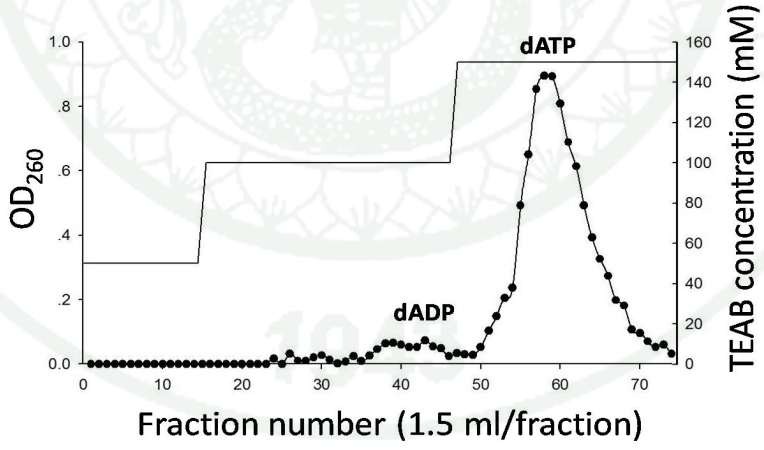

Figure 72 Analysis of dATP synthesis in 100 mM-scale after incubation for 3 hours by DEAE-cellulose column. The TEAB concentration and products of synthesis were shown as black line and black dots. The yield of dADP and dATP were approximately of 6% (fraction numbers 36-46) and 94% (fraction numbers 50-75), respectively.

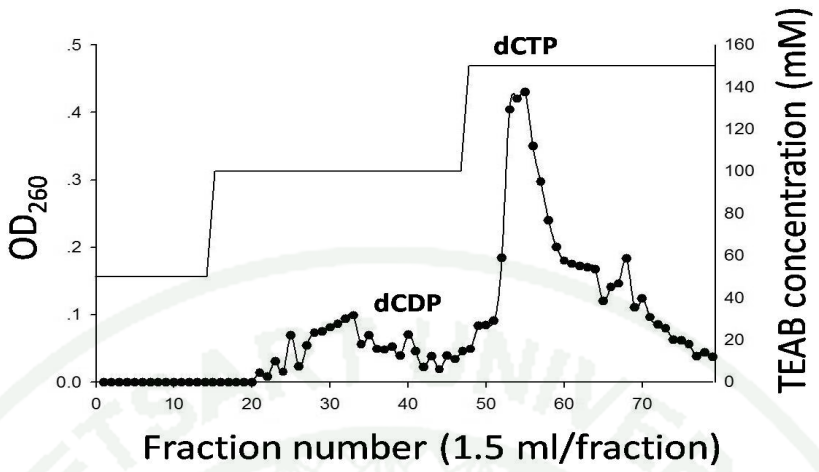

Figure 73 Analysis of dCTP synthesis in 100 mM-scale after incubation for 7 hours by DEAE-cellulose column. The TEAB concentration and products of synthesis were shown as black line and black dots. The yield of dCDP and dCTP were approximately of 10% (fraction numbers 34-43) and 90% (fraction numbers 46-69), respectively.

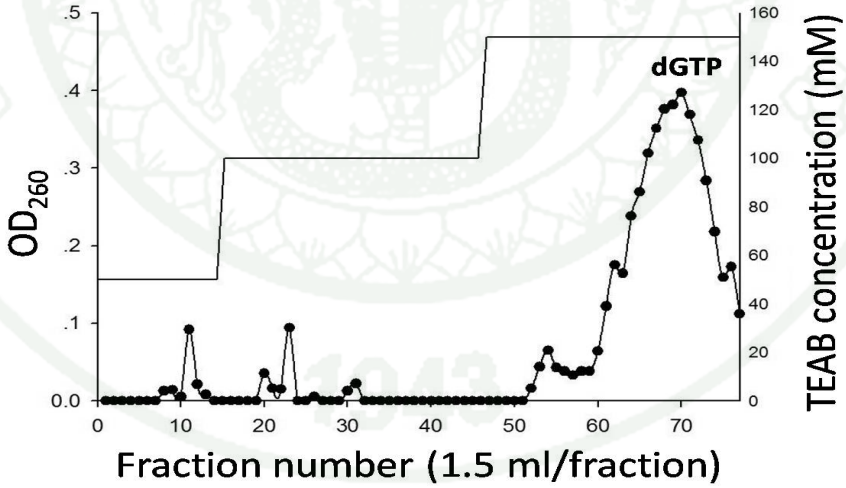

Figure 74 Analysis of dGTP synthesis in 50 mM-scale after incubation for 24 hours by DEAE-cellulose column. The TEAB concentration and products of synthesis were shown as black line and black dots. The yield of dGTP was approximately of 100% (fraction numbers 61-77).

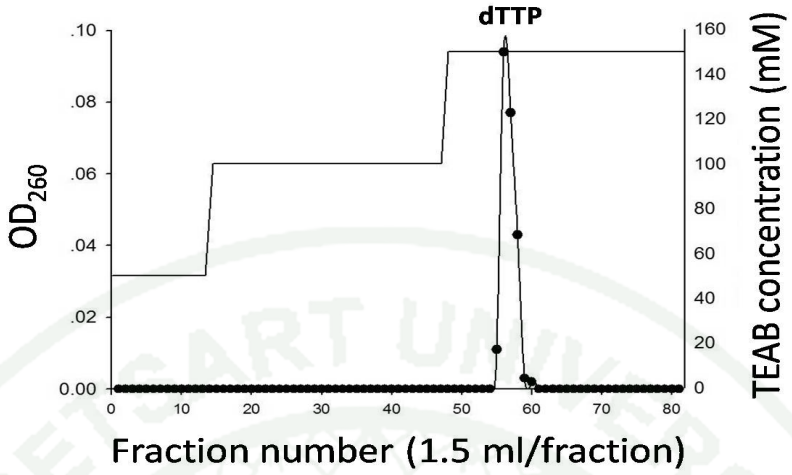

Figure 75 Analysis of dTTP synthesis in 10 mM-scale after incubation for 24 hours by DEAE-cellulose column. The TEAB concentration and products of synthesis were shown as black line and black dots. The yield of dTTP was approximately of 100% (fraction numbers 55-60).

3.6 PCR amplification for dNTP produced in gene amplification

The products from dNTP synthesis were checked by PCR amplification that they actually work in molecular research. After synthesis, the reactions were heat inactivated at 80°C for 15 minutes and centrifuged at 12,000 rpm for 15 minutes for separated aggregated enzyme. Then, the supernatant after centrifugation was precipitated dNTP by 50% ethanol and incubated at room temperature for two times. The precipitation of dCTP, dGTP and dTTP were approximately of 82%, 100% and 96%, respectively. For dATP, the precipitation should supplement with 1.6 M ammonium acetate. The precipitation of dATP was approximately of 82% (Table 15). The precipitated dNTP were resuspended with distilled deionized water and used for amplification at 0.2 mM for final concentration. The PCR amplification was used in protocol for amplification of *pyk* type I gene of *S. coelicolor*. The PCR product was analyzed by 1% agarose gel electrophoresis (Figure 76).

Table 15 The precipitation of dNTP by 50% ethanol

Types of dNTP	mM-scale (maximum rate)	% recovery
dATP	100 mM	82%
dCTP	100 mM	82%
dGTP	50 mM	100%
dTTP	10 mM	96%

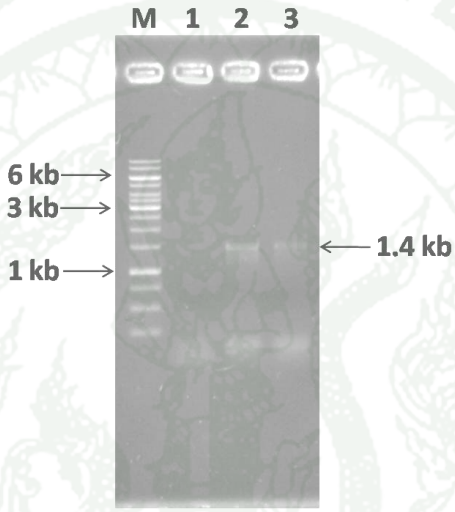

Figure 76 Analysis of PCR amplification by commercial dNTP and produced dNTP by 1% agarose gel electrophoresis. Lane M, DNA ladder; lane 1, PCR product by no template and dNTP, negative control; lane 2, PCR product by using commercial dNTP; lane 3, PCR product by using produced dNTP.

CONCLUSION

From the results and discussion, we can conclude as follows:

1. The nucleotide sequence of the putative type I and II *pyk* gene from *S. antibioticus* had been determined. The complete nucleotide sequence (1,437 bp) of type I *pyk* gene was obtained, whereas only partial sequence (1,173 bp) of the type II had been determined. The deduced amino acid sequence of the putative type I *pyk* gene of *S. antibioticus* is 478 amino acid residues.

2. The type I *pyk* gene of *S. coelicolor* was successfully cloned, overexpressed and purified. Recombinant type I ScPYK was estimated to have molecular weight of 51 kDa, but the recombinant type I ScPYK proteins showed two bands at approximately 51 and 60 kDa by SDS-PAGE. The recombinant type I ScPYK at 60 kDa may have been a phosphorylated form or error of protein translation.

3. In addition, the type I ScPYK formed inclusion bodies when expressed in *E. coli* BL21 (DE3). The inclusion bodies was solubilized by 4 M urea and refolded by dilution method. After refolding, the activity of type I ScPYK can be detected, but it should very low activity and unstable.

4. The predicted structures of type I SaPYK and type I ScPYK were similar. The predicted structures of type I SaPYK and type I ScPYK were similar with PYK from *B. stearothermophilus* that activated by AMP. When analysis of amino acid sequences by multiple sequences alignment and phylogenetic tree, type I SaPYK and type I ScPYK were highest similar with *Microbispora thermodiastatica* (64% and 61% identity) and *Corynebacterium glutamicum* (61% and 58% identity), respectively. In addition, the type I SaPYK and type I ScPYK were classified as the type II group, and were similar to type II PYK from *E. coli*, which is activated by AMP. Thus, the type I SaPYK and type I ScPYK may be AMP-activated enzymes.

5. *E. coli* type I PYK had been successfully used in combination with other kinases such as CMK, ADK or DNK in the synthesis of dNTP at 100 mM scale. Type

II PYK was found to be unstable and unsuitable for large scale synthesis of dNTP. Synthesis of dGTP and dTTP can be accomplished at 50 mM and 10 mM-scale when DNK as dNMP kinase. In the synthesis of dGTP, ATP but not dGTP can be used as the phosphoryl donor. In the synthesis of dTTP, dTTP can be as used as the phosphoryl donor.

LITERATURE CITED

Ahmed, S., A. Craney, M. Pimentel-Elardo and J.R. Nodwell. 2013. A synthetic, species-specific acivator of secondary metabolism and sporulation in *Streptomyces coelicolor*. **ChemBioChem** 14:83-91.

Akbari, N., K. Khajeh, S. Razaie, S. Mirdamadi and M. Shavandi 2010. High-level expression of lipase in *Escherichai coli* and recovery of active recombinant enzyme through *in vitro* refolding. **Protein Expression and Purification** 70:75-80.

Alam, M.T., Merlo, M.E., The STREAM Cousortium, Hodgson, D. A., Wellington, E. M. H., Takano, E., Breitling, R. 2010. Metabolic modeling and analysis of the metabolic switch in *Streptomyces coelicolor*. **BMC Genomics** 11:1471-2164.

Allen, S.C., and H. Muirhead. 1996. Refined three-dimensional structure of cat-muscle (M1) pyruvate kinase at a resolution of 2.6 A^{o}. **Acta Crystallographica** 52:499-504.

Allert, S., I. Ernest, A. Poliszcak, F.R. Opperdoes, P.A.M. Michels. 1991. Molecular cloning and analysis of two tandemly linked genes for pyruvate kinase of *Trypanosoma brucei*. **European Journal of Biochemistry** 200:19-27.

Aloysius, M.M., A.M. Zaitoun, T.E. Bates, A. Albasri, M. Ilyas, B.J. Rowlands and D.N. Lobo. 2009. Complete absence of M2-pyruvate kinase expression in benign pancreatic ductal epithelium and pancreaticobiliary and duodenal neoplasia. **BMC Cancer** 9:1-8.

Anastasiou, D., Y. Yu, W.J. Israelsen, J.K. Jiang, M.B. Boxer, B.S. Hong, W. Tempel, S. Dimov, M. Shen, A. Jha, H. Yang, K.R. Mattaini, C.M. Metallo, B.P. Fiske, K.D. Courtney, S. Malatrom, T.M. Khan, C. Kung, A.P. Skoumbourdis, H. Veith, N. Southall, M.J. Walsh, K.R. Brimacombe, W. Leister, S.Y. Lunt, Z.R. Johnson, K.E. Yen, K. Kunii, S.M. Davidson, H.R. Christofk, C.P. Austin, J. Inglese, M.H. Harris, J.M. Asara, G. Stephanopoulos, F.G. Salituro, S. Jin, L. Dang, D.S. Auld, H.W. Park, L.C. Cantley, C.J. Thomas and M.G. Vander Heiden. 2012. Pyruvate kinase M2 activators promote tetramer formation and suppress tumorigenesis. **Nature Chemical Biology** 8:839-847.

Anderson, A.S. and E.M.H. Wellington. 2001. The taxonomy of *Streptomyces* and related genera. **International Journal of Systematic and Evolutionary Microbiology** 51:797–814.

Anderson, J.C. and S.C. Peck. 2008. A simple and rapid technique for detecting protein phosphorylation using one-dimensional isoelectric focusing gels and immunoblot analysis. **The Plant Journal** 55:881-885.

Andre, C., J.E. Froehlich, M.R. Moll and C. Benning. 2007. A Heteromeric Plastidic Pyruvate Kinase Complex Involved in Seed Oil Biosynthesis in *Arabidopsis*. **Plant Cell** 19:2006-2022.

Arai, A., S. Masuda, A. Matsuyama, S. Murakami ans M. Nakajima. 1998. Molecular cloning and nucleotide sequence of the pyruvate kinase gene of an actinomycete *Microbispora thermodiastatica*. **Applied Microbiology Biotechnology** 49:272-276.

Arnold, K., L. Bordoli, J. Kopp and T. Schwede 2006. The SWISS-MODEL workspace: a web-based environment for protein structure homology modelling. **Bioinformatics** 122:195-201.

Axerio-Cilies, P., R.H. See, R. Zoraghi, L. Worral, T. Lian, N. Stoynov, J. Jiang, S. Kaur, L. Jackson, H. Gong, R. Swayze, E. Amandson, N.S. Kumar, A. Moreau, M. Hsing, N.C. Strynadka, W.R. McMaster, B.B. Finlay, L.J. Foster, R.N. Young, N.E. Reiner and A. Cherkasov. 2012. Cheminformatics-Driven Discovery of Selective, Nanomolar Inhibitors for Staphylococcal Pyruvate Kinase. **ACS Chemical Biology** 7:350-359.

Bakszt, R., A. Wernimont, A. Allali-Hassani, M.W. Mok, T. Hills, R. Hui and J.C. Pizarro. 2010. The Crystal Structure of *Toxoplasma gondii* Pyruvate Kinase 1. **PLoS ONE** 5.

Bao, J. and D.D.Y. Ryu. 2005. Biosynthesis Reaction Mechanism and Kinetics of Deoxynucleoside Triphosphates, dATP and dGTP. **Biotechnology and Bioengineering** 89:485-491.

———. 2007. Total Biosynthesis of Deoxynucleoside Triphosphates Using Deoxynucleoside Monophosphate Kinases for PCR Application. **Biotechnology and Bioengineering** 98:1-11.

Bao, J., G.A. Bruque and D.D.Y. Ryu. 2005. Biosynthesis of deoxynucleoside triphosphates, dCTP and dTTP: reaction mechanism and kinetics. **Enzyme and Microbial Technology** 36:350-356.

Baysdorfer, C. and J.A. Bassham. 1984. Spinach Pyruvate Kinase Isoforms Partial Purification and Regulatory Properties. **Plant Physiology** 74:374-379.

Bello, L.J., and M.J. Bessman. 1963. The Enzymology of Virus-infected Bacteria: IV. Purification and properties of the deoxynucleotide kinase induced by bacteriophage T2. **Journal of Biological Chemistry** 238:1777-1787.

Benjaphokee, S., P. Koedrith, C. Anuesukaree, T. Asvarak, M. Sugiyama, Y. Kaneko, C. Boonchird and S. Harashima. 2011. CDC19 encoding pyruvate kinase is important for high-temperature tolerance is *Saccharomyces cerevisiae*. **New Biotechnology** 29:166-176.

Bentley, S.D., K.F. Chater, A.M. Cerdeno-Tarraga, G.L. Challis, N.R. Thomson, K.D. James, D.E. Harris, M.A. Quail, H. Kieser, D. Harper, A. Bateman, S. Brown, G. Chandra, C.W. Chen, M. Collins, A. Cronin, A. Fraser, A. Goble, J. Hidalgo, T. Hornsby, S. Howath, C.H. Huang, T. Kieser, L. Larke, L. Murphy, K. Oliver, S. O'Neil, E. Rabbinowitsch, M.A. Rajandream, K. Rutherford, S. Rutter, K. Seeger, D. Saunder, S. Sharp, R. Squares, S. Squares, K. Taylor, T. Warren, A. Wietzorrek, J. Woodward, B.G. Barrell, J. Parkhill and D.A. Hopwood. 2002. Complete genome sequence of the model actinomycetes *Streptomyces coelicolor*. **Nature** 417:141-147.

Bergey, D.H. 1919. Thermophilic bacteria. **Journal of Bacteriology** 4:301-306.

Berry, M.B., E. Bae, T.R. Bilderback, M. Glaser and G.N. Phillips, Jr. 2006. Crystal Strcture of ADP/AMP Complex of *Escherichia coli* Adenylate Kinase. **Proteins: Structure, Function, and Bioinformatics** 62:555-556.

Bessman, M.J., I.R. Lehman, E.S. Simms and A. Kornberg. 1957. Enzymatic Synthesis of Deoxyribonucleic Acid II. General properties of the reaction. **Journal of Biological Chemistry** 233:171-177.

Björnsson, A. and L.A. Isaksson. 1993. UGA Codon Context Which Spans Three Codons: Reversal by ms^2i^6A37 in tRNA, Mutation in *rpsD*(S4) or Streptomycin. **Journal of Molecular Biology** 232:1017-1029.

Bornmann, L., B. Hess and H. Zimmermann-Telschow. 1974. Mechanism of Renaturation of Pyruvate Kinase os *Saccharomyces carlsbergensis*: activation by L-Valine and Magnesium and Manganese Ions. **Proceeding of the National Academy of Sciences of the United States of America** 71:1525-1529.

Boulé, J.-B, E. Johnson, F. Rougeon and C. Papanicolaou. 1998. High-Level Expression of Murine Terminal Deoxynucleotide Transferase in *Escherichia coli* Grown at Low Temperature and Overexpression *arg*U tRNA. **Molecular Biotechnology** 10:199-208.

Bourniquel, A.A., F. Desiere and B. Mollet. 2002. Purification and characterization of the pyruvate kinase of *Lactobacillus delbrueckii* subsp. *lactis*. **International Dairy Journal** 12:821-829.

Bradford, M.M. 1976. A rapid and sensitive method of microgram quantities of proteins utilizing the principle of protein-dye binding. **Anal. Biochem** 72:248-264.

Briozzo, P., B. Golinelli-Pimpaneau, A.-M. Gilles, J.-F. Gaucher, S. Burlacu-Miron, H. Sakamoto, J. Janin and O. Barzu. 1998. Structures of *Escherichia coli* CMP kinase alone and in complex with CDP: a new fold of the nucleoside monophosphate binding domain and insights into cytosine nucleotide specificity. **Structure** 6:1517-1527.

Broida, J. and J. Abelson. 1985. Sequence organization and control of transcription in the bacteriophage T4 tRNA region. **Journal of Molecular Biology** 185:545-563.

Brune, M., R. Schunmann and F.W.ttinghofer. 1985. Cloning and sequencing of the adenylate kinase gene *(adk)* of *Escherichia coli*. **Nucleic Acid Reseach** 13:7139-7151.

Brush, G.S., S.K. Bhatnagar and M.J. Bessman. 1990. Bacteriophage T4 Deoxynucleotide Kinase: Gene Cloning and Enzyme Purification. **Journal of Bacteriology** 172:2935-2939.

Bucurenci, N., H. Sakamoto, P. Briozzo, N. Palibroda, L. Serina, R.S. Sarfati, G. Labesse, G. Briand, A. Danchin, O. Barzu and A.M. Gilles. 1995. CMP Kinase from *Escherichia coli* Is Structurally Related to Other Nucleoside Monophosphate Kinases. **Journal of Biological Chemistry** 271:2856-2862.

Chambers, R.W. and H.G. Khorana. 1958. Nucleoside Polyphosphates. VII. The Use of Phosphoramidic Acids in the Synthesis of Nucleoside-5' Pyrophosphates. **Journal of The American Chemical Society** 80:3749-3752.

Chambers, R.W., J.G. Moffatt and H.G. Khorana. 1957. Nucleotside Polyphosphate. IV. A New Synthesis of Guanosine 5'-Phosphate. **Journal of The American Chemical Society** 79:3747-3753.

Chan, M., D.S.H. Tan and T.S. Sim. 2007. *Plasmodium falciparum* pyruvate kinase as a novel target for antimalarial drug-screening. **Travel Medicine and Infectious Disease** 5:125-131.

Chanaton, B. and E. Gottlieb. 2012. Rocking cell metabolism: revised functions of the key glycolytic regulator PKM2 in cancer. **Trends in Biochemical Sciences** 37:309-316.

Chang, L.S., S.R. Lin and C.C. Yang. 2001. Refolding of Taiwan cobra neurotoxin: intramolecular cross-link affects its refolding reaction. **Archives of Biochemistry and Biophysics** 387:289-296.

Changeux, J.-P., and S.J. Edelstein. 2005. Allosteric Mechanisms of Signal Transduction. **Science** 308:1424-1427.

Chen, B.Y. and H.W. Janes. 2002. **PCR Cloning Protocols**. Second ed. Humana Press.

Christofk, H.R., M.G.V. Heiden, M.H. Harris, A. Ramanathan, R.E. Gerszten, R. Wei, M.D. Fleming, S.L. Schreiber and L.C. Cantley. 2008. The M2 splice isoform of pyruvate kinase is important for cancer metabolism and tumor growth. **Nature** 452:230-234.

Cochrane, V. W. 1955. The metabolism of species of Streptomyces VIII. Reaction of the Embden - Meyerhof - Parnas sequence in *Streptomyces coelicolor*. **Journal of Bacteriology** 69:256-263.

Cook, W.J., O. Senkovich, K. Aleem and D. Chattopadhyay. 2012. Crystal Structure of *Cryptosporidium parvum* Pyruvate Kinase. **PLoS ONE** 7.

Corrêa, D.H.A. and C.H.I. Ramos. 2009. The use of circular dichroism spectroscopy to study protein folding, form and function. **African Journal of Biochemistry Research** 3:164-73.

Cottam, G.L., P.F. Hollenberg and M.J. Coon. 1969. Subunit Structure of Rabbit Muscle Pyruvate Kinase. **Journal of Biological Chemistry** 244:1481-1486.

Cytrynska, M., M. Frajnt and T. Jakubowicz. 2001. *Saccharomyces cerevisiae* pyruvate kinase Pyk1 is PKA phosphorylation substrate in vitro. **FEBS Microbiology Letters** 203:223-227.

D'Auria, S., M. Rossi, P. Herman and J.R. Lakowicz. 2000. Pyruvate kinase from the thermophilic eubacterium *Bacillus acidocaldarius* as probe to monitor the sodium concentrations in the blood. **Biophysical Chemistry** 84:167-176.

Denton, H., S.M.A. Brown, C.W. Roberts, J. Alexander, V. McDonald, K.W. Thong and G.H. Coombs. 1996. Comparison of the phosphofructosekinase and pyruvate kinase activities of *Cryptosporidium parvum*, *Eimeria tenella* and *Toxoplasma gondii*. **Molecular and Biochemical Parasitology** 76:23-29.

Dolle, C., and M. Ziegler. 2009. Application of a coupled enzyme assay to characterize nicotinamide riboside kinases **Analytical Biochemistry** 385:377-379.

Dombrauckas, J.D., B.D. Santarsiero and A.D. Mesecar. 2005. Structural basis for tumor pyruvate kinase M2 allosteric regulation and catalysis. **Biochemistry** 44:9417-9429.

Duckworth, D.H. and M.J. Bessman. 1967. The Enzymology of Virus-infeected Bacteria X. A biochemical-genetic study of the deoxynucleotide kinase induced by wild type and amber mutants of phage T4. **Journal of Biological Chemistry** 242:2877-2885.

Edgar, R.C. 2004. MUSCLE: multiple sequence alignment with high accuracy and high throughput. **Nucleic Acid Reseach** 32:1792-1797.

Ferguson, E.C. and J.C. Rathmell. 2008. New roles for pyruvate kinase M2: working out the Warburg effect. **Trends Biochemical sciences** 33:359-362.

Fothergill-Gilmore, L.A., D.J. Rigden, P.A.M. Michels and S.E.V. Phillips. 2000. *Leishmania* pyruvate kinase: the crystal structure reveals the structural basis of its unique regulatory properties. **Biochemical Society Transactions** 28:186–190.

Fricke, J., J. Neuhard, R.A. Kellin and S. Pedersen. 1995. The cmk Gene Encoding Cytidine Monophosphate Kinase Is Located in the rpsA Operon and Is Required for Normal Replication Rate in *Escherichia coli*. **Journal of Bacteriology** 177:517-523.

Galperin, M.Y. and E.V. Koonin. 2000. Who's your neighbor? New computational approaches for functional genomics. **Nature Biotechnology** 18:609-613.

Garcìa-Fruitòs, E., N.Gonzàlez-Montalbàn, M. Martìnez-Alonso, U. Rinas and A. Villaverde. 2009. Systems-Level Analysis of Protein Quality in Inclusion Body-Forming *Escherichia coli* Cells. **Systems Biology and Biotechnology of Escherichia coli**:295-326.

Garrido-Pertierra, A. and R.A. Cooper. 1983. Evidence for two distinct pyruvate kinase genes in *Escherichia coli* K-12. **FEBS** 162:420-422.

Ge, Y. and N.W. Charon. 1997. Identification of a large motility operon in *Borrelia burgdorferi* by semi-random PCR chromosome walking. **Gene** 189:195-201.

Gonzalez, B., F. Ceciliani and A. Galizzi. 2003. Growth at low temperature suppresses readthrough of the UGA stop codon during the expression of *Bacillus subtilis flgM* gene in *Escherichia coli*. **Journal of Biotechnology** 101:173-180.

Guindon, S. and O. Gascuel. 2003. A simple, fast, and accurate algorithm to estimate large phylogenies by maximum likelihoop. **Systematic Biology** 52:696-704.

Gustafsson, C., S. Govindarajan and J. Minshull. 2004. Codon bias and heterologous protein expression. **Trends Biotechnology** 22:346-353.

Hardisson, C., M.B. Manzanal, J.A. Salas and J.E. Suarez 1978. Fine Structure, Physiology and Biochemistry of Arthrospore Germination in *Streptomyces antibioticus*. **Journal of General Microbiology** 105:203-214.

Haug, U., M.N. Wente, C.M. Seiler, D. Rothenbacher, M.W. Buchler, and H. Brenner. 2006. Tumor M2 Pyruvate Kinase as a Stool Marker for Colorectal Cancer: Stability at Room Temperature and Implications for Application in the Screening Setting. **Clinical Chemistry** 52:782-784.

Hohn, T.M., and J.L. Paznokas. 1987. Purification and Properties of Two Isozymes of Pyruvate Kinase from *Mucor racemosus*. **Journal of Bacteriology** 169:3525-3530.

Holyoak, T., B. Zhang, J. Deng, Q. Tang, C.B. Prasannan and A.W. Fenton. 2013. Energetic Coupling between an Oxidizable Cysteine and the Phosphorylatable N-Terminus of Human Liver Pyruvate Kinase. **Biochemistry** 52:466-476.

Hopwood, D.A. 1999. Forty years of genetics with *Streptomyces*: from *in vivo* through *in vitro* to *in silico*. **Microbiology** 145:2183–2202.

Hopwood, D.A., M.J. Bibb, K.F. Chater, T. Kieser, C.J. Bruton, H.M. Kieser, D.J. Lydiate, C.P. Smith, J.M. Ward and H. Schrempf. 1985. **Genetic Manipulation of *Streptomyces*: A Laboratory Manual**. England, The John Innes Foundation, Norwich.

Howhan, P. 2004. **Enzymatic synthesis of deoxynucleoside triphosphates: cloning, overexpression, and purification of cytidine monophosphate kinase,nucleoside diphosphate kinase,and pyruvate kinase from *Escherichia coli***, M.S. Thesis, Kasetsart University.

Huang, H.-D., T.-Y. Lee, S.-W. Tzeng, and J.-T. Horng. 2005. KinasePhos: a web tool for identifying protein kinase-specific phosphorylation sites. **Nucleic Acid Reseach** 33:226-229.

Ignacak, J., and M.B. Stachurska. 2003. The dual activity of pyruvate kinase type M_2 from chromatin extracts of neoplastic cells. **Comparative Biochemistry and Physiology Part B** 134:425-433.

Ikeda, H., J. Ishikawa, A. Hanamoto, M. Shinose, H. Kikuchi,T. Shiba,Y. Sakaki, M. Hattori, and S. Omura. 2003. Complete genome sequence and comparative analysis of the industrial microorganism *Streptomyces avermitilis*. **Nature Biotechnology** 21:526-531

Jakimowicz, D. 2007. Chromosome segregation and cell division during the growth and differentiation of *Streptomyces*. **Postepy Hig Med Dosw** 61:565-575.

Jetten, M.S.M., M.E. Gubler, S.H. Lee and A.J. Sinskey. 1994. Structural and Functional Analysis of Pyruvate Kinase from *Corynebacterium glutamicum*. **Applied and Enviromental Microbiology** 60:2501-2507.

Jocelyn, Q.S., P. Edathil, R. Wu, E.D. Smidansky, C.E. Cameron and B.R. Peterson. 2008. One-Pot Synthesis of Nucleoside 5'-Triphosphates from Nucleoside 5'-*H*-Phosphonates. **Orgenic Letters** 10:1703-1706.

Jurica, M.S., A. Mesecar, P.J. Heath, W. Shi, T. Nowak and B.L. Stoddard. 1998. The allosteric regulation of pyruvate kinase by fructose-1,6-bisphosphate. **Structure** 6:195-210.

Koch, T., N. Lamm and W. Ruger. 1989. Sequencing, cloning and overexpression of genes of bacteriophage T4 between map positions 74.325 and 77.184. **Nucleic Acid Reseach** 17:4392.

Kumar, N.S., E.A. Amandoron, A. Cherkasov, B.B. Finlay, H. Gong, L. Jackson, S. Kaur, T. Lian, A. Moreau, C. Labriere, N.E. Reiner, R.H. See, N.C. Strynadka, L. Thorson, E.W.Y. Wong, L. Worrall, R. Zoraghi and R.N. Young. 2012. Optimization and structure-activity relationships of a series of potent inhibitors of methicillin-resistant *Staphylococcus aureus* (MRSA) pyruvate kinase as novel antimicrobial agents. **Bioorganic & Medicinal Chemistry** 20:7069-7082.

Ladner, W.E. and G.M. Whitesides. 1985. Enzymatic Synthesis of DeoxyATP Using DNA as Starting Material. **Journal of Organic Chemistry** 50:1076-1079.

Larsen, T.M., L.T. Laughlin, H.M. Rayment, I. Rayment and G.H. Reed. 1994. Structure of rabbit muscle pyruvate kinase complexed with Mn^{2+}, K^{+}, and pyruvate. **Biochemistry** 33:6301-6309.

Larsen, T.M., M.M. Benning, G.E. Wesenberg, I. Rayment and G.H. Reed. 1997. Ligand-Induced Domain Movement in Pyruvate Kinase: Structure of the Enzyme from Rabbit Muscle with Mg^{2+}, K^{+}, and L-Phospholactate at 2.7 A^{o} Resolution. **Archives of Biochemistry and Biophysics** 345:199-206.

Larsen, T.M., M.M. Benning, I. Rayment and G.H. Reed. 1998. Structure of the bis(Mg^{2+})-ATP-oxalate complex of the rabbit muscle pyruvate kinase at 2.1 A^{o} resolution: ATP binding over a barrel. **Biochemistry** 18:6247-6255.

Lehman, I.R., M.J. Bessman, E.S. Simms and A. Kornberg. 1957. Enzymatic Synthesis of Deoxyribonucleic Acid I. Preparation of substrates and partial purification of an enzyme from *Escherichia coli*. **Journal of Biological Chemistry** 233:163-170.

Lilie, H., E. Schwarz and R. Rudolph. 1998. Advance in refolding of protein produces in *E. coli*. **Current Opinion in Biotechnology** 9:497-501.

Lin, Y.S., H.M. Kieser, D.A. Hodwood and C.W. Chen. 2006. The chromosomal DNA of *Streptomyces lividans* 66 is linear. **Molecular Microbiology** 10 (5):923-933.

Liu, H.-S., and C.-K. Chang. 2003. Chaperon solvent plug to enhance protein refolding in size exclusion chomatography. **Enzyme and Microbial Technology** 33:424-429.

Loria, R., J. Kers and M. Joshi. 2006. Evolution of Plant Pathogenicity in *Streptomyces*. **Annual Review of Phytopathology** 44:469-487

Lu, Q. and M. Inouye. 1996. Adenylate kinase complements nucleoside diphosphate kinase deficiency in nucleotide metabolism. **Proceeding of the National Academy of Sciences of the United States of America** 93:5720-5725.

Machida, S., S. Ogawa, S. Xiaohua, T. Takaha, K. Fujii and K. Hayashi. 2000. Cycloamylose as an efficient artificial chaperon for protein refolding. **FEBS Letters** 486:131-135.

Malcovati, M. and G. Valentini. 1982. AMP- and Fructose 1,6-Bisphosphate-Activated Pyruvate Kinase from *Escherichia coli*. **Methods in Enzymology** 90:170-179.

Matsuo, K., R. Yonehara and K. Gekko. 2004. Secondary-Structure Analysis of Proteins by Vacuum-Ultraviolet Circular Dichroism Spectroscopy. **Journal of Biochemistry** 135:405-411.

McGregor, J.F. 1954. Nuclear Division and the Life Cycle in a *Streptomyces* sp. **J. gen. Microbiol** 11:52-56.

Mettevi, A., G. Valentini, M. Rizzi, M.L. Speranza, M. Bolognesi and A. Coda. 1995. Crystal structure of *Escherichia coli* pyruvate kinase type I: molecular basis of the allosteric transition. **Structure** 3:729-741.

Mettevi, A., M. Bolognesi and G. Valentini. 1996. The allosteric regulation of pyruvate kinase. **FEBS Letters** 389:15-19.

Mishra, S.K., R.E. Gordon and D.A. Barnett. 1980. Identification of Nocardiae and Streptomycetes of Medical Importance. **Journal of Clinical Microbiology** 11 (6):728-736.

Moffatt, J.G. 1964. A General Synthesis of Nucleoside-5' Triphosphates. **Canadian Journal of Chemistry** 42:599-604.

Monod, J., J. Wyman and J.-P. Changeux. 1965. On the Nature of Allosteric Transition: A Plausible Model. **Journal of Molecular Biology** 12:88-118.

Moran, L.A., H.R. Horton, K.G. Scrimgeour and M.D. Perry. 2012. **Principles of Biochemistry**. Fifth ed. Person Education.

Morgan, H.P., I.W. McNae, K.-Y. Hsin, P.A.M. Michels, L.A. Forthergill-Gilmore and M.D. Walkinshaw. 2010. An improved strategy for the crystallization of *Leishmania mexicana* pyruvate kinase. **Structure Biology and Crystallization Communications** 66:215-218.

Morgan, H.P., I.W. McNae, M.W. Nowicki, V. Hannaert, P.A.M. Michels, L.A. Forthergill-Gilmore and M.D. Walkinshaw. 2010. Allosteric Mechanism of Pyruvate Kinase from *Leishmania mexicana* Uses a Rock and Lock Model. **Journal of Biological Chemistry** 285:12892-12898.

Morgan, H.P., I.W. McNae, M.W. Nowicki, W. Zhong, P.A.M. Michels, D.S. Auld, L.A. Forthergill-Gilmore and M.D. Walkinshaw. 2011. The Trypanocidal Drug Suramin and Other Trypan Blue Mimetics Are Inhibitiors of Pyruvate Kinases and Bind to the Adenosine Site. **Journal of Biological Chemistry** 286:31232-31240.

Muirhead, H., D.A. Clayden, D. Barford, C.G. Lorimerl, L.A. Fothergill-Gilmore, E. Schiltz and W. Schmitt. 1986. The structure of cat muscle pyruvate kinase. **EMBO Journal** 5:475-481.

Muller, R. 1908. Eine Diphtheridee und eine Streptothrix mit gleichen blauen Farbstoff sowie Untersuchungen über Streptothrixarten in allegemeinen. **Abteilung I** 46:195-212.

Munoz, M.E. and E. Ponce. 2003. Pyruvate kinase: current status of regulatory and functional properties. **Comparative Biochemistry and Physiology Part B** 135:197-218.

Murphy, M.M., J. Marsillach, J. Camps, J. Fernandez-Ballart, B. Mackness, M. Mackness, N. Ferre and J. Joven. 2006. Tumor M2 Pyruvate Kinase as a Stool Marker for Colorectal Cancer: Stability at Room Temperature and Implications for Application in the Screening Setting. **Clinical Chemistry** 52:782-784.

Narawongsanont, R. 2010. **Enzymatic Synthesis of Deoxycytidine Triphosphate: Overexpression and Purification of Recombinant Phosphoglycerate Mutase and Enolase from *Escherichia coli*** M.S. Thesis, Kasetsart University.

Nieselt, K., F. Battke, A. Herbig, P. Bruheim, A. Wentzel, Ø.M. Jakobsen, H. Sletta, M.T. Alam, M.E. Merlo, J. Moore, W.A.M. Omara, E.R. Morrissey, M.A. Juarez-Hermosillo, A. Rodríguez-García, M. Nentwich, L. Thomas, M. Iqbal, R. Legaie, W.H. Gaze, G.L. Challis, R.C. Jansen, L. Dijkhuizen, D.A. Rand, D.A. Wild, M. Bonin, J. Reuther, W. Wohlleben, M.C.M. Smith, N.J. Burroughs, J.F. Martin, D.A. Hodgson, E. Takano, R. Breitling, T.E. Ellingsen and E.M.H. Wellington. 2010. The dynamic architecture of the metabolic switch in *Streptomyces coelicolor*. **BMC Genomics** 11.

Ochman, H., A.S. Gerber and D.L. Hartl. 1988. Genetic applications of an inverse polymerase chain reaction. **Genetics** 120:621-625.

Ohnishi, Y., J. Ishikawa, H. Hara, H. Suzuki, M. Ikenoya, H. Ikeda, A. Yamashita, M. Hattori and S. Horinouchi. 2008. Genome sequence of the streptomycin-producing microorganism *Streptomyces griseus* IFO 13350. **Journal of Bacteriology** 190:4050-4060

Olson, E.N., H.-H. Arnold, P.W.J. Rigby and B.J. Wold. 1996. Know you neighbors: Three phenotypes in Null mutants of the Myogenic bHLH gene *MRF4*. **Cell** 84:1-4.

Ou, W.-B., W. Luo, Y.-D. Park and H.-M. Zhou. 2001. Chaperon-like activity of peptidyl-prolyl cis-trans isomerase during creatine kinase refolding. **Protein Science** 10:2346-2353.

Pandza, K., G. Pfalzer, J. Cullum and D. Hranueli. 1997. Physical mapping shows that the unstable oxytetracycline gene cluster of *Streptomyces rimosus* lies close to one end of the linear chromosome. **Microbiology** 143:1493-1501.

Pang, X., X. Zhou, Y, Sun and Z, Deng. 2002. Physical Map of the Linear Chromosome of *Streptomyces hygroscopicus* 10-22 Deduced by Analysis of Overlapping Large Chromosomal Deletions. **J. Bacteriol** 184 (7):1958–1965.

Pilhofer, M., A.P. Bauer, M. Schrallhammer, L. Richter, W. Ludwig, K.-H. Schleifer and G. Petroni. 2007. Characterization of bacterial operons consisting of two tubulins and a kinesin-like gene by the novel Two-Step Gene Walking method. **Nucleic Acid Reseach** 35.

Plaxton, W.C. 1989. Molecular and immunological characterization of plastid and cytosolic pyruvate kinase isozymes from castor-oil-plant endosperm and leaf. **European Journal of Biochemistry** 181:443-451.

Ponce, E., N. Flores, A. Martinez, F. Valle and F. Bolivar. 1995. Cloning of the Two Pyruvate Kinase Isoenzyme Structural Genes from *Escherichia coli*: the Relative Roles of These Enzymes in Pyruvate Biosynthesis. **Journal of Bacteriology** 177:5719-5722.

Poopanitpan, N. 2005. **Cloning, over-expression and purification of deoxynucleotide kinase, adenylate kinase and enolase and enzymatic synthesis of 2'-Deoxyadenosine 5'-Triphosphate**, M.S. Thesis, Kasetsart University.

Pornbanlualap, S. and P. Chalopagorn. 2011. Adenosine deaminase from *Streptomyces coelicolor*: Recombinant expression, purification and characterization. **Protein Expression and Purification** 78:167-173.

Portela, P., S. Howell, S. Moreno and S. Rossi. 2002. *In vivo* and *in vitro* phosphorylation of two isoform of yeast pyruvate kinase by protein kinase A. **Journal of Biological Chemistry** 277:30477-30487.

Portela, P., S. Moreno and S. Rossi. 2006. Characterization of yeast pyruvate kinase 1 as a protein kinase A substrate, and specificity of the phosphorylation site sequence in the whole protein. **Biochemistry Journal** 396:117-126.

Porter, D.H., and J.M. Cardenas. 1980. Analysis of the Renaturation Kinetics of Bovine Muscle Pyruvate Kinase. **Biochemistry** 19:3447-3452.

Price, N.C. and E. Stevens. 1983. The refolding of denatured rabbit muscle pyruvate kinase. **Biochemistry Journal** 209:863-770.

Primrose, S.B. and R.M. Twyman. 2006. **Principles of Gene Manipulation and Genomics**. Seventh ed. Blackwell Publishing.

Procko, E., M.L. O'Mara, W.F.D. Bennett, D.P. Tieleman and R. Gaudet. 2009. The mechanism of ABC transporters: general lessons from structural and functional studied of an antigenic peptide transporter. **FASEB Journal** 23:1287-1302.

Qiu, J., and Y. Zhuo. 2011. Overexpression of the ABC transporter AvtAB increases avermectin production in *Streptomyces avermitilis*. **Applied Microbiology and Biotechnology** 92:337-345.

Rigden, D.J., S.E.V. Phillips, P.A.M. Michels and L.A. Fothergill-Gillmore. 1999. The Structure of Pyruvate Kinase from *Leishmania mexicana* Reveals Details of the Allosteric Transition and Unusual Effector Specificity. **Journal of Biological Chemistry** 291:615-635.

Rodriguez, A.M., C. Olano, C. Vilches, C. Mendez and J. Salas. 1993. *Streptomyces antibioticus* contains at least three oleandomycin-resistance determinants, one of which shows similarity with proteins of the ABC-transporter superfamily. **Molecular Microbiology** 8:571-582.

Sakai, H. 2004. Possible Structure and Functional of the Extra C-Terminal Sequence of Pyruvate Kinase from *Bacillus stearothermophilus*. **Journal of Biochemistry** 136:471-476.

Sambrook, J., E.F. Fritsch and T. Maniatis. 1989. **Molecular Cloning: A Laboratory Manual**. Cold Spring Harbor Laboratory Press. Original edition. New York Original Edition.

Sauer, U. and B.J. Eikmanns. 2005. The PEP-pyruvate-oxaloacetate node as the switch point for carbon flux distribution in bacteria. **FEMS Microbiology Reviews** 29:765-794.

Shirano, Y., and D. Shibata. 1990. Low teperature cultivation of *Escherichia coli* carrying a rice lipoxygenase L-2 cDNA produces a soluble and active enzyme at a high level. **FEBS** 271:128-130.

Singh, J.P., M.D. Smith and J.D. Levin 2000. **Methods of Making Nucleotides**. US PCT/US00/04643

Somani, B.L., G. Valentini and M. Malcovati. 1977. Purification and molecular properties of the AMP-activated pyruvate kinase from *Escherichia coli*. **Biochimica et Biophysica Acta** 482:52-63.

Suzuki, K., S. Ito, A. Shimizu-Ibuka and H. Sakai. 2008. Crystal structure of pyruvate kinase from *Geobacillus stearothermophilus*. **Journal of Biochemistry** 144:305-312.

Swain, S.D., S.L. Helgerson, A.R. Davis, L.K. Nelson and M.T. Quinn. 1997. Analysis of Activation-induced Conformational Changes in $p47^{phox}$ Using Tryptophan Fluorescence Spectroscopy. **Journal of Biological Chemistry** 272:29502-29510.

Tamames, J., G. Casari, C. Ouzounis and A. Valencia. 1997. Conserved clusters of functionally related genes in two bacterial genomes. **Journal of Molecular Evolution** 44:66-73.

Tanaka, K., H. Sakai, T. Ohta and H. Matsuzawa. 1995. Molecular Cloning of the Genes for Pyruvate Kinase of Two Bacilli, *Bacillus phychrophilus* and *Bacillus licheniformis*, and Comparison of the Properties of the Enzymes Produced in *Escherichia coli*. **Bioscience Biotechnology and Biochemistry** 59:1536-1542.

Tani, K., H. Fujii, S. Nagata and S. Miwa. 1988. Human liver type pyruvate kinase: Complete amino acid sequence and the expression in mammalian cells. **Proceeding of the National Academy of Sciences of the United States of America** 85:1792-1795.

Technikova-Dobrova, Z., A.M. Sardanelli and S. Papa. 1991. Spectrophotometer determination of functional characteristics of protein kinase with coupled enzymatic assay. **FEBS** 292:69-72.

Teplyakov, A., P. Sebastiao, G. Obmolova, A. Perrakis, G.S. Brush, M.J. Bessman and K.S. Wilson. 1996. Crytal structure of the bacteriophage T4 deoxynucleotide kinase with its substrates dGMP and ATP. **The EMBO Journal** 15:3487-3497.

Thompson, J.D., D.G. Higgins and T. J. Gibson. 1994. CLUSTAL W: improving the sensilivity of progressive multiple sequence alignment through sequence weighting, position-specific gap penalties and wight matrix choice. **Nucleic Acid Reseach** 22:4673-4680.

Tulloch, L.B., H.P. Morgan, V. Hannaert, P.A. Michels, L.A. Fothergill-Gilmore and M.D. Walkinshaw. 2008. Sulfate removal induces a major conformational chang in *Leishmania mexicana* pyruvate kinase in the crystalline state. **Journal of Molecular Biology** 383:615-626.

Umeyama, T., A. Naruoka and S. Horinouchi. 2000. Genetic and biochemical characterization of a protein phosphatase with dual substrate specificity in *Streptomyces coelicolor* A3(2). **GENE** 258:55–62.

Valentini, G., A. Mattevi, D. Barilla, A. Galizzi and M. L. Speranza. 1997. Recombinant Pyruvate Kinase Type I from *Escherichia coli*: Overexpression and Revised C-Terminus of the Polypeptide. **Biological Chemistry** 378:719-721.

Valentini, G., L. Chiarelli, R. Fortin, M.L. Speranza, A. Galizzi and A. Mattevi. 2000. The allosteric regulation of pyruvate kinase. **Journal of Biological Chemistry** 275:18145-18152.

Valentini, G., L. Chiarellis, R. Fortin, M.L. Speranza, A. Galizzi and A. Mattevi. 2000. The Allosteric Regulation of Pyruvate Kinase: A site-directed mutagenesis study. **Journal of Biological Chemistry** 275:18145-18152.

Valentini, G., L.R. Chiarellis, R. Fortin, M. Dolzan, A. Galizzi, D.J. Abraham, C. Wang, P. Bianchi, A. Zanella and A. Mattevi. 2002. Structure and Function of Human Erythrocyte Pyruvate Kinase: Molecular basis of Nonspherocytic Anemia. **Journal of Biological Chemistry** 277:23807-23814.

Vallejo, L.F., and U. Rinas. 2004. Strategies for the recovery of active proteins through refolding of bacterial inclusion body proteins. **Microbial Cell Factories** 3.

Vasina, J.A., and F. Baneyx. 1997. Expression of Aggregation-Prone Recombinant Proteins at Low Temperatures: A Comparative Study of the *Escherichia coli cspA* and *tac* Promoter Systems. **Protein Expression and Purification** 9:211-218.

Wallace, B.A. and R.W. Janes. 2001. Synchrotron radiation circular dichroism spectroscopy of proteins: secondary structure, fold recognition and structural genomics. **Current Opinion in Chemical Biology** 5:567-571.

Wang, P.-F., W.R.P. Novak, J.S. Cantwell, P.C. Babbitt, M.J. McLeish and G.L. Kenyon. 2002. Expression of *Torpedo californica* creatine kinase in *Escherichia coli* and purification from inclusion bodies. **Protein Expression and Purification** 26:89-95.

Wang, Z., Q. Xiang, G. Wang, H. Wang, and Y. Zhang. 2011. Optimizing expression and purification of an ATP-binding gene gsiA from *Escherichia coli* K-12 by using GFP fusion. **Genetic and Molecular Biology** 34:661-668.

Waskman, S.A. and A.T. Henrici. 1943. The Nomenclature and Classification of The Actinomycetes. **Journal of Bacteriology** 46 (4):337-341.

Waskman, S.A. and H.B. Woodruff. 1941. *Actinomyces antibioticus*, A New Soil Organism Antagonistic to Pathogenic and Non-pathogenic Bacteria. **Journal of Bacteriology** 42:231-249.

Waygood, E.B., and B.D. Sanwal. 1974. The Control of Pyruvate Kinase of *Escherichia coli*. I. Physicochemical and regulatory properties of the enzyme activated by Fructose 1,6-diphosphate. **Journal of Biological Chemistry** 249:265-274.

Waygood, E.B., M.K. Rayman and B.D. Sanwal. 1975. The Control of Pyruvate Kinase of *Escherichia coli*. II. Effectors and Regulatory Properties of the Enzyme Activated by Ribose 5-Phosphate. **Canadian Journal of Biochemistry** 53:444-454.

Weiss, S. 2000. Measuring conformational dynamics of biomolecules by single molecule fluorescence spectroscopy. **Nature Structural Biology** 7:724-729.

Weng, Y.-P., F.-C. Hsu, W.-S. Yang and H.-P. Chen. 2006. Optimization of the overexpression of glutamate mutase S component under the control of T7 system by using lactose and IPTG as the inducers. **Enzyme and Microbial Technology** 38:465-469.

White, T.J., N. Arnheim and H.A. Erlich. 1989. The polymerase chain reaction. **Trends in Genetics** 5:185-189.

Wildermuth, H., and D.A. Hopwood. 1970. Septation during sporulaion in *Streptomyces coelicolor*. **J. gen. Microbiol** 60:51-59.

Wooll, J.O., R.H.E. Friesen, M.A. White, S.J. Watowich, R.O. Fox, J.C. Lee and E.W. Czerwinski. 2001. Structural and Functional Linkages Between Subunit Interfaces in Mammalian Pyruvate Kinase. **Journal of Biological Chemistry** 312:525-540.

Yan, Y. and G. Marriott. 2003. Analysis of protein interactions using fluorescence technologies. **Current Opinion in Chemical Biology** 7:635-640.

Yi, G., S.-H. Sze and M.R. Thon. 2007. Identifying clusters of functionally related genes in genomes. **Bioinformatics** 23:1053-1060.

Zinchenko, A.I., V.N. Barai, L.M. Zalashko, N.E. Poopeiko, T.I. Pricota, G.G. Sivets and I.A. Mikhailopulo. 1990. Enzymatic synthesis of nucleoside 5'-mono and -triphosphates. **Federation of European Biochemical Societies** 260:254-256.

Zoraghi, R., L. Worrall, R.H. See, W. Strangman, W.L. Popplewell, H. Gong, T. Samaai, R.D. Swayze, S. Kaur, M. Vuckovic, B.B. Finlay, R.C. Brunham, W.R. McMaster, M.T. Davies-Coleman, N.C. Strynadka, R.J. Anderson and N.E. Reiner. 2011. Methicillin-Resistant *Staphylococcus aureus* (MRSA) Pyruvate Kinase as a Target for Bis-indole Alkaloids with Antibacterial Activities. **Journal of Biological Chemistry** 286:44716-44725.

APPENDIX

APPENDIX

Bacterial mediums and chemical reagents

LB agar

Peptone	5 g
Yeast extract	5 g
NaCl	5 g
Agar	18 g

Adjust to pH 7.0 by 5N NaOH and adjust volume of medium to 1 L, sterile by autoclaved.

LB broth

Peptone	5 g
Yeast extract	5 g
NaCl	5 g

Adjust to pH 7.0 by 5N NaOH and adjust volume of medium to 1 L, sterile by autoclaved.

YEME (Yeast Extract Malt Extract) medium

Yeast extract	3 g
Peptone	5 g
Glucose	10 g
Sucrose	340 g

Adjust volume of medium to 1L and sterile by autoclaved, add 2 ml of 2.5 M $MgCl_2$ before uses.

Oatmeal agar

Oatmeal	20 g
Agar	18 g
Trace salts solution	1 ml

Adjust volume of medium to 1 L, sterile by autoclaved.

Trace salts solution

$FeSO_4.7H_2O$	0.1 g
$MnCl_2.4H_2O$	0.1 g
$ZnSO_4.7H_2O$	0.1 g

Adjust volume of solution to 100 ml, sterile by filter

Chemical reagents for isolation of plasmids by alkaline lysis method

Solution I

50 mM glucose

25 mM Tris-HCl pH 8.0

10 mM EDTA pH 8.0

Solution II

0.2 N NaOH

1% SDS (Sodium dodecyl sulfate)

Solution III

3 M CH_3CO_2K

TE buffer

10 mM Tris-HCl pH 8.0

1 mM EDTA

6x DNA loading dye

10 mM Tris-HCl pH 7.6

60 mM EDTA

0.03% bromphenol blue

60% glycerol

Cracking buffer, 2x protein loading dye

60 mM Tris-HCl pH 6.8

0.01 % bromphenol blue

1% BME (β-mercaptoethanol)

1% SDS

10% glycerol

10x running buffer for SDS-PAGE

Tris	30.2	g
Glycine	144	g
SDS	10	g

Adjust volumn of buffer to 1L

12% SDS-PAGE, separating gel

1.5 M Tris-HCl pH 8.8	1.25	ml
30% acylamide	2	ml
10% SDS	50	µl
50% glycerol	100	µl
10% ammonium persulfate	25	µl
TEMED	2.5	µl
dH_2O	3.15	ml

4% SDS-PAGE, stacking gel

1.5 M Tris-HCl pH 6.8	468.75	µl
30% acylamide	243.75	µl
10% SDS	18.75	µl
50% glycerol	75	µl
10% ammonium persulfate	9.375	µl
TEMED	1.25	µl
dH_2O	93.75	µl

Coomassie blue solution, staining solution for SDS-PAGE

0.05% Coomassie blue R-250

10% CH_3COOH

50% CH_3OH

Destaining solution I

10% CH_3COOH

50% CH_3OH

Dastaining solution II

7% CH_3COOH

5% CH_3OH

Lysis buffer

20 mM Tris-HCl pH 8.0

50 mM KCl

0.5% Tween 20

0.1% Triton X-100

1 mM EDTA

Sterile by autoclave, add 1 mM PMSF and 2 mM BME before uses.

Lysis buffer for purification of PYK type I of *E. coli*

10 mM Tris-HCl pH 7.5

100 mM KCl

10 mM MgCl2

1 mM EDTA

Sterile by autoclave, add 1 mM PMSF and 2 mM BME before uses.

Buffer A, solution for purification of ADK of *E. coli* by DEAE column

50 mM Tris-HCl pH 8.0

2 mM BME

Buffer B, solution for purification of CMK of *E. coli* by Ni^{2+}-NTA column

20 mM Tris-HCl pH 8.0

500 mM NaCl

10 mM BME

Buffer C, solution for purification of DNK of *E. coli* by Ni^{2+}-NTA column

20 mM Tris-HCl pH 8.0

300 mM KCl

10 mM BME

Buffer D, solution of purification of PYK type I of *E. coli* by DEAE column

50 mM Tris-HCl pH 7.5

2 mM BME

CURRICULUM VITAE

NAME : Ms. Nalumon Thadtapong

BIRTH DATE : September 28, 1987

BIRTH PLACE : Nonthaburi, Thailand

EDUCATION :

YEAR	INSTITUTE	DEGREE/DIPLOMA
2008	Srinakharinwirot Univ.	B.S. (Microbiology)
2013	Kasetsart Univ.	M.S. (Genetic Engineering)